



FINAL REPORT

Solar Heat Pump Seasonal and Peak Demand Energy Analysis

FSEC-CR-1957-13

November 19, 2013

Submitted to:

Craig V. Muccio
General Office, GO
Florida Power & Light
9250 W. Flagler Street, DMO-GO
Miami, Florida 33174

Submitted by:

James B. Cummings
Charles R. Withers, Jr.
Houtan Moaveni
David Hoak

1679 Clearlake Road, Cocoa, FL 32922-5703 • Phone: 321-638-1000 • Fax: 321-638-1010
www.fsec.ucf.edu



A Research Institute of the University of Central Florida

FINAL REPORT
Solar Heat Pump Seasonal and Peak Demand Energy Analysis

FSEC-CR-1957-13
November 19, 2013

FPL PO# 2000052433; C# 4600002848
FSEC Project # 20128241

Submitted to:
Craig V. Muccio
General Office, GO
Florida Power & Light
9250 W. Flagler Street, DMO-GO
Miami, Florida 33174

Prepared by:
James B. Cummings
Charles R. Withers, Jr.
Houtan Moaveni
David Hoak

Florida Solar Energy Center
1679 Clearlake Road
Cocoa, Florida 32922

TABLE OF CONTENTS

LIST OF FIGURES	i
LIST OF TABLES	iv
ACKNOWLEDGEMENTS	vi
EXECUTIVE SUMMARY	vii
1. INTRODUCTION	1
2. PROJECT DESCRIPTION	2
3. SOLAR HEAT PUMP SYSTEM DISCRPTION AND OBSERVATIONS	13
4. COOLING SEASON ENERGY SAVINGS FROM THE SOLAR POWERED HEAT PUMP	28
5. COOLING SEASON PEAK DEMAND SAVINGS PRODUCED BY THE SOLAR HEAT PUMP SYSTEM	36
6. HEATING SEASON ENERGY SAVINGS PRODUCED BY THE SOLAR HEAT PUMP SYSTEM	44
7. HEATING SEASON PEAK DEMAND SAVINGS PRODUCED BY THE SOLAR HEAT PUMP SYSTEM	47
8. ECONOMIC ANALYSIS OF VARIOUS SYSTEM CONFIGURATIONS	52
9. SUMMARY AND CONCLUSIONS	65
APPENDIX A: Performance Analysis of Components of the Stand Alone System	68
APPENDIX B: Improving Solar Heat Pump System control to Achieve Maximum Peak Demand Savings	71

List of Figures

Figure ES-1. Monitored mini-split heat pump EER for Standard and Economy modes as a function of daily outdoor temperature with indoor temperature held constant at about 76°F.	xvi
Figure 1. The Building Science Lab is a 2000 ft ² , highly instrumented lab building located on the FSEC Campus	3
Figure 2. SolarWorld SW 250 I_V Curves at 25°C cell temperature	6
Figure 3. SolarWorld SW 250 PV module efficiency versus irradiance and cell temperature	6
Figure 4. Ambient air temperature, PV module temperature, and solar radiation on a typical summer day (September 3, 2012) with near full sun	7
Figure 5. Building Science Lab building with 8 PV panels in the foreground. The outdoor unit of the 1.5-ton mini-split heat pump can be seen along the south wall of the building. Batteries, charge controller, inverter, and 8 batteries are located in the lab building room closest to the PV panels	9
Figure 6. Battery SOC versus Battery Resting Voltage (data from battery manufacturer)	17
Figure 7. Twenty-four hour space temperature profiles in the Building Science Lab with only the mini-split conditioning the space. Temperature is shown for the central zone (blue line) and 4-room average (red line). The mini-split is powered on these particular days by PV solar for about half the day and from the utility grid for the remainder of the day, while the central ducted system does not operate during the entire 7-day period. It can be seen that room temperature rises in direct proportion to the cooling load.	23
Figure 8. Monitored mini-split EER for Standard and Economy modes as a function of daily outdoor temperature with indoor temperature held constant at about 76°F.	27
Figure 9. Cooling energy delivered by the solar heat pump system as a function of daily solar radiation for <u>Standard</u> thermostat control mode when using the eight battery storage bank.....	30
Figure 10. Delivered mini split cooling versus solar radiation using <u>Economy</u> control mode when using the eight battery storage bank.....	30
Figure 11. Daily MH Lab cooling load versus delta-T (out – in) when using attic ducts.....	31
Figure 12. Measured cooling EER for the central ducted 3-ton SEER 13 MH Lab heat pump as a function outdoor temperature. Duct losses are not considered when calculating EER.	31
Figure 13. Solar ratio, which is used to convert solar radiation on the horizontal to solar radiation at PV array tilt, varies as a function of day of the year. Solstice day increases from 1 to 183 from December 21 to June 21, and then decreases from 183 to 1 from June 21 to December 21.....	32

List of Figures (cont.)

Figure 14. During the 8-day period August 29-September 5, 2012, the central ducted system does not cycle ON during the hours of 4 to 6 PM (EDT) because the mini-split, which is in Standard mode, meets the entire building cooling load during those peak hours. Therefore, the solar heat pump system meets 100% of the cooling demand on the peak hours of those 8 hot summer days.	36
Figure 15. Twenty-four hour cooling power consumption profile for Standard and Economy mini-split operation when using 8 batteries, plus cooling power consumption for the MH Lab SEER 13 central system. Figure 15 has added economy profile to Figure 14.	37
Figure 16. Twenty-four hour cooling power consumption profile for Standard and Economy mini-split operation when using 4 batteries, plus cooling power consumption for the MH Lab SEER 13 central system.....	38
Figure 17. The red line is a measured 24-hour space temperature profile in the Building Science Lab for a 7-day period with only the mini-split conditioning the space, with space temperature setpoints used by the mini-split (blue line) and central system (orange line) illustrated.....	42
Figure 18. Daily heating load (Btu/day) versus delta-T (out – in) for the MH Lab excluding duct losses.....	45
Figure 19. Measured system 15-minute heating EER for the 3-ton SEER 13 MH Lab heat pump as a function outdoor temperature..	45
Figure 20. Twenty-four hour composite of solar heat pump operation on a cold two-day period, with average morning low of 33°F and nearly cloudless skies.....	48
Figure 21. Twenty-four hour composite of solar heat pump operation on a cold two-day period, showing heating power for the mini-split operating on solar (blue line) and on the grid (green line), and heating power for the central 5-ton system (purple line).	49
Figure 22. Composite of three moderately cold days in late March shows that there is insufficient stored battery energy to allow the solar heat pump to operate during the 6 to 8 AM peak period... ..	50
Figure 23. Utility Grid-Interactive PV System.	55
Figure 24. Grid Interactive monthly 24-hour profile PV system supply/demand energy flows.	56
Figure 25. “As-tested” Stand-Alone Solar Heat Pump System.	57
Figure 26. Solar Powered Heat Pump System	59
Figure 27. Bimodal PV System.	61
Figure 28. Equipment cost versus SEER rating for four sizes of mini-split heat pumps based on an on-line survey, including a best-fit line for the 1-ton units. (Source: survey performed by Carlos Colon in 2011.).....	63

List of Figures (cont.)

- Figure A-1.** System Operation Energy Flow Patterns and Definitions..... 68
- Figure A-2.** Calculated Performance Ratio (PR) values are determined based on monitored data from the “as-tested” solar heat pump system for each month of the year. 69
- Figure A-3.** Performance Ratio plotted versus Production Factor based on monitored data. ... 69
- Figure B-1.** Battery SOC versus Batter Resting Voltage (data from battery manufacturer). 72

DRAFT

List of Tables

Table ES-1. Annual cooling energy required by the MH Lab SEER 13 central system and annual energy savings provided by the solar heat pump system using 5 different system configurations.	viii
Table ES-2. Peak cooling energy required by the MH Lab SEER 13 central system and peak demand reduction provided by the solar heat pump system for 4 different system configurations.	ix
Table ES-3. Annual heating energy required by the MH Lab SEER 13 central system and annual energy savings provided by the solar heat pump system based on two operating modes.....	ix
Table ES-4. Seasonal savings and payback period for four solar heat pump system designs taking into account maintenance and component replacement costs over a 20-year period.....	xii
Table ES-5. TMY3 projected demand and annual energy savings for the FPL territory.....	xvii
Table 1. A composite of average measured daily outdoor temperature, PV module temperature, and solar radiation for the period August 3 – September 3, 2012. The average panel temperature during this hot summer period is about 126°F at peak temperature and 114.4°F for the solar radiation-weighted average PV module temperature for this period.	8
Table 2. Advantages and disadvantages of three types of deep discharge batteries.....	10
Table 3. Data for a warm and sunny spring day (April 11, 2013) showing outdoor and indoor temperatures, solar radiation, PV system energy output (PVw), mini-split and central system energy consumption, and mini-split sensible cooling for the solar heat pump with 8-batteries and Economy mode. Time is DST.	22
Table 4. Data for a hot and sunny summer day (July 8, 2013) showing outdoor and indoor temperatures, solar radiation, PV system energy output (PVw), mini-split and central system energy consumption, and mini-split sensible cooling for the solar heat pump with 4-batteries and Economy mode. Time is DST.	25
Table 5. Regression analysis results for cooling derived from monitored data of 100% mini-split (M-S) operation and 8 batteries. Calculated cooling energy savings (last column) are based on typical summer values with daily average temperature of 76°F indoors and 80°F outdoors, with solar radiation of 5500 Wh/m ² -day.	29
Table 6. Annual cooling energy required by the MH Lab SEER 13 central system (first data row) and annual energy savings provided by the solar heat pump system for 5 different system configurations (data rows 2–6).	34
Table 7. Peak cooling energy required by the MH Lab SEER 13 central system and peak demand reduction provided by the solar heat pump system for 4 different system configurations	40

List of Tables (cont.)

Table 8. Regression analysis results for heating derived from monitored data of 100% mini-split (M-S) operation and 8 battery Economy control mode. Calculated heating energy savings (last column) are based on daily average temperature of 72°F indoors and 50°F outdoors, with solar radiation of 5500 Wh/m ² -day.	44
Table 9. Annual heating energy required by the MH Lab SEER 13 central system and annual energy savings provided by the solar heat pump system using 2 different system configurations.	46
Table 10. Seasonal savings and payback period for four solar heat pump system designs taking into account maintenance and component replacement costs over a 20-year period.	54
Table A-1. Analysis of the solar heat pump system PV strings (1 module per string) over the period July 15, 2012 – July 15, 2013 finds that PV module mismatch produces losses of 6 to 7% for each of the four strings of panels.	70

DRAFT

ACKNOWLEDGEMENTS

The authors would like to acknowledge assistance and guidance provided by Dave Click, Principal Research Scientist at the Florida Solar Energy Center, support and encouragement from Craig Muccio – project monitor from Florida Power and Light, and for financial support for this research from Florida Power and Light.

DRAFT

EXECUTIVE SUMMARY

A research project was conducted to evaluate the potential annual and peak electrical energy reduction resulting from the addition of a solar powered mini-split heat pump system to an existing home with central heat and cooling in the Florida Power and Light service territory. Experiments were performed to characterize the performance of a solar powered mini-split heat pump over a 12-month period and to determine seasonal and peak demand savings for both heating and cooling periods. The 1.5-ton mini-split heat pump, along with 2 kW of photovoltaic (PV) panels, 8 deep discharge batteries, a charge controller, and an inverter were installed in a 2000 ft² facility called the Building Science Lab building on the Florida Solar Energy Center (FSEC) campus. Instrumentation was installed to record solar and outdoor temperature, indoor temperature and relative humidity (RH), and electrical energy flows from PV, batteries, inverter, and utility grid to heat pump.

The mini-split heat pump was a 1.5-ton Fujitsu model with 19.2 SEER and 10.0 HSPF energy efficiency ratings. Cooling capacity of the system is variable and ranges from 7000 to 23,000 Btu/h. Heating capacity is variable and ranges from 7000 to 29,000 Btu/h. The mini-split has two modes of operation; 1) Standard and 2) Economy. In Standard cooling mode, the supply air temperature is about 46°F when the return air is about 75°F. This 29°F temperature drop is unusually large for an A/C system. The cold coil (and cold supply air) yields excellent indoor RH control, with typical RH levels being 39-42% in the lab building (it is an unoccupied building without mechanical ventilation but had water vapor added to the space at a rate of about 8 pounds/day). In Economy mode, the compressor cooling capacity is reduced much of the time and the supply air was delivered typically at a temperature of about 52°F. This supply air temperature is still sufficiently cold to provide good RH control, typically about 46% indoor RH on hot and humid summer days. It was found that Economy mode allows the system to operate considerably more efficiently and utilize the available solar energy considerably more effectively.

Experiments were operated variously with Standard and Economy modes, with 8 batteries and 4 batteries acting as storage, and with the mini-split operated from solar alone or from the utility grid. A 5-ton central ducted heat pump, with a SEER rating of approximately 11, operated as back-up to the mini-split heat pump when the space conditioning load could not be otherwise met.

Energy analysis. Electrical energy flows were monitored for the PV system, the charge controller, the batteries, the inverter to the mini-split heat pump, and the utility grid to either the mini-split or the central system.

Regression analysis was performed to characterize cooling and heating energy delivered to the Building Science Lab by the solar powered mini-split heat pump, by the mini-split heat pump when operating from the utility grid, and by the central ducted heat pump. While the experiments were carried out in the Building Science Lab, seasonal energy savings and peak demand reduction were determined for the MH Lab. The MH Lab is a highly instrumented 1600 ft² lab wood frame house, space conditioned by a split direct-expansion 3-ton SEER 13 heat

pump having central air distribution through essentially leak free ducts in the attic space. MH Lab cooling and heating loads and heat pump performance characteristics had been characterized in previous experiments. Seasonal and peak energy consumption and savings from operation of the solar mini-split heat pump (and also from operation of the mini-split from the grid when the solar resource was depleted) were characterized for the MH Lab based on regression analysis equations and Typical Meteorological Year (TMY3) data from four Florida cities (weighted to characterize the FPL service territory).

Seasonal cooling savings. Cooling savings were characterized for a variety of experimental configurations versus the 3-ton SEER 13 central heat pump which serves the MH Lab. Annual cooling energy consumption for the SEER 13 system with attic ductwork (in all cases weighted for the FPL service territory) was 6204 kWh when operating by itself. When the solar-powered mini-split was operated, between 34% and 54% of the annual cooling load was satisfied by the solar heat pump depending upon the number of batteries used and whether Standard or Economy mode was employed (Table ES-1). Economy mode yielded about 24% greater annual cooling energy savings compared to Standard mode. The larger battery bank (8-batteries) yielded about 32% greater annual cooling energy savings compared to 4 batteries. The title of last row in Table ES-1 uses the term “100% mini-split” meant to indicate that this system is free to operate at all times even if solar generated power is not available. The central system was also still able to operate if the mini-split could not keep up with the load. Additional savings resulted when the mini-split operated on grid power after the solar resource was depleted. In total, when operated from solar and the grid, savings of 4442 kWh/y or 72% of space cooling energy that would have otherwise been consumed in the MH Lab house by the central system, are achieved.

Table ES-1

Annual cooling energy required by the MH Lab SEER 13 central system and annual energy savings provided by the solar heat pump system using 5 different system configurations.

	Annual Cooling kWh	Annual Savings %
MHL SEER 13 Average Annual kWh	6204	0%
8 Battery Economy kWh Savings	3322	53.5%
8 Battery Standard kWh Savings	2683	43.3%
4 Battery Economy kWh Savings	2516	40.6%
4 Battery Standard kWh Savings	2101	33.9%
100% Mini-Split Economy kWh Savings¹	4442	71.6%

¹ These savings assume that the mini-split also operates on the grid when the solar resources has been depleted, is limited, by assumption, to meeting no more than 80% of the space cooling load during hours when it operates on the utility grid, and the PV system uses 8 batteries.

Peak demand cooling savings. Cooling peak demand savings were characterized for a variety of experimental configurations versus the MH Lab central heat pump. Peak cooling demand for the hottest hours of the hottest TMY3 day for each of the four FPL cities was determined based on regression analysis. Generally, the solar heat pump is very effective at meeting cooling

demand during the 3-5 PM peak period. Depending upon which of the solar heat pump configurations was active, peak demand savings ranged from 69% to 100% (Table ES-2). Peak demand savings were about 20% higher with Standard mode than with Economy mode. Likewise, peak demand savings were about 20% higher with 8 batteries than with 4 batteries. Maximum peak demand savings were 2.25 kW for the solar heat pump.

Table ES-2

Peak cooling energy required by the MH Lab SEER 13 central system and peak demand reduction provided by the solar heat pump system for 4 different system configurations.

	Cooling Peak kW	Peak Reduction %
MHL SEER13 Cooling Peak Demand	2.25	0%
8 Battery Standard Peak Reduction	2.25	100.0%
8 Battery Economy Peak Reduction	1.91	85.1%
4 Battery Standard Peak Reduction	1.91	84.9%
4 Battery Economy Peak Reduction	1.55	69.1%

Seasonal heating savings. Early in the heating evaluation period, it was determined that the solar heat pump system would not meet a substantial portion of the heating load with 4 batteries or under Standard control mode. Therefore, the heating experiments focused on operation with 8 batteries with Economy control mode. (Clarification: Economy mode yielded greater solar heating savings because the mini-split operated at about 34% higher efficiency in Economy mode versus Standard mode.) Heating savings were characterized for one experimental configuration (Economy with 8 batteries) versus the MH Lab central heat pump. Annual heating energy consumption for the SEER 13 system with attic ductwork (in all cases weighted for the FPL service territory) was 260 kWh when operating by itself, based on the regression equations and TMY3 data. When the solar-powered mini-split was operated, 213 kWh (or 82%) of the annual heating load was satisfied by the solar heat pump (Table ES-3). In total, when operated from solar and the grid, 232 kWh/y or 89% of space heating energy that would have occurred by the central system, are saved.

Table ES-3

Annual heating energy required by the MH Lab SEER 13 central system and annual energy savings provided by the solar heat pump system based on two operating modes.

	Annual Heating kWh	Annual Savings %
MHL SEER 13 Average Annual	260	0%
8 Battery Economy Savings	213	81.9%
100% Mini-Split Economy Savings²	232	89.2%

² These savings are based on the assumption that the mini-split operating on the grid meets no more than 80% of the space heating load that would otherwise be met by the SEER 13 central system.

Peak demand heating savings. There was insufficient peak heating data to perform regression analysis. The research team examined a representative sample experimental peak demand periods on cold winter mornings and found that in no case did the solar heat pump operate at all during the 6-8 AM (EST) period. It is concluded, therefore, that the solar heat pump system was unable to achieve any peak demand savings on winter mornings, because the batteries could not carry sufficient electrical energy forward through a cold night to keep the system operating.

Lessons learned.

1. The tested solar heat pump system can meet over 70% of the annual space conditioning energy usage, but does not yield attractive economic returns, with typical payback on the order of 20 years when taking into account maintenance and periodic equipment replacement (for batteries, inverters, and mini-split) .
 - a. On the other hand, the solar heat pump system does produce substantial cooling peak demand reduction which can be attractive to the utility.
 - b. It also provides some space conditioning and potentially 120V alternating current service to the customer during periods when the grid goes down
2. Batteries are the weak link in the solar heat pump system. When subjected to nearly daily cycling from 45% to 90% state-of-charge (SOC), the batteries exhibited evidence of significantly diminished storage capacity by the end of 12 months.
 - a. It is noteworthy that the battery manufacturer recommends that only about 50% of total battery storage capacity be used on a regular basis. However, even limiting battery discharge to about 50% of full capacity, the 8 AGM batteries used in this work had essentially failed by the end of 12 months of service.
3. The inverter proved to be more inefficient than originally anticipated (84% monitored efficiency). It will be important, for future stand-alone applications, to find higher efficiency inverters.
4. A bimodal inverter (able to both receive from and deliver to the central grid) is needed in order to use excess solar energy that is available on sunny days with limited space conditioning loads.
 - a. Based on the findings of this research effort, it is recommended that an inverter for this type of stand-alone system be bimodal, that is having the capability to also send power to the electric utility grid. Converting this system to bimodal would make the overall yearly solar heat pump system operation more energy efficient because excess PV power that is not needed by the mini-split heat pump on mild autumn, winter, and spring days could then be put to good use (that is, the excess power could be sent back to the grid). As it was, there were a significant number of days when a significant portion of the available solar could not be used, because of limited cooling or heating load on the building.
5. An optimized stand-alone bimodal system design is proposed in this report that will make the system more cost-effective by delivering all of the available solar energy either to the mini-split or to the utility grid and by greatly extending the life of the batteries.

- a. This bimodal system can operate in grid-integrated mode or as a stand-alone system. Compared to the “as-tested” system, there are two main differences.
- b. The first difference is that the inverter can also deliver excess solar to the utility grid, allowing essentially all potential solar power to be put to effective use, either going to the solar heat pump or directed to the grid.
- c. The second difference is that in normal everyday operation this bimodal system will limit the battery SOC range to only about 5% of full capacity. With this small cycling range, it is expected that battery life will increase by an order of magnitude. However, the system can still be effective as a stand-alone back-up system because when the utility grid goes down the batteries can be exercised across a larger range of SOC (to 50% or more of full capacity) in order to allow the system to deliver significant back-up solar power to the home.

Economic analysis summary and conclusions. Economic analysis was performed for a total of four solar heat pump configurations. Additionally, three other variations of the “as-tested” solar heat pump system were examined.

All seven of the designs had battery back-up with the exception of 1) a grid-tied solar system with a separate mini-split heat pump system (operating in parallel but not integrated); this was the baseline against which the other system designs were compared. Other examined designs included 2) the “as-tested” solar heat pump system, 3) the dc-powered solar heat pump system which was originally proposed but was unavailable for testing, and 4) an optimized bimodal ac-powered solar heat pump system. Three additional variations of the “as-tested” system also examined were; 5) operation of the system with 4 batteries versus 8 batteries, 6) operation of the system with a lower or a higher efficiency mini-split heat pump, and 7) operation of the system with expanded PV/battery capacity.

- Table ES-4 presents a summary of economic analysis results for the four primary solar heat pump system design variations (economic analysis of the three additional variations on the “as-tested” system are presented later in the report). While energy savings analysis derived from the year-long monitoring and regression analysis is available for the “as-tested” system, that analysis is not available for the other configurations. Therefore, the economic performance of the other configurations has been examined using a solar simulation tool called PV-DesignPro-S. In order to provide internally consistent results, the analysis has also been performed for the “as-tested” system using the same PV-DesignPro-S software. Therefore, analysis results from PV-DesignPro-S for all four of the primary system configurations are presented in the table. The following information is presented in Table ES-4: Solar generated electricity
- Electrical energy savings that result from the operation of the mini-split using solar generated electricity as a result of avoided electrical energy use that the central ducted SEER 13 system would have used
- Electrical energy savings that result when the mini-split heat pump operates on the grid when the solar resource has been depleted. The savings occur because the mini-split is essentially two times as efficient as the central ducted system

- Gross and net system cost
- Payback period taking into account maintenance and replacement costs for batteries, inverters, and mini-split.

Table ES-4

Seasonal Savings and Payback Period for Four Solar Heat Pump System Designs Taking into Account Maintenance and Component Replacement Costs over a 20-year Period

	PV produced kWh/y	PV+M-S avoided kWh/y	Mini-split on grid savings kWh/y	Seasonal savings kWh/y	Gross system cost	Net system cost¹	Payback period years
Grid-integrated	2968	3877	1274	6151	\$11,200	\$7840	12
“As-tested” ²	2734	5386	539	5925	\$15,200	\$10,640	20
DC	2441	4247	-	4247	\$12,860	\$9002	22
Bimodal	2968	3877	1274	6151	\$13,600	\$9520	17

¹ after 30% Federal tax credits

² Economy mode with 8 batteries

All of the systems employed a mini-split heat pump. In all cases a substantial portion of the seasonal energy savings occurred as a result of the high efficiency of the mini-split heat pump. The ac-powered mini-split had a net efficiency that was 1.97 times that of the central SEER 13 ducted heat pump (which has an effective SEER of 9.75 after including 25% attic duct system losses). The dc-powered mini-split’s net efficiency was 1.74 times that of the central system. The fact that in most cases all of the solar power was being delivered through the mini-split means that the mini-split can be thought of as an amplifier, in effect doubling (or nearly doubling) the delivered savings that the solar system would otherwise have provided. In the case of the baseline system (grid-tied system with the mini-split heat pump operating in parallel), the solar power is not actually delivered through the mini-split but can in effect be thought to be substantially delivered through the mini-split.

There is another source of seasonal energy savings apart from solar powering of the mini-split, and that is operation of the mini-split from the grid when the solar resource has been depleted. While the solar heat pump system meets about 54% of the heating and cooling load of the house (MH Lab, in this case; see Table ES-1), the remaining space conditioning load can be substantially met by operation of the high efficiency mini-split operating from the utility grid. The “as-tested” solar heat pump system in our lab building had a relay installed that allowed the mini-split to switch seamlessly from solar to grid power when the solar resource was depleted. For this analysis, the research team assumed that 80% of the remaining heating and cooling load that had not been met by the solar heat pump would, in fact, be met by the mini-split operating off of the grid. The fact that the mini-split could provide the required space conditioning at approximately twice the efficiency of the central ducted heat pump meant that the energy represented by the remaining 46% of the yearly load not met by solar would then be effectively cut in half. As a result, about 72% of the energy use that would have occurred with the central ducted system was saved by the mini-split heat pump system when operating from solar and the grid.

This is a key point. While the 2 kW of solar panels can typically deliver about 2400 to 3000 kWh annually to end uses in a typical year (depending upon which system is being examined), the delivered energy savings (from avoided space conditioning energy consumption by the SEER 13 central, ducted system) increases to the 4200 to 6200 kWh per year range when tied in with a high efficiency mini-split.

In spite of the energy savings enhancement provided by the mini-split, the economic benefits are not particularly attractive strictly from yearly energy savings. For most of the examined systems, the payback period is on the order of 17-22 years. The grid-tied (baseline) system (2 kW of PV with a SEER 19.2 mini-split heat pump, but no batteries) has a payback of about 12 years.

The reader may have noticed that the predicted annual kWh savings of the “as-tested” system based on monitored data, regression analysis, and TMY3 data is about 25% lower than that predicted by the simulation tool PV-DesignPro-S. Inevitably, measured data (with simplified modeling based on regression analysis) and complex modeling using PV-DesignPro-S do not provide the same answers. There are too many variables to account correctly for all effects. Furthermore, models are only as good as the software developer and the data upon which the model was constructed and verified. The PV-DesignPro-S modeled results tend to yield greater annual savings.

It would be difficult for the research team to point to any one item or group of items that explains the difference between these modeling approaches. However, based on the research team’s observations, it is likely that battery charging issues and load scheduling may contribute significantly to the modeled differences.

- In our 12-month experiments, the research team observed that the batteries go through three stages – BULK, ABSORB, and FLOAT. In BULK, the batteries are able to accept energy at a high rate and can accept all of the solar available from the PV panels. As State of Charge (SOC) approaches 90%, charging goes into ABSORB mode, and the rate of energy acceptance by the batteries is cut substantially, so that about 50% of the available solar may be thrown away while in this charging mode. When charging goes into FLOAT, perhaps 90-95% of the available solar is thrown away. It is uncertain whether the PV-DesignPro-S model can fully account for the energy acceptance rate of the batteries that occurs in actual system operation, since these charging rates change from minute to minute as solar input and load output fluctuate in real time.
- Regarding load, the PV-DesignPro-S model assumes a single, typical daily load profile for each day of a given month. This simplification may well miss important outcomes from the variability which occurs in real weather patterns. For example, in the month of March, real weather may include 6 days of cold weather, followed by other days when neither heating nor cooling is required, and then mixed with days of significant space cooling. While the solar heat pump system will provide certain savings results when exposed to the variability of real weather and building loads, the predicted system performance based on average daily load may yield different annual savings. It is

difficult to predict how load profile simplifications like this can affect the annual predicted space conditioning savings.

- Nevertheless, the authors feel that the modeling results across the four primary system configurations, and three variations on the “as-tested” system, are sufficiently representative of actual seasonal performance that the relative economic performance of the systems can be meaningfully compared.

In order to observe differences in annual energy savings, the PV-DesignPro-S model was run for the various configurations based on a single TMY3 weather station (Melbourne). Melbourne was chosen to make comparison to the 12-months of our measured lab results (in Cocoa) most comparable. The objective of this exercise was not to provide service territory-weighted annual savings for the FPL service territory but rather to allow internally consistent comparison of each system to all of the others and to identify the relative economic performance of the systems. Following is a partial list of economic results and conclusions.

- All of the solar heat pump systems with battery back-up have a payback period on the order of 17-22 years. On the other hand, the grid-tied system with mini-split heat pump operating in parallel (but no battery storage) showed a payback period of about 12 years.
- A direct current-powered solar heat pump system is projected to have a similar level of cost-effectiveness compared to the “as-tested” system. On one hand, it would deliver slightly more solar space conditioning (because there are no inverter losses) and is estimated to be less costly. On the other hand, the ac-powered mini-split can provide additional annual cooling and heating energy savings by operating on grid power during periods when the solar resource has been depleted.
- A bimodal, optimized stand-alone solar heat pump system (as described earlier) would provide greatly expanded battery life and therefore greatly expanded functionality. On the other hand, as the system was modeled, it yields a longer payback period because the system expends more of its solar energy providing uninterruptable power to other end uses (i.e., computers, communications, refrigeration, and lighting) besides the mini-split, which unlike the high-efficiency mini-split, do not have the capability of amplifying the energy output of the solar system.

While cooling and heating savings do not make a compelling economic case for the solar heat pump systems (though the grid-tied solar heat pump system without batteries has a much shorter payback), cooling season peak demand savings is an attractive feature from an electric utility perspective, with fairly reliable 2.2 kW peak savings. If incentives are made available to the customer, the payback periods would be even more attractive. On the other hand, the systems with battery backup provide additional functionality which can offer significant value to the customer. The ability of the systems operating on alternating current to provide uninterruptable power to the house and power for both short-term and more extended grid power disruption can be seen as a major bonus. The ability of the optimized bimodal system to provide those functions and optimize battery life (which has been identified as major issue in this research project) will make it an attractive option for many consumers.

Strategies for Achieving Maximum Seasonal Energy Savings

During the 12-months of experiments, the research team made observations regarding how the solar heat pump system can be operated for maximum savings. Most of these observations relate to how operation in Economy mode yields substantial energy efficiency benefit.

Greater cooling energy savings can be achieved by operating the solar heat pump in Economy mode versus Standard mode, for three reasons.

1. In Economy mode, the supply air is significantly warmer, about 54°F compared to 46°F. Heat pumps operate more efficiently when they are pushing energy flows against a smaller temperature differential. In Economy mode, monitored cooling EER (Energy Efficiency Ratio) is 34% higher compared to Standard control mode when outdoor temperature is 82°F (Figure ES-1). From the regression analysis equations, it can be calculated that the mini-split operates with 17.6 EER in Economy mode compared to 13.1 EER in Standard mode.
2. The fact that the supply air is about 8°F warmer means that the heat pump in Economy mode is providing proportionately less latent cooling (less water vapor removal from the room air) and is expending more of its space cooling energy on lowering room air temperature (sensible cooling). It therefore meets the thermostat setpoint sooner.
 - a. Instead of producing typical 40% indoor RH (which it does while operating in Standard control mode), it produces about 46% indoor RH while operating in Economy control mode.
 - i. 40% indoor RH is significantly lower than is necessary for most applications (46% RH is sufficiently low for essentially all circumstances), and the energy used to draw the humidity down to the lower level is largely wasted. Humidity in the 38 - 40% range can lead to drying of skin and eyes, and can contribute to static electricity discharges.
 - ii. One could however argue that a lower indoor RH can produce similar occupant comfort at a higher temperature, which means that the thermostat could be raised by say 1°F with the lower RH. This would, however, require some thermostat adjustment on the part of the occupants, and it is uncertain that this sort of adjustment actually occurs in real homes.
 - iii. Another way to say this is that in Economy mode the system is spending less of its energy on latent cooling (moisture removal) and more of its energy on lowering the space (drybulb) temperature. Since thermostats control based on room air temperature, higher equipment operating SHR leads to reduced space cooling energy use.
3. When the mini-split is in Economy mode, it draws about 600 W compared to about 1000W in Standard mode. The relevance of the lower power draw in Economy mode to system efficiency relates to how this power draw interacts with the batteries. The smaller power draw of Economy mode tends to keep the system operating for an extended period. By contrast, the larger power draw of Standard mode tends to trigger premature cut-out of the inverter. As a result, more of its operation time (when in Economy mode) occurs at night when outdoor temperatures are cooler and the system operates more efficiently.

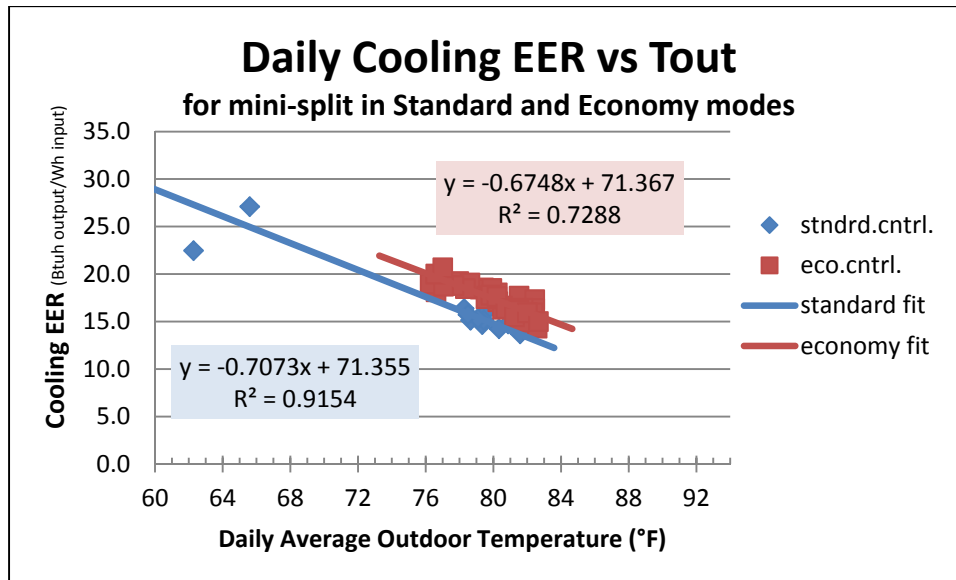


Figure ES-1. Monitored mini-split heat pump EER for Standard and Economy modes as a function of daily outdoor temperature with indoor temperature held constant at about 76°F.

Top Findings

This research project was primarily designed to measure the performance of a solar-powered mini-split heat pump with battery backup. Analysis was also performed for three additional system variations that were not tested in the lab based on simulations using the PV-DesignPro-S software. The simulations evaluated the economic merit of other system variations, including grid tied, dc-powered mini-split, and bimodal inverter options. Based on the economic analysis, the top two options with the best return on investment were:

1. Grid integrated PV no battery backup (12 years)

This is the only option evaluated that did not have battery backup. Because there are no expensive batteries, this system requires much less investment, but provides no benefit during storm events where grid power may not be available.

2. Bimodal inverter with 4 battery (17 years)

This system utilizes a bimodal inverter, permitting PV power to go to the mini-split, to the batteries, or to the grid when excess PV power is available. This system also employs electrical energy exchange between the grid and batteries to keep batteries within a narrow range of higher SOC which would extend battery life. While this system has a considerably longer payback period compared to the grid-tied system with no batteries, it has the significant advantage of providing uninterruptable power supply during periods of short power outages and providing power back-up during more extended periods of power outage.

Other major findings were:

- Money spent on upgrading the efficiency of the mini-split is more cost-effective than adding additional PV capacity, with payback periods of 8 years and 20 years, respectively.
- Operating with 4 batteries instead of 8 is more cost effective, but yields less effective back-up power during grid outages, reduced summer peak reduction, and about 4 hours less solar cooling on an average summer day.
- Better charge controllers are needed to more effectively manage battery SOC for optimum battery life. Drawing charges down to about half capacity requires careful monitoring on the part of the customer.
- Repeated cycling of the batteries (of about 45% typically on a daily basis) brings about shortened battery life and reveals significant performance and economic weakness of the batteries in this type of solar heat pump system. A bimodal system which reduces the daily range of SOC cycling from a 45% limit to about a 95% limit is projected to greatly extend battery life.
- Table ES-5 presents peak demand and annual energy savings developed from monitored data and modeling based on regression analysis and TMY3 weather input. Summer peak demand savings from solar ranged from 69% to 100%. Winter peak demand savings from solar was 0% in all cases. On the other hand, when the mini-split was also enabled to operate off of the grid, peak demand reduction was 45%. Seasonal space conditioning savings ranged from 33% to 72%.

Table ES-5
TMY3 Projected Demand and Annual Energy Savings for the FPL Territory.

	Summer Peak Demand (kW)	Summer Peak Demand Reduction	Winter Peak Demand (kW)	Winter Peak Demand Reduction	Annual Cool+Heat kWh	Annual Savings
MHL SEER 13	2.25	-	2.16	-	6464	-
8 Battery Economy Savings	1.91	85.1%	2.16	0%	3535	55%
8 Battery Standard Savings	2.25	100.0%	2.16	0%	2768²	43%
4 Battery Economy Savings	1.55	69.1%	2.16	0%	2569²	40%
4 Battery Standard Savings	1.91	84.9%	2.16	0%	2133²	33%
100% Mini-Split Economy Savings	1.91	85.1%	0.98¹	45.4%	4674	72%
Grid Tied No Batteries Savings	2.25	100.0%	0.98¹	45.4%	5674³	88%

¹ Due to limited heating season data, winter peak demand and demand savings are estimated based on the assumption that during the peak hour (34°F ambient temperature) the mini-split meets 70% of the heating requirement while the SEER 13 central ducted system meets 30% of the heating requirement.

² Due to limited heating season data, annual heating energy savings have been estimated for three of the tested configurations. Because space heating represents such a small portion of the total space conditioning energy in the heavily south-Florida weighted region (about 4%), even significant errors in these heating estimates would yield very small errors in annual space conditioning.

³ Based on 4674 kWh/y saved through PV and MS economy + 1000 kWh/y from PV power to other household use or utility grid per PV-DesignPro-S simulation.

1. INTRODUCTION

Renewable sources of energy, such as wind power and solar electricity, are being more widely implemented within homes. The power generated by these sources is in the form of direct current (dc). If this energy is to be used to power appliances within the home (or delivered to the electric grid), the dc current must, in nearly all cases, be converted to alternating current (ac), because nearly all household appliances use ac power. This conversion process requires a relatively expensive inverter and involves some loss in overall system efficiency. The research team was lead to believe that the inverter that was installed in this system would have a conversion efficiency of about 90 to 95%. Based on our monitored results, however, it was found that the actual operating inverter efficiency was 84% (see Appendix A for details on measured solar heat pump system component efficiency). To avoid the extra first cost and system inefficiency associated with dc to ac conversion, it may make sense to operate dc appliances within the home.

One home end-use that can be provided in the form of dc power is space heating and cooling. Dc-powered mini-split heat pumps have, in recent years, been introduced to the marketplace. One specific product (the SplitCool heat pump) was available in the marketplace at the time that the original proposal was written in 2011 but not when the project was scheduled to start. More on why FSEC was unable to test the SplitCool product and why an ac-powered solar heat pump was actually tested is presented in Section 2.

The company marketing the SplitCool product stated verbally that this heat pump would have energy efficiency equivalent to a SEER 17 rating (though no actual rating was available and no literature to that effect existed). The dc-powered unit would have a system efficiency equivalency of SEER 20.2 if compared to an ac-powered system with an 84% efficient inverter. The ac-powered mini-split actually tested in this project had a SEER rating of 19.2. Consequently, based on the SEER ratings of the dc- and ac-powered units, and the 84% inverter efficiency, the dc heat pump system would then have had an efficiency advantage of 5% compared to the ac heat pump.

2. PROJECT DESCRIPTION

This project originated when Florida Power and Light (FPL) requested that a solar powered heat pump be examined to determine seasonal and peak demand savings in a typical residential application. The Florida Solar Energy Center (FSEC) proposed that a dc-powered mini-split heat pump, along with photovoltaic (PV) panels and batteries, be installed in the 2000 ft² Building Science Lab located on the FSEC campus. A dc-powered 1.5-ton SplitCool mini-split had been identified for use in the experiments. When it was time to purchase the proposed SplitCool dc heat pump, it was learned that this product was between production cycles and it was not clear when it would be available. It was then decided, with approval from FPL, to test an ac-powered heat pump, using an inverter to convert the dc power to ac power. Since it was an objective of the project to examine the efficiency benefits of avoiding an inverter (use dc power from PV source to heat pump load), FSEC proposed to install energy meters that would monitor energy flows and allow characterization of inverter operating efficiency (as well as the efficiency of all other elements of the Solar Heat Pump system). An assessment of solar heat pump system component efficiency (and associated derate factors) is presented in Appendix A.

When discussing this change in scope of work, it was pointed out to FPL that a significant advantage of the ac system would be the capability of powering other household appliances (e.g., refrigerator, computer, lighting, etc.) in times of grid power outage. It was also pointed out that there would be other significant benefits of examining the ac-powered version of the solar-powered heat pump; 1) ac-powered mini-split heat pumps would likely have lower price and greater reliability (because of their high-volume production and opportunity to work out the bugs), 2) some mini-split heat pumps have SEER ratings as high as 27.2 (or 42% higher than that of unit tested in this project), 3) finding service personnel to make repairs would be easier, and 4) finding replacement parts would be more practicable. Furthermore, having a dc-to-ac inverter would allow transfer of electrical energy from the PV/battery system to the utility grid during periods when the PV system produces more power than is required by the heat pump. It should be noted that the type of inverter used in this project does not allow transfer of electrical energy to the grid, though this type of inverter is now available on the market.

2.1 Building Science Lab

The solar heat pump experiments were carried out in the Building Science Lab located on the FSEC campus (Figure 1). This 2000 ft² building has a slab foundation, concrete block walls with R-5 rigid board insulation, and 153 ft² of single-pane window glazing area. R-19 insulation batts are located on top of a suspended T-bar ceiling (2' x 4' panels), which is located 9.5 feet above the floor. The approximately 6-foot high space between the ceiling and the roof deck can be either vented or unvented (by opening up to 21 8"x16" vent openings, or not), and during these experiments was unvented. The nearly flat roof assembly has a dark roof membrane, about 2.5 inches of lightweight concrete, a low-emissivity (0.28 emissivity typical) reflective galvanized metal deck underneath the concrete, and no insulation (as stated before, insulation batts are located on the ceiling).



Figure 1. The Building Science Lab is a 2000 ft², highly instrumented lab building located on the FSEC campus.

The floor plan of the Building Science Lab has one large room in the central zone surrounded on the east by four spaces (offices, entry foyer, bathroom, and storage room) and on the west by two rooms (office and mechanical room). The central zone is fully open to unrestricted air flow and represents 50% of the total floor area. A single floor fan was located on the north side of the central zone and operated continuously to move air in a circular motion in the central zone. Doors to all of the rooms (except the mechanical room, bathroom, and storage room) remained open throughout the experiments.

A 5-ton central, ducted heat pump serves the building. The AHU is located in the mechanical room and the supply ductwork is positioned in the ceiling space. This central system has a SEER rating of approximately 11 based on performance testing.

Some internal loads were introduced into the space. One bank of lights remained operating at all times, drawing 720 W. The floor fan (55 W) and a computer combined with miscellaneous smaller electricity consumption (134 W) operated continuously. The batteries, charge controller, and inverter were all located in the southwest office; they give off a significant but unspecified amount of heat to the space. During the cooling season (but not the heating season), latent load (water vapor) was introduced to the space by means of a positive displacement pump and a mist-generating humidifier. This humidifier, which has a fan that moves about 400 cfm, throws small water droplets into the air which then evaporate, adding water vapor to the air. A positive displacement pump delivers water to the humidifier continuously at a rate of 8.4 pound/day. The evaporation of this amount of water represents 368 Btu/h of sensible space (evaporative) cooling. By comparison, the 63 W of humidifier fan

power represents 215 Btu/h of space heating. So on a net basis, the humidifier provides 153 Btu/h of sensible space cooling, equal to 1.3% of a ton of continuous cooling.

The Building Science Lab has a measured airtightness of 4.6 ACH50, meaning that it is of approximately average airtightness compared to typical new Florida homes. Tracer gas decay tests were performed, and it was found that typical natural air infiltration rate (natural means air infiltration driven by wind and temperature differential) was 0.28 ach (air changes per hour), which converts to about 80 cfm of air exchange with outdoors. No intentional ventilation was provided to the space.

2.2 The Stand-Alone Solar Heat Pump System Design

It is common practice when designing a PV system to first review the total electricity usage of the building. This provides insight into what size of PV system will be compatible with the application. This electricity usage and cost data for the building is then typically reviewed to ensure that the system would not produce more than the expected load would consume on a month-to-month basis. Most stand-alone systems are inherently more complex, with more complicated interactions between components, than regular grid-interactive PV systems. The stand-alone PV system sizing is directly proportional to the heat pump load as it requires a balance between energy generation and energy demand. The system design is an iterative process until the system output matches the load requirement. In common practice, a stand-alone PV system is designed to meet the average daily load, which in this case is for space cooling and heating from a mini-split heat pump. Installing a larger system will result in considerable excess solar power generation on days with little or no space conditioning load, which would result in considerable PV-generated electricity being thrown away. If the stand-alone system has the capability of selling excess electricity to the grid, then there is little downside to a larger system size. An optimized, bimodal solar heat pump system is proposed in Section 8 which incorporates bimodal electrical energy flow (from the grid and to the grid) and avoids stranded solar electricity.

As stated earlier, the solar heat pump experiments were carried out in the Building Science Lab. This 2000 ft² facility has a peak cooling load of about 2 tons. The Fujitsu 18RLXFW mini-split heat pump has a nominal capacity of 1.5-tons but maximum capacity of 1.92 tons (23,000 Btu/h). The nominal capacity of the mini-split heat pump, namely 1.5 tons, was selected due to the fact that the original solar powered dc heat pump (brand name SplitCool) had a nominal capacity rating of 1.5 tons. As it turns out, this was a fairly appropriately size for the Building Science Lab. At its maximum capacity, it is very nearly able to meet the cooling load of the building on the hottest days.

Selecting an appropriate PV system size is a multiple step iterative process. First, a simplified hourly load profile for a typical day for each month was developed for the mini-split heat pump. Required battery capacity, which is defined as the product of the current in amps (A) multiplied by the number of hours the current is flowing, is calculated by dividing average daily electrical load by the nominal inverter efficiency, nominal direct current system voltage (24 V), allowable

depth of discharge, and battery discharge-rate derating factor. For many stand-alone solar systems, an autonomy factor is taken into account. However, since additional power could be imported from the grid during periods of below average sunshine, this step was neglected in the design of the “as-tested” system.

Deep-discharge lead acid batteries were selected for the system as they are the most appropriate for the amount of required storage and the frequency of cycling that would be occurring in this system.

- The number of battery strings was determined by dividing the required battery capacity by the nominal battery capacity (305 Ah) supplied by the manufacture. In order to size the PV array, the array peak current was calculated from the simplified average daily load divided by the nominal battery efficiency, nominal system voltage (24 V), a derating factor (0.95), and monthly peak sun hours for Cocoa.
- The number of PV module strings was determined by dividing the array peak current by the nominal PV module maximum power current (provided by the manufacturer).
- Finally, the number of PV modules to be installed in series was calculated based on the maximum array voltage, which needs to be higher than the battery bank voltage (in order to charge the batteries). It should be noted that the system was designed to optimize energy yield and maximize the levelized cost of energy produced throughout the system’s lifetime. A widely used software tool, PV-DesignPro-S, was used to simulate annual system performance, using TMY3 hourly weather data for Cocoa. A description of the selected components for the PV system is included here as follows.

2.2.1 Photovoltaic Array

Several PV module types were available for selection. Monocrystalline PV modules have the highest efficiency. Amorphous PV modules are also available. However, since their efficiency is about 3 times lower than that of the polycrystalline, a good deal of roof surface area, mounting hardware, and installation labor is required. Polycrystalline PV modules represent a reasonable compromise between efficiency and cost. Eight (8) SolarWorld modules (SW 250 Mono) were selected for this system. Each module is rated to produce 250 W under standard test conditions (STC) of 1000 W/m² and 25°C (77°F). Figure 2 shows the I-V (current-voltage) curves for the selected SolarWorld modules at 25°C cell temperature.

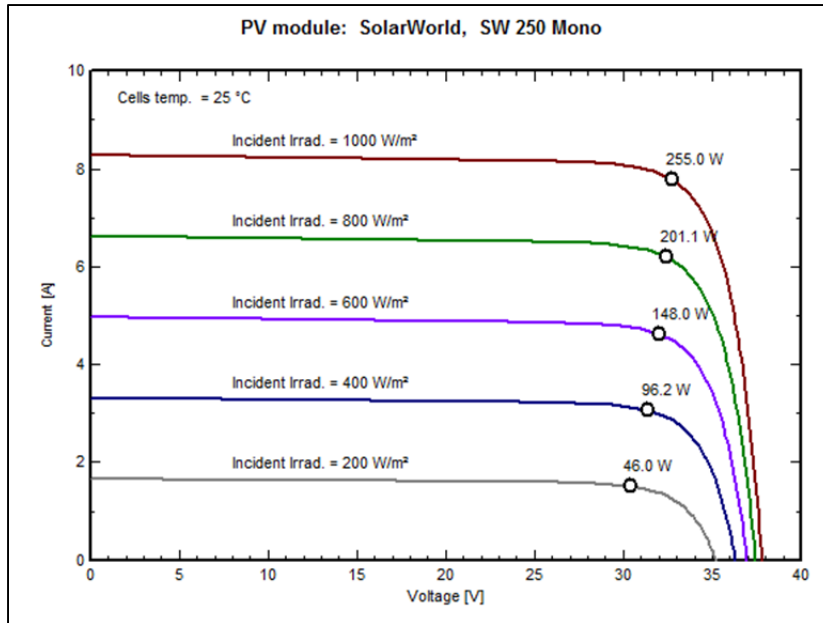


Figure 2. SolarWorld SW 250 I_V Curves at 25°C cell temperature.

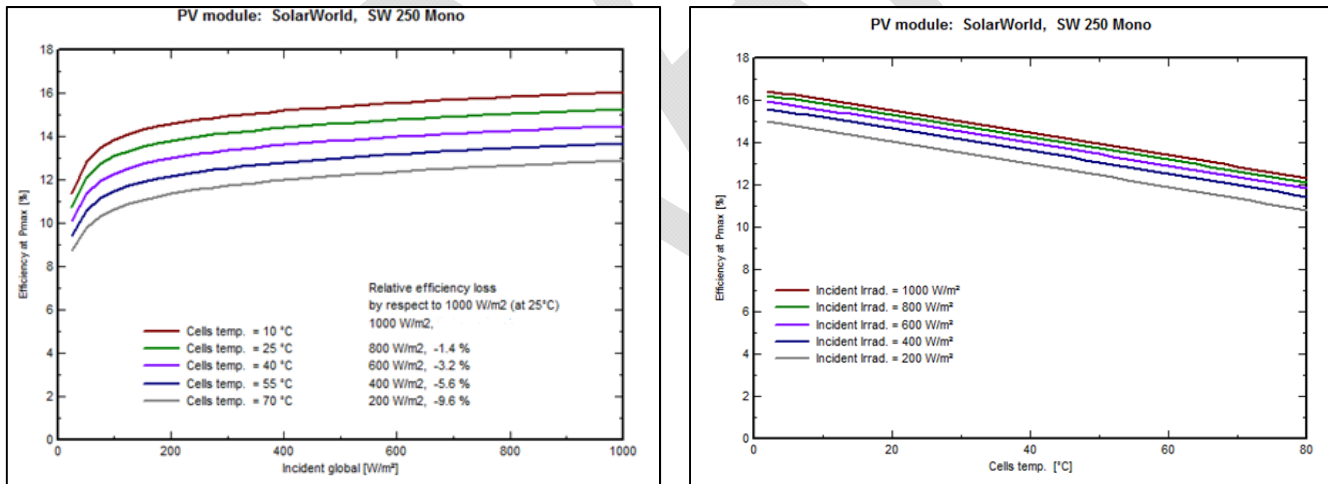


Figure 3. SolarWorld SW 250 PV module efficiency versus irradiance and cell temperature.

Each PV module has a surface area of 1.593 m² (17.14 ft²) and combined, the 8 modules have a total surface area of 12.74 m² (137.1 ft²). The PV array nameplate capacity at Standard Test Conditions (STC) is 2 kWdc and was installed in four strings of two modules in series. Each module is rated to produce 250 W under STC of 1000 W/m² and 25°C (77°F). They are also rated at 183.3 W under 800 W/m² and 25°C (77°F). Under STC, they have a rated efficiency of 14.91%, which means that 14.91% of the solar energy striking the top surface of the module is converted to electrical energy. However, typical PV panel temperature conditions are considerably warmer than 77°F, even as high as 150°F. At warmer temperatures, PV system efficiency declines. A formula can be

used to adjust typical PV panel electrical output as a function of panel temperature and the module temperature coefficient of power (MTCOP). Percent change in PV module output = (MTCOP) x (T_{module} – 25°C), with the value of MTCOP = -0.5% for typical mono- or poly crystalline cell modules. During the peak sun hours of September 3, 2012, for example, the panel reached a temperature of 145°F, as can be seen in Figure 4. Based on this temperature and the MTCOP of -0.5%, the calculated panel efficiency at this peak temperature would be 12.09% (0.811 x 14.91% = 12.09%). While the rated capacity is 250 W, the actual operating capacity at this peak summer hour would be 203 W under full sun and 145°F panel temperature.

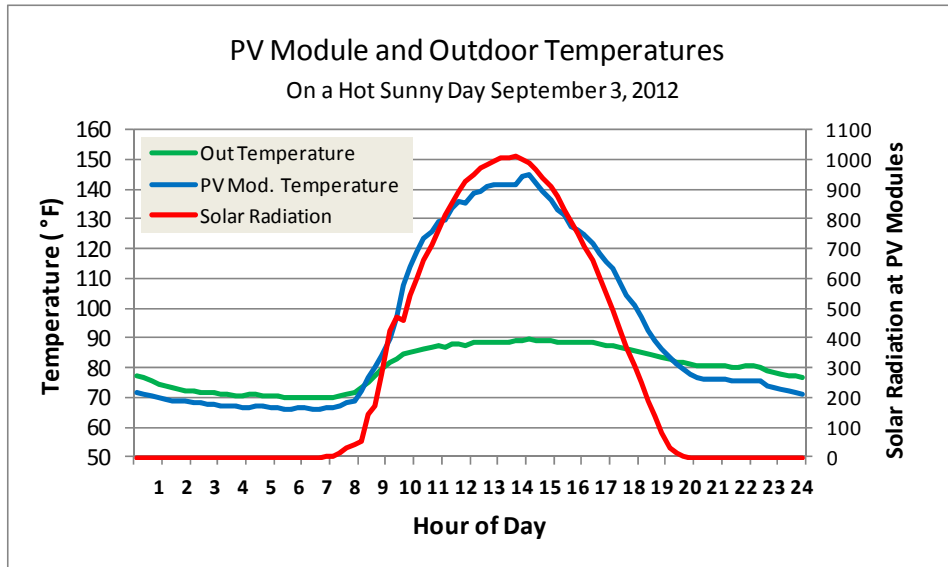


Figure 4. Ambient air temperature, PV module temperature, and solar radiation on a typical summer day (September 3, 2012) with near full sun.

However, panel efficiency is considerably higher than 12.09% for average summer conditions. Table 1 provides an average daily profile of ambient temperature, PV module temperature, and solar radiation for the 32-day period of August 3 through September 3, 2012. The solar radiation-weighted average PV module temperature turns out to be 114.4°F for this period. PV module efficiency reduction is calculated, then, to be 13.36% during typical summer weather or 10.4% lower than the nominal rating.

For this project, all PV source and output circuit wiring was secured to module frames and mounting rails. Each circuit of the PV modules was protected by an inline overcurrent protective device of proper voltage and current rating (15 A). The PV array was grounded using appropriate grounding clips. The PV modules were installed on pre-fabricated tilted roof units, sloped at an angle of 20 degrees, and oriented to the south (Figure 5). This tilt is fairly typical of many older homes in Florida. Newer homes often have a steeper roof which would tend to decrease solar electricity production in the summer and increase production in the winter.

Table 1

A composite of average measured daily outdoor temperature, PV module temperature, and solar radiation for the period August 3 – September 3, 2012. The average panel temperature during this hot summer period is about 126°F at peak temperature and 114.4°F for the solar radiation-weighted average PV module temperature for this period.

	Hour	T ambient	T pv-module	SOLAR
		°F	°F	W/m²
	1.00	77.21	74.16	0
	2.00	76.74	73.74	0
	3.00	76.31	73.32	0
	4.00	75.90	73.08	0
	5.00	75.51	72.79	0
	6.00	75.06	72.35	0
	7.00	74.95	72.25	0
	8.00	75.76	73.67	32.93
	9.00	78.97	79.60	119.88
	10.00	82.83	98.24	372.00
	11.00	85.71	115.38	565.70
	12.00	87.27	122.85	646.16
	13.00	88.18	126.84	705.24
	14.00	88.49	125.63	689.10
	15.00	87.92	119.64	618.29
	16.00	86.26	111.65	512.32
	17.00	85.11	104.33	387.27
	18.00	83.48	94.83	234.51
	19.00	81.75	86.21	108.44
	20.00	80.15	79.81	27.91
	21.00	79.07	76.68	9.80
	22.00	78.55	75.81	0
	23.00	77.98	74.92	0
	24.00	77.55	74.34	0
AVG		80.70	89.67	209.56
SUM				5029.55



Figure 5. Building Science Lab building with 8 PV panels in the foreground. The outdoor unit of the 1.5-ton mini-split heat pump can be seen along the south wall of the building. Batteries, charge controller, inverter, and 8 batteries are located in a lab building room closest to the PV panels.

2.2.2 Inverter and Charge Controller

The inverter needs to convert dc power to ac power in sufficient quantity up to the mini-split's maximum power draw. In cooling mode, the mini-split's maximum draw is rated at 1350 W. In heating mode, the maximum draw is rated at 1800 W. "Maximum Power Input" for the mini-split, however, was listed on the product specification sheet as 3.01 kW in both cooling and heating modes. Because of uncertainty regarding the actual full power draw, the research team selected a 4.0 kW inverter. The inverter was capable of providing a high percentage of its full rated output into one phase for extended periods of time, without allowing the voltage on the unloaded leg to spike. The inverter, which was purchased and installed as part of the solar heat pump system, was a Midnight Solar, Inc. Magnum MNEMS4024PAECL150 (\$3528.57 from Midnight Solar, Inc., Arlington, VA, phone 360 403-7207). It is a pre-wired combination system that includes a 4.0 kW inverter and the PV/battery system charge controller. It has the capability of delivering 240V AC power to a load (in this case, a mini-split heat pump) from a 24-V bank of batteries and also directly from the PV system. It does not have the capability to deliver power from the solar system to the grid. The charge controller size and model was determined based on array configuration and specifications.

2.2.3 Batteries

Lead-acid batteries are the most commonly used type for small-scale stand-alone PV systems. The battery bank designed and installed for this system contained 8 deep-discharge lead acid batteries (Sun Xtender PVX-3050T, Solar Battery Manufactured by Concorde Battery Corporation) of the absorbed glass mat (AGM) type. Sizing of the battery bank was determined

by the inverter input voltage (24 V) and PV-output storage requirements. The characteristics of AGM batteries are per manufacturer literature:

- They are not vented and are maintenance free.
- They produce relatively little hydrogen, but still must have some ventilation.
- They use much less electrolyte (battery acid), are considered “Non-spillable”, and can be shipped “HAZMAT Exempt by any means”.

There are three typical deep-discharge lead acid battery types; flooded, gel, and AGM. There are advantages and disadvantages to each type (Table 2).

Table 2
Advantages and disadvantages of three types of deep discharge batteries.

	Flooded	Gel	AGM
ADVANTAGES	Lowest cost	Longer life	No HAZMAT transport requirements
			Resistant to overcharging problems
DISADVANTAGES	Spillage danger	Overcharging can “fry” the battery	More costly
	Vapor discharge		Fewer cycles

According to Trojan Battery Company (the largest manufacturer of deep-cycle batteries and which manufactures all three battery types), deep-cycle flooded batteries have the lowest cost, provide the most cost-effective storage solution, and “are very versatile and should be the first choice for renewable energy systems where maintenance can be carried out and ventilation is available.” Proper maintenance is critical, especially keeping the hydrogen production well ventilated and adding distilled water to keep the plates submerged on a regular basis.
[\[http://www.trojanbatteryre.com/Tech_Support/ComparingFlood2VRLA.html\]](http://www.trojanbatteryre.com/Tech_Support/ComparingFlood2VRLA.html).

Gel-type batteries have a higher cost but offer longer life. They are, however, more vulnerable to damage from overcharging.

The AGM battery type, while the most expensive, is considered by many to be the most compatible with residential applications because of greater safety and fewer maintenance requirements. Furthermore, there is less risk of damaging AGM batteries compared to flooded or gel types from overcharging. Nevertheless, the homeowner must still take a number of battery maintenance steps to achieve good battery life, even with the AGM batteries.

The battery bank nominal capacity was 14.64 kWh. The price paid for these 8 batteries was \$2638. The batteries were placed in an enclosure separate from other PV system components and vented to the room using a muffin fan.

2.3 Solar Heat Pump

The solar heat pump system consists of a Fujitsu 18RLXFW 1.5-ton mini-split heat pump, 8 solar panels (250 W x 8 = 2000 W nominal capacity), 8 batteries, a charge controller, and an inverter. The batteries have total storage capacity of 14.64 kWh. However, only about 6.5 kWh of storage was available in the typical daily operational range of 45% to 90% SOC (state of charge represents the amount of energy stored in the batteries at a given time compared to the maximum amount that can be stored in the batteries). In order to enhance control of the heat pump, a timer with relay was installed to activate or deactivate the inverter power (to the mini-split) to prevent short-cycling of the mini-split heat pump and provide extended periods for solar charging of the batteries. The timer was typically set to shut off inverter power to the mini-split for the period from 7 AM to 1 PM during the cooling season, allowing the battery bank the opportunity to reach substantially full charge by the time the mini-split would start operation at 1 PM. Later in the experiments, when the size of the battery bank was cut in half (from 8 to 4 batteries) to examine an alternative system configurations, power to the mini-split was initiated earlier so that the system was typically starting at about 9 AM. During the heating season, several different timer schedules were used.

A relay was also installed which would allow transfer of the mini-split from the inverter (solar power) to utility grid power. This configuration, when selected, would permit the mini-split to continue to operate for the remainder of the day on the utility grid after the solar resource had been exhausted. This has the advantage that the homeowner could then use the high efficiency mini-split to displace much of the space conditioning that would normally be done by the central system. This option would be available to the homeowner only if the installed solar heat pump system used an ac mini-split. If a dc-powered mini-split were installed, there would be no option to run the mini-split off of the utility grid.

2.4 Three Experimental Configurations

Three experimental configurations were examined.

1. BASELINE OPERATION

- a. Cooling season; the mini-split was operated (enabled) with power from the inverter for up to 18 hours per day from 1 PM till 7 AM, depending upon whether there was enough PV power available for the entire period. The 5-ton central heat pump was operated for the hours of 7 AM till 1 PM, plus any additional hours during which the solar power was no longer available. This 7 AM to 1 PM period was also a period in which the batteries could be charged from approximately 45% SOC to approximately 90% SOC (assuming bright sun but less if the day had more cloud cover).
- b. Heating season; the mini-split was operated (enabled) with power from the inverter for up to 19 hours per day from 5:30 AM till 12:30 AM (with some variations prior to settling on this schedule). Actual solar powered operation time, as was also true for cooling, depended upon whether there was enough PV power available for the entire

period. The 5-ton central heat pump was operated for the hours of 12:30 AM till 5:30 AM, plus any additional hours during which the solar power was depleted. The period of actual operation varied depending upon the amount of solar radiation and outdoor temperature (colder days created more heating load and earlier heat pump shut-down). Charging of the batteries from approximately 45% SOC to approximately 90% SOC (assuming bright sun and less if more cloudy) would occur during the period of sun-up to sun-down since there would typically be limited heating load during the sunny hours of the day, especially after 10 AM.

2. 100% MINI-SPLIT OPERATION

- a. Cooling season; in this configuration, the operation was identical to that of the BASELINE cooling experiments except that the mini-split system would switch over to the FPL grid and continue to operate in place of the central 5-ton system.
- b. Heating season; in this configuration, the operation was identical to that of the BASELINE heating experiments except that the mini-split system would switch over to the FPL grid and continue to operate in place of the central 5-ton system.

3. 100% 5-TON OPERATION

- a. Cooling season; generally once every 5 to 10 days, the batteries were allowed to go through their full charging cycle (BULK, ABSORB, and FLOAT). To enable this full charging cycle, the mini-split was disconnected from the solar/batteries/inverter. In most cases, the 5-ton heat pump was operated (more specifically, enabled) 24 hours per day during those battery full-charge periods.
- b. Heating season; generally it was not necessary to force the mini-split off in order to allow the batteries to go through their full charging cycle (BULK, ABSORB, and FLOAT), so therefore it was unnecessary to go into 100% 5-ton mode. The reason this was different from the cooling season is that during normal operation heating would typically only last for 3 to 5 days at a time, after which the batteries could then naturally go to full charge.

The experiments described above were carried out over a 12-month period. Data was collected for both the cooling and heating seasons in 15-minute time increments and stored on the FSEC central computer system.

3. SOLAR HEAT PUMP SYSTEM DESCRIPTION AND OBSERVATIONS

A number of general observations can be made regarding the solar heat pump system which consists of the mini-split heat pump plus photovoltaic panels, charge controller, batteries, and inverter.

3.1 The Mini-split Heat Pump

The Fujitsu 18RLXFW mini-split heat pump has a nominal capacity of 1.5-tons. It consists of an outdoor unit (compressor and condenser coils) and an indoor fan coil unit (FCU). The FCU was located outdoors along the south wall of the large central room. It has oscillating vanes to throw air side to side. Horizontal vanes adjust themselves to throw air upward during cooling operation and downward during heating operation.

This heat pump has a SEER rating of 19.2 and HSPF (Heating Season Performance Factor) of 10.0. It is a variable capacity system. While it is nominally rated at 18,000 Btu/h for cooling and 21,600 Btu/h for heating, its capacity can vary from 7000 to 23,000 Btu/h in cooling and 7000 to 29,000 Btu/h in heating. Therefore, maximum cooling and heating capacities are 28% and 34% greater than the nominal rating. During much of the year, the mini-split does not cycle off but rather modulates its cooling or heating capacity in response to a temperature differential between room temperature (as detected by the return air sensor) and the space temperature thermostat set-point. So, unlike a fixed-capacity system which will cycle on and off throughout the day, the mini-split may remain on continuously for 24 hours per day on typical warm to hot summer days. During cooler spring and fall days, however, the mini-split (in cooling mode) is likely to cycle on and off during portions of the day, especially during the cooler overnight hours.

The standard mini-split thermostat is a hand-held unit that looks a lot like a TV remote and can be located anywhere in the room. It operates in tandem with a temperature sensor located inside the return air plenum of the FCU. The thermostat location, therefore, does not impact space temperature control since the sensor detecting room temperature is located in the return plenum. The system can also be installed with a more standard, wall-mounted thermostat (connected by wire to the mini-split) which we purchased and installed. Contrary to our expectations, however, it provided little additional functionality and actually used the same temperature sensor located in the return plenum of the FCU. Because the thermostat sensor is not (under normal circumstance) directly exposed to the room air, the FCU cycles the fan on (if the mini-split has cycled off) on a regular basis (15-20 times per hour) in order to sample room conditions at a low fan speed (at about 50% of normal low-speed operation).

During periods of low cooling load (such as on mild spring or autumn days), when the cooling load falls below 7000 Btu/h, the mini-split will cycle on and off. In order to better control the system, the research team pulled the temperature sensor out (about 15 inches out) of the FCU return so it would more readily detect room space temperature. With the sensor now located outside of the FCU, it would no longer in theory be necessary for the FCU fan to cycle on to detect room temperature. However, even though the temperature sensor was relocated outside of the FCU, the

research team was unable to disable the cycling of the FCU fan, so this fan cycling continued to operate during all periods when the FCU was off.

This fan cycling has an important implication for indoor relative humidity (RH) control, for periods of low cooling load, such as during warm/humid days in autumn. With the system off, the fan cycles on for about 25-30% of the time (at a low fan speed) sampling room air temperature, but in doing this it evaporates moisture from the coil and drain pan whenever the fan moves air through the FCU. The evaporated moisture returns to the room increasing indoor RH. In actual practice, however, this fan cycling does not represent a large problem. Because the mini-split can operate continuously down to as little as 7000 Btu/h, there are few daytime hours during the cooling season when this fan cycling (with no compressor operation; so the coil is warm) occurs. This most commonly occurs during nighttime periods during the autumn and spring seasons. It can, however, reduce the ability of the mini-split to control indoor RH during those periods, because of this moisture evaporation.

The Fujitsu mini-split has two modes of operation; 1) Standard and 2) Economy. In Standard cooling mode, the supply air temperature is about 46°F when the return air is about 75°F. This 29°F temperature drop is unusually large for an A/C system. The cold coil (and cold supply air) yields excellent indoor RH control, with typical RH levels being 39-42% in the lab building (it is an unoccupied building but had water vapor added to the space at a rate of about 8 pounds/day). In Economy mode, the compressor cooling capacity is reduced much of the time and the supply air was delivered at a temperature of about 52°F. This supply air temperature is still sufficiently cold to provide good RH control, typically about 46% indoor RH on hot and humid summer days. It was found that Economy mode was a much better choice for operation with the solar system (in terms of efficiency), allowing the system to operate considerably more efficiently and allowing it to operate up to 70% more hours on the available solar energy.

3.2. Inverter and Charge Controller

Based on the findings of this research effort, it is recommended that an inverter for this type of stand-alone system be bimodal, that is having the capability to also send power to the electric utility grid. Converting this system to bimodal would make the overall yearly solar heat pump system operation more energy efficient because excess PV power that is not needed by the mini-split heat pump on mild autumn, winter, and spring days could then be put to good use (that is, the excess power could be sent back to the grid). As it was, there were a significant number of days when a significant portion of the available solar could not be used, because of limited cooling or heating load on the building.

3.3 Batteries

Batteries are a key element of a stand-alone system or even of a grid-integrated system that can operate in a stand-alone fashion when the utility grid goes down.

3.3.1 Battery State of Charge and System Cycling

As indicated earlier, SOC represents the amount of energy stored in the batteries at a given time compared to the maximum amount that can be stored in the batteries. SOC then varies from 0% to 100%. It is the nature of batteries in general and these batteries in specific that the full range of stored energy is not available for use on each cycle. To be more accurate, it is not so much that the full stored energy is not available, but rather that draining the batteries below a specific level on a repeated basis will shorten the life of the batteries. The manufacturer recommends that it “is always good to have twice the battery capacity that an application requires. This will promote long battery life and also reduce the amount of recharge time” (source: Sun Xtender product brochure document No. 6-0103, Rev 4/09).

Therefore, during the cooling season, the typical daily cycle would take the batteries from about 90-95% SOC down to about 45% SOC. Thus only 45-50% of the full battery capacity was being regularly used.

It might seem surprising that 90-95% was the typical upper level SOC instead of 100%. This occurs for a practical reason related to the way that (the rate at which) the batteries are charged. There are three modes of charging; BULK, ABSORB, and FLOAT. Most of the time, charging occurs in BULK mode. During our experiments, it was found that in BULK mode, all of the available PV energy could be delivered into the batteries. This is a rate issue. The amount of PV power being generated under full sun could be delivered into the batteries while in BULK mode. (It is also relevant to note that during the cooling season, a significant portion of the PV power is shunted directly to the inverter and on to the mini-split, bypassing the batteries. During the heating season, by contrast, most of the PV power delivered to the mini-split had to be stored in the batteries during sunny hours and then delivered to the mini-split during the overnight and early morning hours.)

However, as SOC approaches 85-90%, the batteries go into ABSORB and then FLOAT modes, where anywhere from 50% to 95% of the available solar is discarded as the batteries go through their final stages of charging. The reason that 50% to 95% of the available solar is thrown away during ABSORB and FLOAT modes, respectively, is because the rate at which energy is delivered into the batteries is substantially slowed (for ABSORB mode) and greatly slowed (for FLOAT mode). This is one of several ways in which batteries are the weak link in the solar heat pump system, namely that it is necessary to fully charge the batteries on a regular basis and when doing so, a significant portion of the solar is thrown away.

Periodic full charging is important to the health of the batteries. The manufacturer states that it “is recommended that batteries be recharged to 100% at least every 5-10 cycles”, which for this application means once every 5 to 10 days. While we might have achieved 90-95% SOC on most sunny days, the research team also took steps to push SOC to 100% every 10 days or so.

- During the period from late-October through early May, getting the batteries to 100% SOC on a regular basis is typically not a problem for two reasons. First, periods of substantial heating are intermittent, and the milder days in-between require less heating power and

therefore commonly allow the batteries to reach 100% charge. Second, during the warmer periods of November through April, when some cooling is needed, there are intermittent days with smaller cooling loads which allow for full battery charge even while the mini-split system operates a portion of the time.

- During the period of May through late-October (the primary cooling season), more attention needs to be paid to intermittently achieving 100% SOC. Throughout most of this period, all of the available PV power can be (will be) consumed by space cooling (in a properly sized solar heat pump system), and so without intervention, the battery would rarely reach 100% SOC. It becomes necessary, therefore, to interrupt the normal system operation and force the charging process to go into ABSORB and then FLOAT modes, thus achieving 100% SOC. This forced intervention results in periods of discarded solar energy, since the ABSORB and FLOAT modes necessitate throwing away significant amounts of solar energy during those portions of the charging cycle. Therefore, good battery maintenance practice requires some scheduling of battery full-charge periods and by necessity some waste of solar energy.
 - In our experiments, the research team dealt with this during the primary cooling season by shutting down the mini-split for a day once every 7 to 10 days and allowing the batteries to be charged to 100% SOC while the central 5-ton A/C system was used to condition the space.
 - In our typical daily operation schedule, we shut down the mini-split from 7 AM till 1 PM (by means of a relay controlled by a timer), during which time the battery would often go from about 45% SOC to about 90% SOC.
 - An alternative approach to achieving 100% SOC could also be implemented, which would use power from the electric utility grid to charge the batteries overnight. This approach might provide some advantages to the electric utility since it would allow it to sell electricity to the customer during night hours (perhaps controlled by the “On-Call” system) when excess capacity is often available, thus shifting system demand from daytime hours to nighttime hours. The FSEC research team did not explore this option and some experimentation would likely be needed to optimize the scheduling of these charging patterns.
- Once the batteries reach about 85-90% SOC, they go into the ABSORB cycle which typically operates for 2 hours (this length of time is user selectable), then goes into FLOAT for a period of about 2 hours.
- It was not clear whether the batteries need to get to the full 100% SOC to maintain good battery health, or whether getting to say 98% SOC achieves essentially the same outcome.

It should be noted that the inverter/charge controller used in these experiments has a SOC indicator, but its accuracy is sufficiently poor that the user knows very little about the actual SOC. Therefore, throughout the entire project, the research team did not know actual SOC.

There is an exception to this statement. SOC can be accurately known when the battery is in “resting” state that is when no energy is being delivered into the batteries or being drawn from the batteries. During the hotter days of the year (high of say 84°F or above), battery energy (for the 8-battery bank) is typically depleted sometime during the night, often between 12 AM and 4 AM, at which time the mini-split turns off. During the period between mini-split turn off and sunrise, no power flows into or out of the battery bank, and the batteries are therefore resting. A battery voltage reading taken when the batteries are resting provides an accurate reading of SOC. Data provided by the battery manufacturer (Figure 6) allows an accurate determination of SOC based on battery voltage.

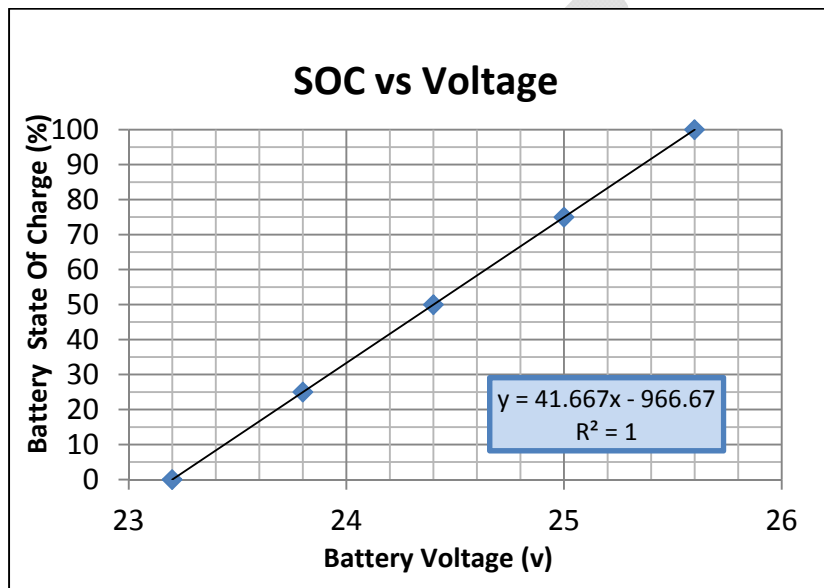


Figure 6. Battery SOC versus Battery Resting Voltage (data from battery manufacturer).

3.3.2 Cooling and Heating Season Battery Requirements

The eight 6-volt deep-discharge batteries used in these experiments were configured in two parallel banks of four batteries in series, creating a nominal 24V DC power system. Each battery is rated at 305 amp-hours of energy storage, which converts to 1.83 kWh. The 8-battery bank then has a total rated storage capacity of 14.64 kWh. Since the batteries were exercised on a daily basis typically across a 45% to 90% SOC range, the effective battery storage capacity was about 6.6 kWh. Total power produced by the nominal 2 kW PV array on a typical summer day is on the order of 8 kWh, or about 20% more than what the batteries can hold across the 45% to 90% SOC range. On the other hand, since the mini-split typically consumes about 4 kWh during the period from 1 PM to sunset (summer weather), the eight batteries therefore have more than sufficient capacity for the portion that needs to be carried forward into the evening and night hours.

During the cooling season, the time periods when cooling is required and the PV system produces power are closely matched, with a typical 3 hour lag. Peak power from the PV system typically occurs about 1:30 PM (DST) while the peak cooling load occurs about 4:30 PM (DST). As a result, much of the mini-split power consumption occurs during the hours of PV energy production.

Consequently, it is not necessary to carry a large portion of the PV energy into the night. Therefore, the amount of PV energy that must be carried forward (by means of battery storage) during the cooling season is smaller compared to the storage need for heating. This has important design implications for whether this stand-alone system is optimized for the space-cooling season or designed for both cooling and heating. If designed for space cooling only (or for cooling as the primary task), the battery bank could be somewhat smaller.

During the heating season, by contrast, relatively little of the PV power is typically used by the mini-split during hours when the sun is shining. On a typical cold Florida winter day (low 40°F and high 60°F), most of the heating load occurs during the hours of 10 PM and 10 AM. During the other 12 hours of the day, the heating system would generally be off or operating only intermittently till after sundown. As a consequence, perhaps 80% or more of the PV energy to be used for space heating must be stored in the batteries and used 8 to 12 hours later. Therefore, the battery bank must be on the order of 2 or 3 times as large for optimal heating season performance.

3.3.3 Maintenance Issues and Battery Degradation

One important characteristic of stand-alone systems is that they employ batteries for energy storage, and batteries require maintenance. Therefore, when trying to optimize energy savings, battery life and health must be taken into account. While the AGM-type batteries do not require water-adding maintenance, they do require following of a regular charging schedule (e.g., taking SOC to 100% once every 10 days or less). There is a tension, then, between using as much of the available solar energy (produced by the PV panels) as possible while still protecting the life of the batteries. This means letting cooling and heating operate as many hours as possible while avoiding draining the batteries below 45% SOC on a frequent basis but still achieving 100% SOC on a regular basis (once every 7-10 days).

The Sun Xtender PVX-3050T owner's manual states that "For maximum life, batteries must be periodically recharged to 100% capacity. Continually recharging to less than 100% may result in premature capacity loss. It is recommended that batteries be recharged to 100% at least every 5-10 cycles." For this application, this means that the batteries must be charged to 100% once every 5 to 10 days. During the approximately 6 months of substantial cooling loads, this means that the mini-split heat pump must be disabled for a full day (or a large fraction of a day) at least once every 10 days so that the batteries can go through their full charging cycle, which includes BULK, ABSORB, and FLOAT. During other portions of the year, cooling and heating loads are sufficiently small or intermittent so that the batteries are typically charged to 100% every few days or week as a result of normal weather patterns.

Alternatively, the batteries could be brought to 100% SOC during the overnight hours using the utility grid, once a week, or so. On the days when overnight charging occurs, it would be preferable to disable the timer which locks out operation of the mini-split till 1 PM. On the overnight charging days, the mini-split could be operated from the grid for the period that the batteries are being charged.

Additionally, once every 6 to 12 months the bank of batteries should be “equalized”, which is another form of required maintenance. This involves applying a steady charge to the batteries through the inverter for a period of 8 hours. To achieve this, a 240V source must be provided to the inverter while solar production is curtailed.

With regular use, battery capacity diminishes over time, sometimes at different rates per cell within the battery, resulting in a shortened battery life. In a bank of batteries, when these voltages differ too much from battery to battery, each battery can take on a unique charge/discharge profile. As a result, some of the batteries in the bank become overcharged while others are undercharged. To bring these battery voltages back to balance, an equalization charge may be required once every 6 to 12 months. Equalization is a process during which the entire bank of batteries is overcharged for a period of time to bring the voltage of each battery in the bank and each cell within each battery to the same value. The desired outcome from an equalization charge would be nearly identical battery charge/discharge characteristics for all batteries and battery cells.

It is important to note that equalization is somewhat damaging to the batteries in that some electrolyte is lost in the charge process. In a sealed AGM battery, such as the PVX-3050T, the lost electrolyte cannot be replaced so equalization is only used when substantially lower battery capacity is detected.

By March 2013 (after about 8 months of system operation), battery performance for the as-tested system showed signs of deterioration. The primary indicator of this battery degradation was a sharp downward spike in battery voltage after battery voltage had declined to about 23.8V, with this occurring on a daily basis. After an 8-hour equalization was implemented, no improvement in battery performance could be detected.

By early June 2013, some of the batteries had deteriorated to the point where they were causing sudden dips in voltage of the 8-battery bank on a nightly basis. In this new battery-failure-induced pattern, battery voltage would decline slowly into the nighttime hours, and then suddenly a plunge in battery voltage would occur, cutting out the inverter which then causes a potentially premature shutdown of the mini-split heat pump for the night.

Tracking of voltage of individual batteries over a several day period identified that 3 of the 8 batteries were experiencing more rapid voltage drop. At that point, the 4 best-performing batteries were identified, and these were assembled into a four-battery bank. From June 6 through July 15, 2013, the system was operated with only 4 batteries instead of the original 8 batteries. This allowed us to evaluate the performance of the solar heat pump system with the smaller bank of batteries.

The reduction in battery capacity caused a significant but not critical reduction in the ability of the system to deliver PV power to the task of space cooling, because (as discussed earlier) the batteries did not have to carry as much PV-power forward. If we had attempted to operate the system with 4 batteries during heating weather on a regular basis, the outcome would have been less satisfactory. In fact, operation of the solar heat pump system with 4 batteries had been

implemented early in the winter season, and it was quickly identified that a larger battery bank (8 batteries) was crucial for the heating season.

By July 15, 2013, even the 4 batteries which had performed the best began to deteriorate badly. This bank of 4 batteries started to cycle the inverter off on the order of every 15 minutes (due to collapsing battery voltage). As a result, the mini-split was, by the second week of July, short-cycling in a manner that would diminish the operational efficiency of the system and perhaps endanger the mini-split compressor.

In order to better understand normal battery operation and the problems occurring with the batteries, the research team requested answers to a number of questions from the manufacturer.

Q: What is the typical battery SOC at the point when it goes into ABSORB mode and then again the SOC at the point when it goes into FLOAT mode.

A: The SOC at which charging goes from BULK to ABSORB depends upon V_{abs} (voltage at which the batteries go into Absorption mode) which in turn depends upon the net charging rate (net charging rate = rate of charging [ROC] minus rate of discharge [ROD]). SOC at V_{abs} can range from 80% up to about 95% depending upon net charging current. Higher net charging current gives lower SOC at V_{abs} . Because our charging rate was continuously variable (because of varying energy input from solar and varying discharge to the variable capacity heat pump), SOC at V_{abs} was in continuous flux.

Q: “How often does the battery need to be fully charged to 100% SOC, in order to maintain the batteries health? Can it be charged to less than 100% - say 95% - and achieve the same health?”

A: It should be charged to 100% (not 95% or even 98%) every 7-10 days, otherwise the plates will become sulfated.

Q: Can you explain why our batteries died at the end of 12 months of service.

A: Based on their understanding of how we used the batteries, they concluded that the research team “chronically undercharged the batteries, leading to premature sulfation of the cells”.

Q: Is there any way of conditioning the batteries in their current state that might help restore the batteries?

A: Periodic “conditioning charge” per Section 5.5 of the Manufacturer’s Technical Manual is recommended. You can implement a conditioning charge to equalize the batteries in each string? You might consider a voltage balancer, such as:
<http://cpc.farnell.com/camdenboss/ceq6a/balancer-battery-6v/dp/BT05600>.

Note that the research team has continued to perform some remediation work on the batteries with preliminary indications of some success in restoring a portion of the battery functionality. No conclusive outcome can be reported at this time.

3.3.4 Conclusions Regarding the Battery Bank

Batteries are expensive. The 8 AGM batteries with total capacity of 14.64 kWh cost nearly the same as the 8 PV panels, which had nominal 2 kW electrical energy production rating. Since the original purchase of the heat pump system components in May 2012, the price for PV panels has declined by about 30% while the cost of batteries has remained fairly stable.

Not only are the batteries expensive, they appear to represent a weak link in the solar heat pump system. By the end of 12 months, the 8 batteries had reached a point where they were not functioning effectively. Members of the research team believe that reasonable steps were taken to follow the manufacturer's instructions regarding fully charging the batteries every 7-10 days and taking the 8-battery bank through an equalization process once every 6 to 12 months (as recommended). Nevertheless, the batteries appear to have reached, or nearly reached, the end of their life by July 2013. It seems unlikely that most homeowners will work as hard as the research team did to comply with battery maintenance recommendations.

Since battery cost and life-expectancy have been identified as a major weak link in this solar heat pump system, an alternative (optimized with bimodal inverter) solar heat pump system design is presented later in this report that may go a long way toward extending the life of the batteries and improving the overall functionality and cost-effectiveness of the system. Battery life would be greatly extended by reducing the range of SOC operation to perhaps 80-85% under most day-to-day operation. Power from the grid would prevent the SOC from falling below 80%, while excess energy would be sold to the grid once SOC reached 85%. Periodic charging of the batteries to 100% SOC would occur from the grid. See Section 8.4 for more details about the proposed optimized bimodal solar heat pump system.

3.4 Typical Operation of the Solar Heat Pump System

Tables 3 and 4 illustrate environmental conditions and solar heat pump operation for a mild cooling day and a hot cooling day, respectively. Throughout much of the cooling season, the project research team employed a timer to cut-out mini-split operation for the period 7 AM to 1 PM (DST).

- In Table 4 it can be seen that the PV/battery system provides sufficient power to operate the mini-split for all hours of the day (18 hours) except for the 6-hour period from 7 AM to 1 PM (DST). From this table, the following operating characteristics can be observed. During the hours of 9 AM to 1 PM, the PV system is charging the batteries at a rate of about 1265 W, taking them from about 45% to about 75% SOC during this period (this period has essentially full sun). Battery voltage rises during this six hour period from 23.4 V to 28.1 V.
- For the remainder of the bright sunlight hours (from 1 PM to 6 PM), the PV mini-split draws about 580 W (in Economy mode) while the PV system delivers an average of about 880 W

over a five-hour period, leaving 300 W net power to go to the batteries. The net charging rate of about 300 W to the batteries for this six-hour period would then bring the SOC up to perhaps 85-90%.

Table 3

Data for a warm and sunny spring day (April 11, 2013) showing outdoor and indoor temperatures, solar radiation, PV system energy output (PVw), mini-split and central system energy consumption, and mini-split sensible cooling for the solar heat pump with 8-batteries and Economy mode. Time is DST.

Day	Hour	Toutdoors	Tindoors	Solar	PVw	PVw/	Battery	Mini-split	Mini-split	Mini-split	Mini-split	Central
		°F	°F	W/m ²	Wh/h	solar (ratio)	voltage V	heat pump Wh/15-min	heat pump Wh/h	runtime (%)	sensible cooling Btu/h	heat pump Wh/h
2013101	1:00	74.2	74.9	0	0	0	24.6	93	373	95%	6807	0
2013101	2:00	74.2	74.8	0	0	0	24.6	86	342	94%	6610	0
2013101	3:00	73.9	74.8	0	0	0	24.5	82	328	85%	5943	0
2013101	4:00	73.2	74.7	0	0	0	24.5	72	288	83%	5678	0
2013101	5:00	73.1	74.7	0	0	0	24.4	66	264	76%	5115	0
2013101	6:00	73.0	74.8	0	0	0	24.3	67	268	76%	4902	0
2013101	7:00	72.8	74.5	0	0	0	24.3	45	180	63%	3581	0
2013101	8:00	73.1	74.6	41	54	1.67	24.7	0	0	0%	0	810
2013101	9:00	75.1	75.2	172	364	2.24	25.3	0	0	0%	0	740
2013101	10:00	77.5	75.7	517	969	1.88	25.9	0	0	0%	0	1010
2013101	11:00	78.5	74.8	673	1217	1.81	26.3	0	0	0%	0	1430
2013101	12:00	80.0	75.7	887	1524	1.72	27.1	0	0	0%	0	1130
2013101	13:00	79.8	74.8	991	1350	1.37	28.1	0	0	0%	0	1510
2013101	14:00	80.9	76.3	1027	1320	1.29	28.1	129	517	94%	6504	0
2013101	15:00	80.2	76.2	974	808	0.83	26.4	145	580	100%	7285	0
2013101	16:00	79.9	76.4	817	784	0.96	26.2	147	588	100%	7301	0
2013101	17:00	79.2	76.8	632	772	1.25	26.2	145	579	100%	7359	0
2013101	18:00	78.3	76.8	409	705	1.73	26.0	150	598	100%	7503	0
2013101	19:00	76.8	76.6	171	269	1.56	25.4	141	565	100%	7419	0
2013101	20:00	75.4	76.1	34	24	1.40	25.2	132	529	100%	7469	0
2013101	21:00	75.3	75.8	0	0	0.0	25.0	129	514	100%	7638	0
2013101	22:00	75.3	75.5	0	0	0.0	25.0	124	496	100%	7739	0
2013101	23:00	75.1	75.3	0	0	0.0	24.8	120	478	100%	7865	0
2013102	0:00	75.1	75.1	0	0	0.0	24.7	108	431	100%	7701	0
AVG		76.2	75.4	306.0	423.3	0.8	25.5	82.5	329.9			276.3

As can be seen in Table 3, indoor temperature tends to be cooler during nighttime hours and then goes to a slightly warmer temperature for 7 AM to 1 PM when the 5-ton central system is operating. Subsequently, indoor temperature rises substantially for the time period of 1 PM to 7 PM with mini-split operation, and then declines overnight. What explains this pattern of indoor temperature variation?

First, during the six-hour period from 7 AM to 1 PM, the 5-ton central system provides all of the space conditioning and its thermostat is set to about 0.5 to 1°F warmer than the mini-split. So the 7 AM to 1 PM period averages about 0.5°F warmer than that produced by the mini-split during the nighttime hours. Second, the mini-split allows indoor temperature to drift upward during periods when the cooling load increases. This can be seen in Table 3 during the hours from 1 PM to 7 PM where the mini-split operation allows average temperature to rise to 76.6°F, or about 1.9°F warmer than during night hours.

The explanation for this mini-split induced temperature variation is illustrated in Figure 7. This figure presents indoor temperature in the central zone (where the mini-split thermostat is located) and in the building as a whole (4-room average) during a 7-day period when only the mini-split was operating. To understand why the mini-split produces this indoor temperature pattern, it is necessary to understand how the mini-split varies its capacity (recall that it is a variable capacity system, with capacity ranging from 7000 to 23,000 Btu/h). The mini-split increases its cooling capacity based on deviation of space temperature from the set point. A large temperature deviation is required before the mini-split will push its capacity to higher levels.

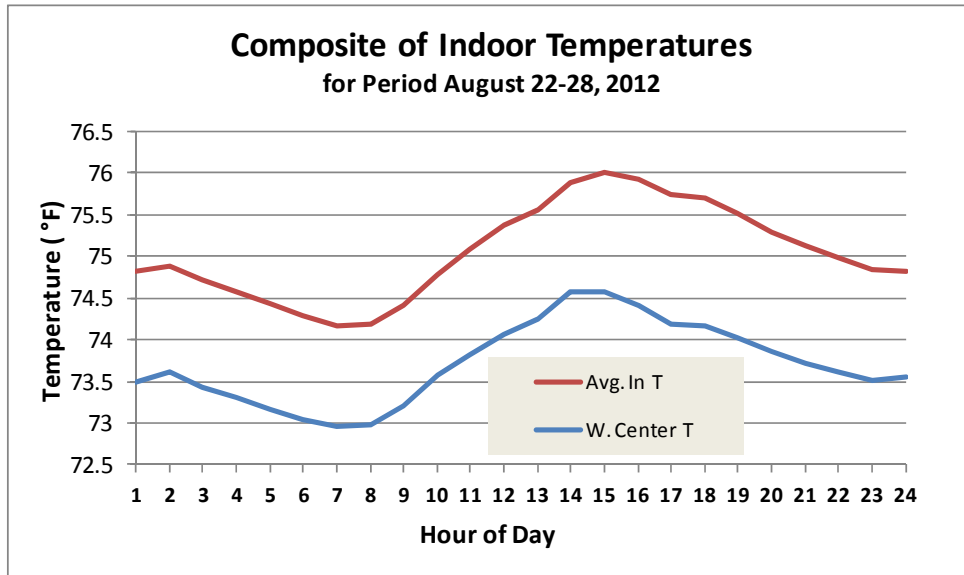


Figure 7. Twenty-four hour space temperature profiles in the Building Science Lab with only the mini-split conditioning the space. Temperature is shown for the central zone (blue line) and 4-room average (red line). The mini-split is powered on these particular days by PV solar for about half the day and from the utility grid for the remainder of the day, while the central ducted system does not operate during the entire 7-day period. It can be seen that room temperature rises in direct proportion to the cooling load.

The 5-ton central system has a SEER rating of approximately 11 while the Fujitsu mini-split has a SEER rating of 19.2. Referring back to Table 3, the relative performance of the mini-split and the central ducted 5-ton system can be seen for the three hours of 10 AM to 1 PM (79.4°F outdoors and 75.1°F indoors) versus the five hours of 1 PM to 6 PM (79.7°F outdoors and 76.3°F indoors). The central, ducted system consumes an average of 1357 W compared to 572 W for the mini-split for cooling loads that are approximately comparable, indicating savings of about 58% by using the mini-split. This suggests that the central system in the Building Science Lab has an effective SEER value of 8.1 after figuring in approximately 26% losses due to the attic duct system (note: the attic temperature ranges, on average, from 80°F to 92°F for all days with average outdoor temperature of 77°F and higher.) Typical cooling season operating patterns can be seen in Tables 3 and 4, for a mild cooling day and a hot and humid day, respectively.

Table 3 has data from a warm (but not hot) and very sunny spring day. The PV system combined with 8 batteries and operating in Economy mode provides sufficient energy to operate the solar heat pump (in cooling mode) for the entire 24-hour period, except for the 7 AM to 1 PM period when a timer is used to intentionally disable inverter power to the mini-split (the batteries are allowed to charge substantially during that 7 AM to 1 PM period). Some additional solar heat pump characteristics can also be observed.

1. Room temperature rises from about 74.5°F just before sunrise and rises to a high of 76.8°F in the late afternoon, a rise of 2.3°F from low to high.
2. The mini-split heat pump draws a daily average of 330 W, or 119% of the power being drawn by the central heat pump for the average hour.
3. Starting about noon, the PV system charging starts to decline as the system moves into the ABSORB mode, where some of the solar must be discarded as the permitted charging rate is lowered (by the charge controller) below the rate of the entering solar resource.
 - a. This can be observed in the column titled PVw/solar (ratio).
 - b. A ratio of 1.8 or higher indicates that charging is in BULK mode.
 - c. During the hours of 12 (noon) to 5 PM, this ratio declines from about 1.8 to as low as 0.83, indicating that the batteries have dropped into ABSORB mode and as much as 55% of the available solar is discarded during specific hours.
4. Battery voltage declines overnight to a low of 24.3 V, and then rises throughout the sunlight hours largely in proportion to the intensity of the solar radiation.
5. It can be seen that the mini-split operates continuously from 1 PM through midnight (see mini-split runtime column) and then cycles off a number of times during the overnight hours.
6. While the mini-split has a nominal cooling capacity of 18,000 Btu/h which would correspond to about 13,000 Btu/h of sensible cooling (this cooling is associated with lowering the air temperature), throughout much of the day. It can be seen that the sensible capacity runs no higher than about 7800 Btu/h, or 60% of full nominal sensible capacity. If the system were operated in Standard rather than Economy mode, sensible capacity would increase significantly.
7. It is interesting that while the central system operates for only 25% of the day (6 hours), it consumes 45% of the day's total space cooling energy use. There are two primary reasons for the relative energy consumption discrepancy.
 - a. The mini-split heat pump consumes about 58% less energy per unit of cooling compared to the 5-ton central system in the BS Lab, including distribution system losses.
 - b. The thermostat controlling the 5-ton system maintains a space temperature of about 75.2°F while the mini-split allows room temperature to rise to about 76.8°F during the hotter hours of the day. Therefore, the 5-ton unit is actually meeting a larger space cooling load during the hours that it is operating.

In a second example, Table 4 shows data from a hot and very sunny summer day (July 8, 2013). The mini-split was also operating in Economy mode, but it was operating with a reduced battery bank (4 batteries) and the timer (controlling the inverter) disabled power to the mini-split for only one hour from 7 AM to 8 AM. A number of differences can be observed in the system operating characteristics as a result of the hotter temperatures, changed timer schedule, and 4-battery storage. Solar power is sufficient to operate the solar heat pump (in cooling mode) for just over 11 hours on this day. Some additional solar heat pump characteristics can also be observed.

1. Room temperature rises from about 75.0°F just before sunrise to a high of 77.3°F in the late afternoon, a similar pattern to that seen in Table 4.
2. The mini-split heat pump draws an average of 290 W, or 23% of the power being drawn by the central heat pump for the average hour.

Table 4

Data for a hot and sunny summer day (July 8, 2013) showing outdoor and indoor temperatures, solar radiation, PV system energy output (PVw), mini-split and central system energy consumption, and mini-split sensible cooling for the solar heat pump with 4-batteries and Economy mode. Time is DST.

Day	Hour	Toutdoors	Tindoors	Solar W/m ²	Battery voltage V	PVw Wh/h	PVw/ solar (ratio)	Mini-split heat pump Wh/15-min	Mini-split heat pump Wh/h	Mini-split runtime (%)	Mini-split sensible cooling Btu/h	Central heat pump Wh/h
		°F	°F									
2013189	1:00	79.4	75.0	0	24.7	0	0	0	0	0%	0	1850
2013189	2:00	79.3	75.0	0	24.7	0	0	0	0	0%	0	1810
2013189	3:00	78.9	75.5	0	24.7	0	0	0	0	0%	0	1540
2013189	4:00	78.5	75.1	0	24.6	0	0	0	0	0%	0	1090
2013189	5:00	78.2	74.9	0	24.6	0	0	0	0	0%	0	1670
2013189	6:00	77.9	75.5	0	24.6	0	0	0	0	0%	0	840
2013189	7:00	77.5	75.0	12	24.6	4	1.24	0	0	0%	0	1580
2013189	8:00	79.1	75.7	38	25.1	64	1.66	0	0	0%	0	820
2013189	9:00	81.7	75.5	155	25.5	199	1.40	0	0	1%	22	1780
2013189	10:00	84.7	75.8	471	25.8	854	1.80	110	442	93%	6503	800
2013189	11:00	86.4	75.7	660	26.4	1207	1.83	114	454	96%	6586	1240
2013189	12:00	87.6	75.5	795	27.5	1313	1.66	110	441	92%	6270	1060
2013189	13:00	88.6	76.0	944	28.3	1029	1.09	125	501	95%	6494	810
2013189	14:00	88.4	77.1	962	27.8	946	0.98	160	642	100%	7647	0
2013189	15:00	88.2	77.0	927	26.2	820	0.88	158	631	100%	7648	780
2013189	16:00	87.5	77.3	773	26.1	704	0.92	137	546	100%	7404	720
2013189	17:00	87.1	76.8	663	26.1	823	1.27	165	660	100%	7951	1690
2013189	18:00	86.4	76.9	456	25.6	789	1.74	197	788	100%	9086	800
2013189	19:00	85.1	77.0	229	24.9	379	1.65	207	828	100%	9619	810
2013189	20:00	82.8	76.9	36	24.4	71	1.80	201	803	100%	9754	730
2013189	21:00	81.0	77.0	0	24.4	0	0	54	216	27%	2654	1120
2013189	22:00	80.2	76.4	0	24.8	0	0	0	0	0%	0	1820
2013189	23:00	79.9	76.1	0	24.8	0	0	0	0	0%	0	2080
2013190	0:00	79.7	74.9	0	24.8	0	0	0	0	0%	0	2250
AVG		82.7	76.0	546.7	25.5	707.62	1.44	129.6	289.7			1237.1

3. Starting about 9:15 AM, battery voltage rises to about 26 V which is the level at which inverter power is restored to the mini-split. The battery charging rate starts to decline as the system moves into the ABSORB mode around 11:30 AM, where some of the solar must be discarded as the permitted charging rate is lowered below the rate of the entering solar resource. This can be observed in the column titled PVw/solar (ratio). A ratio of 1.8 or higher indicates that charging is in BULK mode and that all of the available solar is being successfully delivered into

the batteries. During the hours of 11:30 AM to 5 PM, this ratio declines from about 1.8 to as low as 0.88, indicating that as much as 50% of the available solar is being discarded during specific hours.

4. Because of the limited battery capacity (4 batteries) and the relatively large power draw (over 800 W) of the mini-split (a large power draws pulls battery voltage down more precipitously), battery voltage declines to 24.4 by 8:15 PM at which time the mini-split turns off. The mini-split remains off until battery voltage reaches 26 V around 9:15 AM the next day.
5. In spite of the much earlier mini-split shut-down, the solar heat pump operates at relatively high capacity throughout the peak cooling hours. The central heat pump meets about 30% of the space cooling load, on average, from 9 AM to 8 PM, while the solar heat pump meets about 70% of the load. However, because the central ducted system is about 58% less energy efficient than the mini-split, it uses more energy during that period than the mini-split.
6. It can be seen that the mini-split operates nearly continuously from about 9 AM through 8 PM and remains off till about 9 AM the following morning.
7. While the mini-split has a nominal cooling capacity of 18,000 Btu/h which would correspond to about 13,000 Btu/h of sensible cooling (sensible cooling is associated with lowering the air temperature), throughout much of the day, sensible capacity runs no higher than about 9750 Btu/h, or 75% of full nominal sensible capacity. The mini-split cooling output would likely increase to a higher level if the system was operated in Standard mode.

3.5 Strategies for Achieving Maximum Seasonal Energy Savings

The customer can achieve maximum cooling energy savings by operating the mini-split in Economy mode versus Standard mode, for three reasons.

1. In Economy mode, the supply air is significantly warmer, about 54°F compared to 46°F. Heat pumps operate more efficiently when they are pushing energy flows against a smaller temperature differential. In Economy mode, cooling EER (Energy Efficiency Ratio) is 34% higher compared to Standard control mode when outdoor temperature is 82°F (Figure 8). From the regression analysis equations, it can be calculated that the mini-split operates with 17.6 EER in Economy mode compared to 13.1 EER in Standard mode.
2. The fact that the supply air is about 8°F warmer means that the heat pump in Economy mode is providing proportionately less latent cooling (less water vapor removal from the room air) and is expending more of its space cooling energy on lowering room air temperature (sensible cooling). It therefore meets the thermostat setpoint sooner.
 - a. Instead of producing typical 40% indoor RH while operating in Standard control mode, it produces about 46% indoor RH while operating in Economy control mode. 40% indoor RH is significantly lower than is necessary for most applications (46% RH is sufficiently low for essentially all circumstances), and the energy used to draw the humidity down to that level is largely wasted. Humidity in the 38 - 40% range can lead to drying of skin and eyes, and can contribute to static electricity discharges.

- b. One could argue that a lower indoor RH can produce similar occupant comfort at a higher temperature, which means that the thermostat could be raised by say 1°F with the lower RH. This would, however, require some thermostat adjustment on the part of the occupants, and it is uncertain that this sort of adjustment actually occurs in real homes. Another way to say this is that in Economy mode the system is spending less of its energy on latent cooling (moisture removal) and more of its energy on lowering the space (drybulb) temperature. Since thermostats control based on room air temperature, higher equipment operating SHR leads to reduced space cooling energy use.
4. When the mini-split is in Economy mode, it draws about 600 W compared to about 1000 W in Standard mode. The relevance to system efficiency relates to how this power draw interacts with the batteries. The smaller power draw of Economy mode tends to keep the system operating for an extended period. By contrast, the larger power draw of Standard mode tends to trigger premature cut-out of the inverter. As a result, more of its operation time (when in Economy mode) will occur at night when outdoor temperatures are cooler and the system will operate more efficiently.

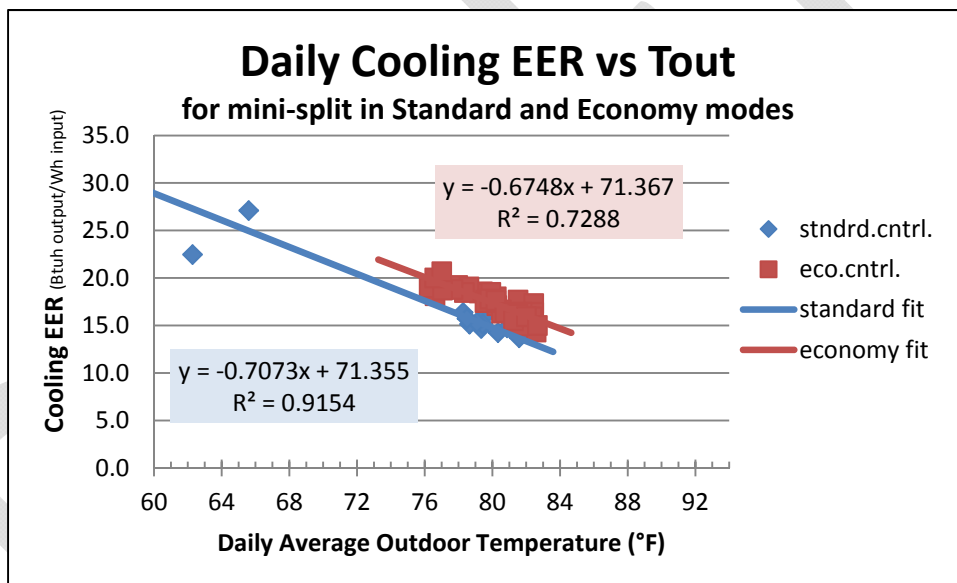


Figure 8. Monitored mini-split EER for Standard and Economy modes as a function of daily outdoor temperature with indoor temperature held constant at about 76°F.

4. COOLING SEASON ENERGY SAVINGS FROM THE SOLAR POWERED HEAT PUMP

The solar heat pump system produces electrical power when the sun shines onto 2 kW of PV panels and delivers it to the house. However, the energy savings experienced by the homeowner is amplified because all of the solar power is delivered to the building by means of a 1.5-ton mini-split heat pump, which has cooling (and heating) efficiency which is essentially twice that of the central SEER 13 ducted system in the MH Lab. Space conditioning energy savings have also been assessed when operating in both Economy and Standard control modes and with the number of batteries at 8 and 4.

Additional savings occur when the high efficiency mini-split heat pump is operated using utility grid power after the solar resource has been depleted. Operation of the mini-split on the utility grid offsets a portion of the electrical energy which would otherwise be used by the less efficient central ducted system.

While the experiments were carried out in the Building Science Lab, the energy savings have been calculated as if the cooling and heating provided by the mini-split had been delivered into the MH Lab, a three bedroom two bath 1600 ft² home. Measured data had been collected in the MH Lab over a couple-year period to determine the cooling and heating loads over a wide range of outdoor temperatures. Regression analysis was completed so that the space cooling and heating loads could be predicted from TMY3 data. From experiments carried out in the Building Science Lab over the past 12 months, regression analysis has also been performed to characterize the cooling and heating energy that can be delivered to the MH Lab using the solar powered heat pump.

4.1 Cooling Season Energy Savings Calculation Methodology

Typically the difference between outdoor and indoor temperature (delta-T) accounts for 85%-95% of the variability in delivered cooling energy. However, the solar heat pump is designed to meet only a portion of the house space conditioning load (it turned out to be about 55% for the entire year), the solar powered mini-split heat pump delivered cooling energy predominantly as a function of the amount of solar radiation striking the PV panels. On the other hand, it was also a function of outdoor temperature. To account for the driving forces of both solar and delta-T, multivariate regression analysis was performed. This yielded equations which predict daily cooling energy delivered by the solar mini split system as a function of daily solar radiation and average outdoor temperature. Delivered cooling (DC) is calculated by the following equation:

$$DC = M1 \times \text{solar radiation at tilt (W/m}^2\text{)} + M2 \times \text{Outdoor Temperature (}^\circ\text{F)} + C$$

where M1 = solar coefficient, M2= temperature coefficient, and C = constant

Table 5 presents the results of the multivariate analysis for 5 different experimental variations.

Table 5

Regression analysis results for cooling derived from monitored data of 100% mini-split (M-S) operation and 8 batteries. Calculated cooling energy savings (last column) are based on typical summer values with daily average temperature of 76°F indoors and 80°F outdoors, with solar radiation of 5500 Wh/m²-day.

	# days	M1	M2	C	r ²	kBtu/d
100% M-S economy	27	0.00469	13.039	-806.664	0.855	262.2
8 battery economy	68	0.01185	5.8794	-372.914	0.545	162.6
8 battery standard	38	0.01436	-3.654	322.678	0.618	109.3
4 battery economy	35	0.00990	-3.045	290.215	0.684	101.0
4 battery standard	13	0.00866	2.498	-148.399	0.774	99.1

While regression analysis has been completed using solar radiation and outdoor temperature, cooling energy versus both cannot be shown in a two-dimensional plot. Instead cooling energy delivered to the Building Science Lab has been plotted vs daily total solar radiation for Standard control mode using the eight battery storage bank (Figure 9). The plot shows measured delivered cooling versus solar radiation only as blue data points. However, the red data points show the predicted cooling energy based on both variables (solar and temperature). Figure 10 shows delivered cooling versus solar radiation for the mini-split using the Economy thermostat control mode with 8 battery bank. By examining the best-fit lines and equations of Figures 9 and 10, it can be seen that Economy mode yields considerably greater delivered cooling for a given amount of solar radiation.

In both Figure 9 and Figure 10, it can be seen that a significant amount of scatter is eliminated when outdoor temperature is also taken into account. The fact that r² values improve from 0.559 to 0.859 and from 0.243 to 0.446 in Figures 9 and 10, respectively, confirms what can be seen visually, that including the effect of outdoor temperature significantly improves uncertainty in the predicted delivered cooling.

For each day of the year, the amount of cooling electrical energy savings (based on cooling energy provided to the MH Lab by the solar heat pump) is determined (calculated) in a 4-step process.

- STEP 1: Determine the maximum amount of solar-powered cooling that could be delivered to the MH Lab based on daily solar radiation for each TMY3 day using the best-fit (“predicted”) equations from Table 5.
- STEP 2: Determine the cooling load of the MH Lab for each individual day in the following manner. For each day of the TMY3 data, daily average outdoor temperature is used to determine delta-T (T_{out} – 77°F). Total cooling load for that day is then calculated based on delta-T for that day and the best-fit equation in Figure 11.
- STEP 3: The lesser of Step 1 or Step 2 is then the actual cooling delivered to the MH Lab for that day of the (TMY3) year.
 - The reason for this step: the solar heat pump system cannot deliver space cooling to the MH Lab that exceeds the cooling load of the MH Lab for each specific TMY3 day.

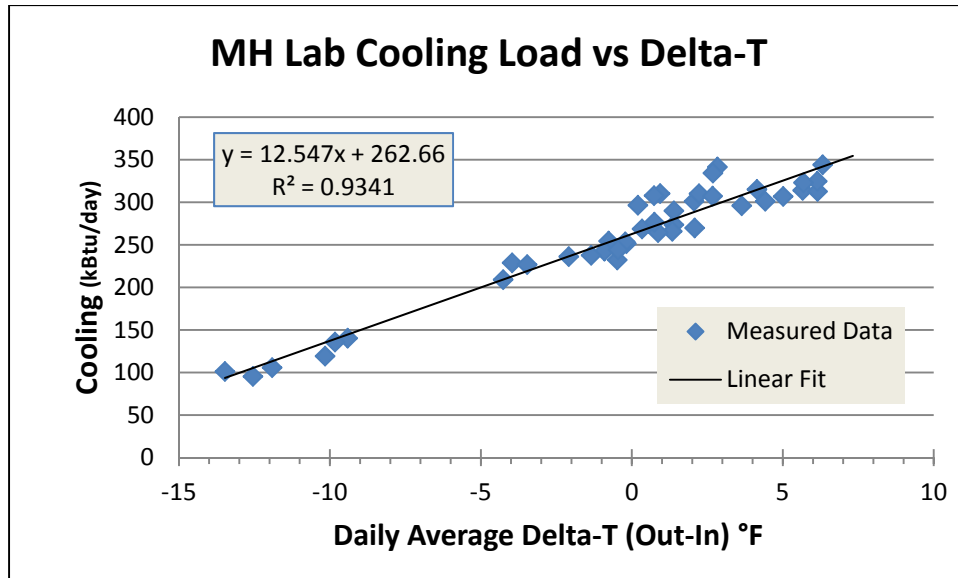


Figure 11. Daily MH Lab cooling load versus delta-T (out – in) when using attic ducts.

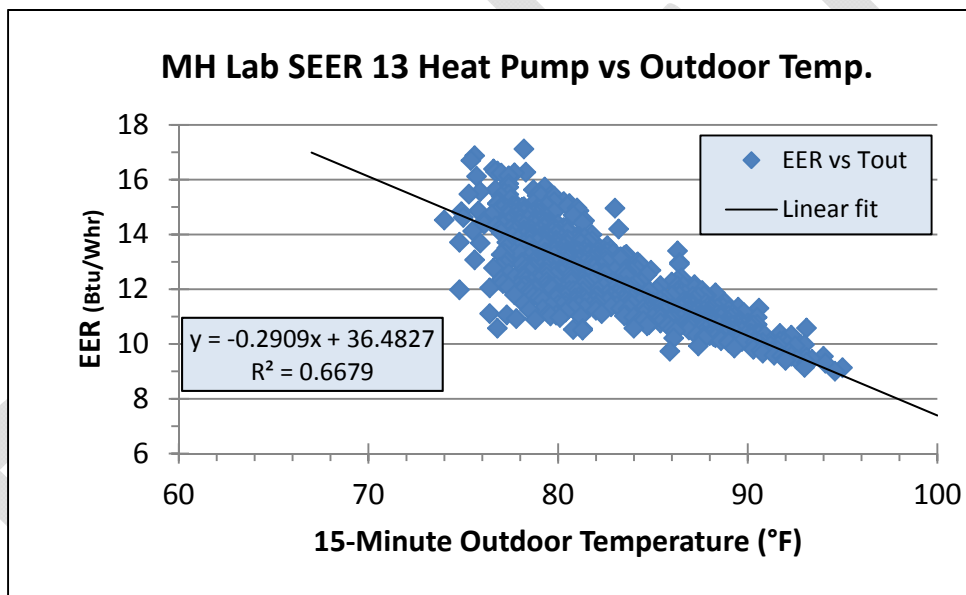


Figure 12. Measured cooling EER for the central ducted 3-ton SEER 13 MH Lab heat pump as a function outdoor temperature. Duct losses are not considered when calculating EER.

These calculations are performed for each day of the year for which cooling is required (based on TMY3 data) for each of the four FPL service territory cities. Weighting for the four cities are as follows; Daytona Beach (15.17%), Miami (43.19%), West Palm Beach (22.43%), and Fort Meyers (19.21%). Similar calculations with identical weighting will also be performed for the heating season.

4.1.1 Example Calculation of Cooling Energy Savings from the Solar Heat Pump System

Following is an example of delivered cooling calculation for a particular TMY3 day (in this case, January 29, 1995) in Miami, which has average daily average conditions of 73.5°F drybulb temperature and 2472 Wh/m² solar radiation on the horizontal.

Over the past year, solar radiation was measured at the Building Science Lab at the PV panel tilt. However, since TMY3 solar radiation represents solar on the horizontal, it has to be converted to solar radiation incident at the tilt angle of the PV panels. Conversion is done based upon a regression of the solar ratio (horizontal solar versus PV tilt solar) versus the day of year from solstice. Days from December 21 to June 21 increase from 1 to 183 and days from June 21 to December 21 decrease from 183 to 1. The solar ratio was developed based on measurements from two pyranometers, one horizontal and one at PV tilt. The solar ratio and best-fit line are represented in Figure 13. Each TMY3 day is assigned a “day from solstice”, which is then used to calculate the solar ratio multiplier. For the case of January 29, this day is given the solstice day number of 40. Applying the regression equation, the solar ratio is calculated to be 0.8586. The TMY3 solar on the horizontal is then converted to solar at PV tilt by dividing TMY3 horizontal solar by the solar ratio, yielding 2879 Wh/day on the PV tilt (2472/0.8586 = 2879).

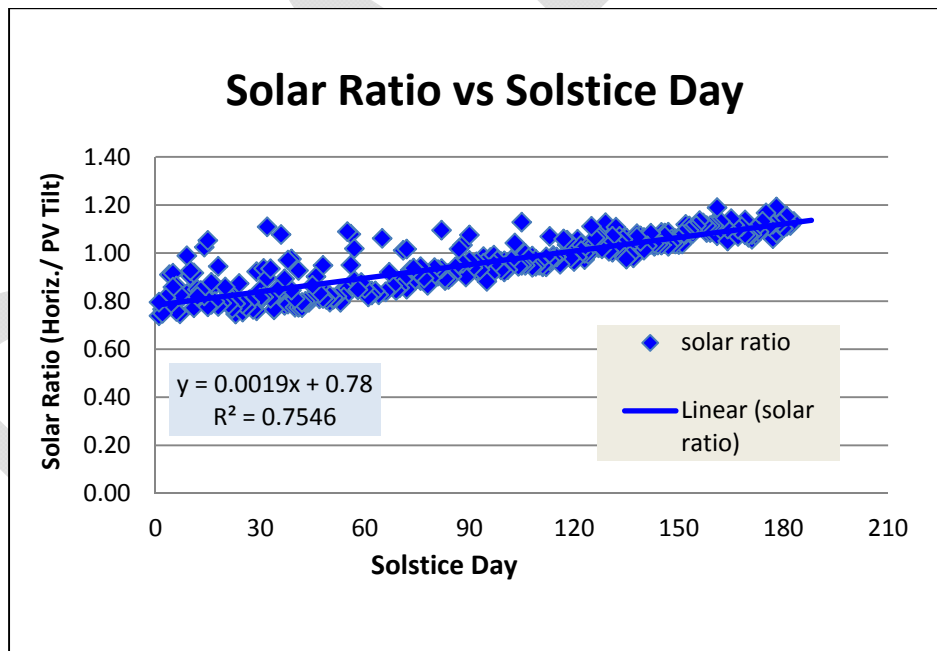


Figure 13. Solar ratio, which is used to convert solar radiation on the horizontal to solar radiation at PV array tilt, varies as a function of day of the year. Solstice day increases from 1 to 183 from December 21 to June 21, and then decreases from 183 to 1 from June 21 to December 21.

Following the calculation steps laid out in Section 4.1, electrical energy savings for January 29, 1995 is calculated as follows.

STEP 1 -- POTENTIAL SOLAR HEAT PUMP COOLING DELIVERY: Based on the solar radiation of 2879 Wh/m²-day of TMY3 solar on the PV tilt and the regression equations (from Table 5; not from

Figures 9 and 10), the potential space cooling that could be provided by the solar heat pump is 93,457 Btu/d when using Economy mode and 95,380 Btu/d when in Standard mode.

STEP 2 -- REQUIRED COOLING LOAD: Based on an average daily ambient temperature of 73.5°F, a delta-T of -3.5°F (73.5°F – 77°F = -3.5°F), and the best-fit equation for MH Lab cooling load (Figure 11), the MH Lab space cooling load is calculated to be 216,500 Btu/d (when the MH Lab is located in Miami on January 29, 1995).

Step 3 – DETERMINE ACTUAL SPACE COOLING DELIVERED: The smaller of Steps 1 and 2 is 93,457 Btu/d when operating in Economy mode and 95,380 Btu/d in Standard mode.

Step 4 – DETERMINE COOLING ENERGY SAVINGS: Cooling electrical energy savings provided by the solar heat pump to the MH Lab house is determined by dividing delivered cooling (Step 3) by the EER of the MH Lab central system which is obtained from the best-fit regression equation from Figure 12. In this case, EER for that day is calculated to be 15.09 Btu/Wh ($Y = -0.2909 (73.5^\circ\text{F}) + 36.483 = 15.09$). The energy savings of 93,457 Btu/d (in Economy mode) yields electrical energy savings of 6.19 kWh/d ($93,457 / 15.09 = 6193$) and the energy savings of 95,380 Btu/d (in Standard control mode) yields electrical energy savings of 6.32 kWh/d ($95,380 / 15.09 = 6321$).

4.2 Seasonal Cooling Energy Savings from the Solar Heat Pump

Annual cooling energy consumption and cooling energy savings are shown in Table 6 based on TMY3 weather data for four Florida cities and calculations outlined in Section 4.1.

When the mini-split heat pump is operated only when solar power (from PV and batteries) is available (in other words, the mini-split is not operated on grid power and the central system picks up where the solar heat pumps drops out), annual cooling savings from 33.9% to 53.5% are achieved depending upon the system operational configuration.

- When the mini-split is operated with 8 batteries and Economy mode (with warmer supply air), this configuration yields 3322 kWh (or 53.5%) annual cooling savings.
- When the mini-split is operated with 8 batteries and Standard mode (with colder supply air), this configuration yields 2683 kWh (or 43.3%) annual cooling savings.
- When the mini-split is operated with 4 batteries and Economy mode (with warmer supply air), this configuration yields 2516 kWh (or 40.6%) annual cooling savings.
- When the mini-split is operated with 4 batteries and Standard mode (with colder supply air), this configuration yields 2101 kWh (or 33.9%) annual cooling savings.

Table 6

Annual cooling energy required by the MH Lab SEER 13 central system (first data row) and annual energy savings provided by the solar heat pump system for 5 different system configurations (data rows 2–6).

	Daytona kWh	Miami kWh	West Palm Beach kWh	Ft. Myers kWh	4 city weight-avg kWh	Annual savings %
S13 MHL annual kWh	4749	6745	6109	6246	6204	
8 Bat. Economy kWh savings	2584	3594	3275	3346	3322	53.5%
8 Bat. Standard kWh savings	2430	2738	2704	2736	2683	43.3%
4 Bat. Economy kWh savings	2269	2575	2527	2569	2516	40.6%
4 Bat. Standard kWh savings	1700	2246	2078	2122	2101	33.9%
100% MS Economy kWh savings ¹	3400	4830	4374	4472	4442	71.6%

¹ These savings assume that the mini-split cooling output is limited, by assumption, to meeting no more than 80% of the space cooling load during hours when it operates on the utility grid.

We can conclude that there are large seasonal cooling energy savings benefits of operating the mini-split in Economy mode versus Standard mode.

- With 8 batteries, annual savings increase by 24% going from 2683 to 3322 kWh when going from Standard to Economy modes.
- With 4 batteries, annual savings increase by 20% going from 2101 to 2516 kWh when going from Standard to Economy modes.

There are also large seasonal cooling energy savings resulting from operating the mini-split using 8 batteries compared to 4 batteries.

- When operating in Economy mode, annual savings increase by 32% going from 2516 to 3322 kWh when going from 4 batteries to 8 batteries.
- When operating in Standard mode, annual savings increase by 28% going from 2101 to 2683 kWh when going from 4 batteries to 8 batteries.

4.3 Additional Cooling Season Savings from Operating the Mini-split from the Utility Grid

Because of the considerable efficiency advantage of the mini-split system compared to the central ducted heat pump system, an additional system design feature was also examined in this project that would allow the mini-split to run 100% of the time. A relay was installed in the Building Science Lab that would automatically switch the mini-split power from inverter (PV power) to the utility’s grid when the batteries had run out of energy (more specifically the battery SOC had declined to a specified level). With this relay and control setup (which we would recommend to customers who purchase this “stand-alone” solar powered heat pump system), the mini-split can operate 24 hours per day (on the PV/battery power for as long as that is available and then on grid power when the solar power has been depleted), and thus displace a large proportion of the home’s yearly heating

and cooling energy requirements. This switch-over relay worked flawlessly through the year of data collection and automatically switched over to the grid when the batteries had drained to a specified (user-selectable) level.

Considerable savings can occur in this mode. Consider, for example, if the central system has a SEER 13 rating and delivers its energy to the space through attic ductwork with 25% average overall energy losses, then the central system net efficiency equates to SEER 9.75 ($SEER\ 13 * (1 - 0.25) = 9.75\ SEER$). Since the mini-split has no ductwork and therefore no duct-related losses, its efficiency will not be reduced below its SEER rating of 19.2. (Note that other mini-split systems that could be used in this type of application have SEER ratings as high as 27.2, and could therefore yield even greater savings in this mode of operation.) Therefore, the mini-split operation by itself, apart from the solar energy delivered to the house, could save 30-70% on seasonal cooling energy savings compared to the central system, depending upon the SEER ratings of the mini-split and central systems, the SEER rating of the central system, and the energy losses of the ductwork serving the central system. Operating the mini-split during all hours when the solar resource has been depleted increases annual cooling energy savings by 34% from 3322 to 4442 kWh (Table 6). When the mini-split is operated from solar power and then also powered from the utility grid when the solar resource has been depleted, annual cooling energy savings from the solar heat pump system is then 72%.

5. COOLING SEASON PEAK DEMAND SAVINGS PRODUCED BY THE SOLAR HEAT PUMP SYSTEM

The peak cooling demand period of most interest to FPL occurs during the hour of 4 to 5 PM. The combination of solar radiation and battery storage on hot summer afternoons ensures that the mini-split will be operating continuously during those peak hours in all circumstances, and using solar power alone. The only question that remains to be determined is – “What proportion of the space cooling is met by the mini-split during that hour.”

There are several factors which determine whether the mini-split will meet the entire cooling load during those peak hours (recall that the mini-split is a variable capacity system). Figure 14 illustrates a typical pattern of cooling energy use when the mini-split is in Standard control using the 8 battery bank for a hot 8-day summer period. Based on timer control, solar power is delivered from the inverter to the mini-split starting at 1 PM EDT (blue line). By 2 PM the central ducted system (dotted red line) has cycled off because the mini-split setpoint is below that of the central system. From 2 PM to 6 PM, then, the central ducted system cycles off completely, and the solar heat pump system meets 100% of the cooling demand for the peak hour(s). The solid red line shows the predicted SEER 13 cooling electrical energy consumption for the MH lab house, based on regression analysis, when no other supplemental cooling occurs.

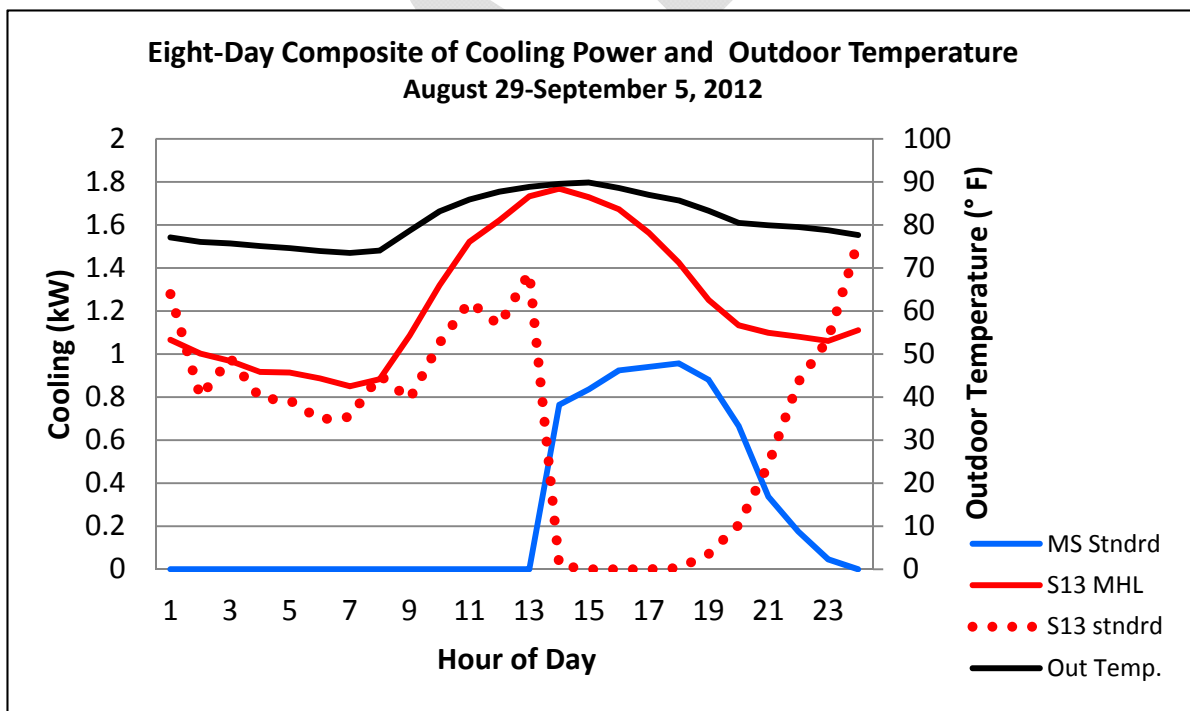


Figure 14. During the 8-day period August 29-September 5, 2012, the central ducted system does not cycle ON during the hours of 4 to 6 PM (EDT) because the mini-split, which is in Standard mode, meets the entire building cooling load during those peak hours. Therefore, the solar heat pump system meets 100% of the cooling demand on the peak hours of those 8 hot summer days.

Based on regression analysis, it was found that operation of the solar heat pump with 8 batteries and Standard control yields 100% peak demand reduction. For all days of the year, the combination

of solar energy from the PV modules and energy stored in the 8-battery bank allows the mini-split to operate on solar power alone and meet the entire space cooling load peak demand (Figure 14 and Table 7).

Figure 15 illustrates hourly space cooling operation for another data set. Cooling power is shown for a total of 17 days, allowing for comparison of Economy and Standard control modes. The red line represents the electrical demand produced by the MH Lab central system when the solar heat pump system is taken off line. When the solar heat pump system is activated, it can be seen that the central ducted system does not operate at all for the 4-5 PM period (blue dots) since the mini-split (in Standard control mode) meets 100% of the space cooling load at that time. When the system is switched to Economy mode, the solar heat pump does not meet all of the peak cooling demand because the central SEER 13 system cycles on occasionally during those peak hours (green dashed line in Figure 15).

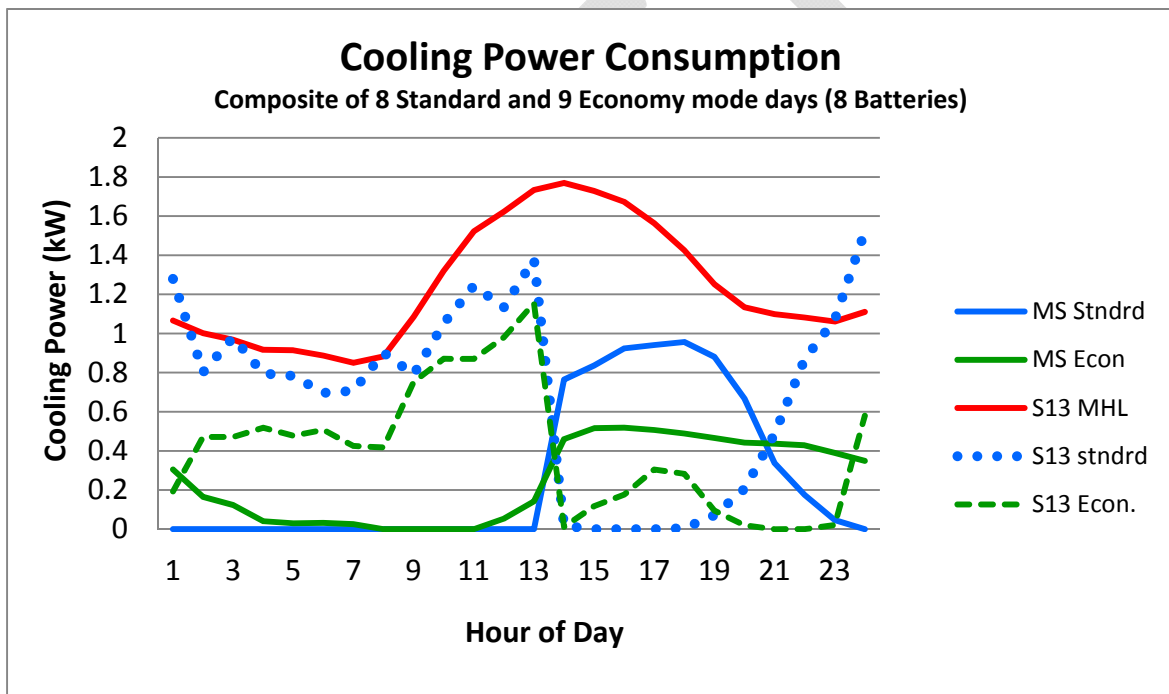


Figure 15. Twenty-four hour cooling power consumption profile for Standard and Economy mini-split operation when using 8 batteries, plus cooling power consumption for the MH Lab SEER 13 central system. Figure 15 has added economy profile to Figure 14.

When in Standard mode and the battery bank is reduced to 4 batteries, the solar heat pump does not meet all of the peak cooling demand. It can be seen that the central system cycles on occasionally during those peak hours (Figure 16). When in Economy mode and the battery bank is reduced to 4 batteries, the solar heat pump does not meet nearly the entire peak cooling demand and the central system cycles on more frequently during those peak hours.

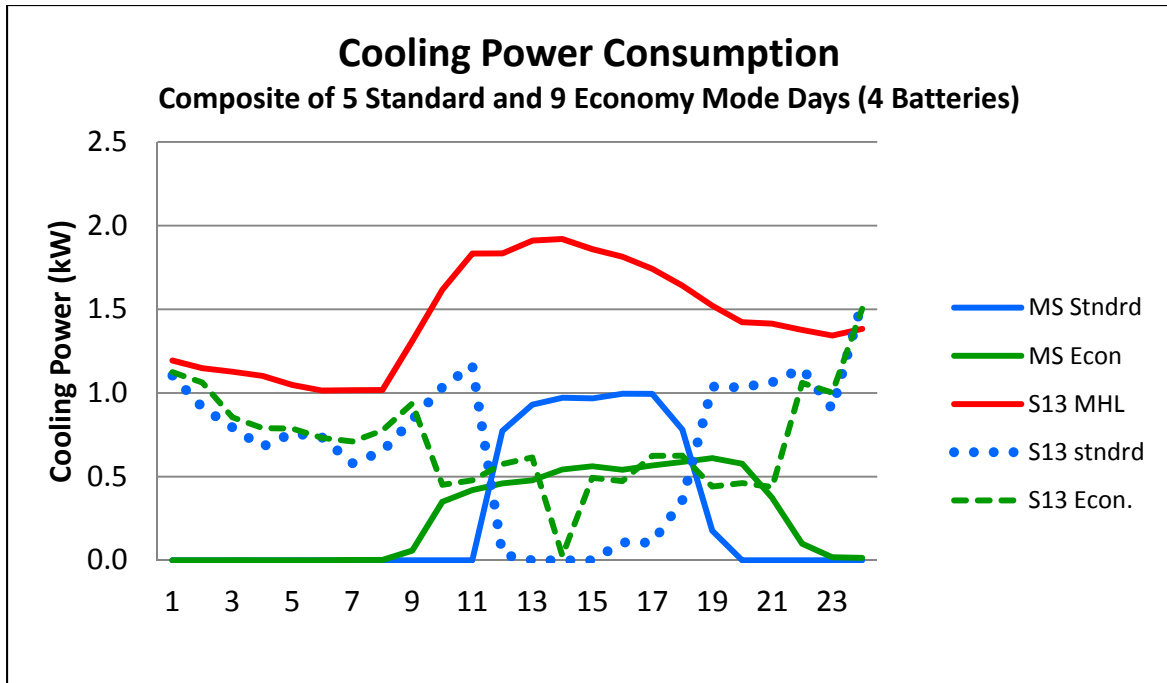


Figure 16. Twenty-four hour cooling power consumption profile for Standard and Economy mini-split operation when using 4 batteries, plus cooling power consumption for the MH Lab SEER 13 central system.

Figures 15 and 16 are complicated and this section will therefore benefit from further explanation.

- The cooling energy consumption patterns shown in Figure 15 are a combination of monitored data and simulated energy consumption, all based on a composite derived from a number of days and representative of typical summer temperature and solar. Table 7 also shows relative peak demand for the hottest summer hours based on TMY3 data for the four chosen FPL market cities.
- The solid blue line in Figure 15 is measured energy consumption of the solar heat pump (provided by the PV/battery system) when operating in Standard mode.
- The solid green line is the measured energy consumption of the solar heat pump (provided by the PV/battery system) when operating in Economy mode.
- The blue dotted line is the simulated energy consumption of the MH Lab central system if the solar heat pump (mini-split) were operating in the MH Lab in Standard mode.
- The green dashed line is the simulated energy consumption of the MH Lab central system if the solar heat pump (mini-split) were operating in the MH Lab in Economy mode.
- The red solid line (labeled S13 MHL) is the regression analysis-based simulated energy that the SEER 13 MH Lab central system would have consumed if the solar heat pump (mini-split) were not operating.
- The peak demand reduction produced by the solar heat pump with Standard control and 8 batteries would then be the gap between the red line and the dotted blue line in Figure 15.

- The peak demand reduction produced by the solar heat pump with Economy control and 8 batteries would then be the gap between the red line and the dashed green line in Figure 15.
- The peak demand reduction produced by the solar heat pump with Standard control and 4 batteries would then be the gap between the red line and the dotted blue line in Figure 16.
- The peak demand reduction produced by the solar heat pump with Economy control and 4 batteries would then be the gap between the red line and the dashed green line in Figure 16.

The following can be learned from Figures 15 and 16 regarding the 31 days represented in those composite plots.

- When the solar heat pump operates in Standard mode with 8 batteries, 100% of the peak demand which would have occurred during the 4-5 PM period by operation of the central ducted system is met by the solar heat pump.
- When the solar heat pump operates in Economy mode with 8 batteries, approximately 80% of the peak demand which would have occurred during the 4-5 PM period by operation of the central ducted system is met by the solar heat pump.
- When the solar heat pump operates in Standard mode with 4 batteries, approximately 95% of the peak demand which would have occurred during the 4-5 PM period by operation of the central ducted system is met by the solar heat pump.
- When the solar heat pump operates in Economy mode with 4 batteries, approximately 65% of the peak demand which would have occurred during the 4-5 PM period by operation of the central ducted system is met by the solar heat pump.
- While the solar heat pump operated continuously throughout the peak demand hours for both Standard and Economy modes, only the Standard control mode allows the mini-split to operate at a sufficiently high capacity to meet the entire cooling load.
- An interesting control option would be conceivable, namely that advanced algorithms could be implemented that would result in Economy mode operation most of the time (thus achieving maximum seasonal operation efficiency) but Standard mode operation during periods when peak demand reduction is advantageous. This control approach could result in operational outcomes that are maximized for both the customer and the electric utility.

Table 7 summarizes TMY3 modeled peak demand for the MH Lab central system (as if the solar heat pump were not available) and also the peak demand reduction yielded by operation of the solar heat pump with various battery and control mode configurations for peak cooling load periods for the 4 representative cities of the FPL service territory. These results are obtained from simulation of peak demand based on calculation using the hottest 4-5 PM (EDT) hours of the hottest TMY3 day for each city.

Table 7

Peak cooling energy required by the MH Lab SEER 13 central system and peak demand reduction provided by the solar heat pump system for 4 different system configurations.

HOURLY ENDING	MHL SEER13 Cooling Peak Demand					Peak Demand Reduction			
	Daytona kW	Miami kW	WPB kW	Ft. Myers kW	weight-avg kW	8 batt-standard kW	8 batt-economy kW	4 batt-standard kW	4 batt-economy kW
4:00 PM	2.51	2.01	2.51	2.51	2.29	2.29	1.95	1.95	1.58
5:00 PM	2.35	1.93	2.35	2.51	2.20	2.20	1.87	1.87	1.52
AVG	2.43	1.97	2.43	2.51	2.25	2.25	1.91	1.91	1.55
Peak Demand reduction %						100.0%	85.1%	84.9%	69.1%

The following can be learned from Table 7.

- When operated with 8 batteries in Standard mode, the solar heat pump produces 100% demand reduction which is equal to a 4-city weighted average 2.25 kW reduction.
- When operated with 8 batteries in Economy mode, the solar heat pump produces 85% demand reduction which is equal to a 4-city weighted average 1.91 kW reduction.
- When operated with 4 batteries in Standard mode, the solar heat pump produces 85% demand reduction which is equal to a 4-city weighted average 1.91 kW reduction.
- When operated with 4 batteries in Economy mode, the solar heat pump produces 69% demand reduction which is equal to a 4-city weighted average 1.55 kW reduction.

There are three factors which determine the extent of demand reduction produced by the solar heat pump for the 4 to 5 PM period on the hottest days.

- The first factor is the capacity of the mini-split. While this 1.5-ton unit has nominal cooling capacity of 18,000 Btu/h, the unit actually has capacity up to 23,000 Btu/h. It appears to be true of nearly all variable-capacity systems, including mini-split heat pumps, that maximum capacity is considerably greater than the nominal capacity. When one considers that mini-split heat pumps experience no duct losses, it then has capacity approximately equivalent to a central ducted system of about 3-ton capacity when duct conduction and duct air leakage losses are included. In many cases, then, the 1.5-ton mini-split will be able to meet or nearly meet the peak cooling load of many mid-sized homes. In the case of the Building Science Lab, the peak cooling load is about 2 tons. (The MH Lab also has a peak cooling load of about 2 tons, when operating with the attic duct system.) Therefore, this 1.5-ton mini-split can meet the cooling load of either of these buildings even on the hottest days.
- The second factor is whether the system is operated in Standard or Economy modes. For a given amount of daily solar radiation, the solar powered mini-split provides almost 50% more daily cooling when operating in Economy mode. On the other hand, when operating in Standard mode, the mini-split draws nearly 60% more power. Therefore, it makes the most sense for the homeowner to operate in Economy mode under most circumstances. In Economy mode, and with the central ducted system operating at about 1°F higher

temperature than the mini-split setting, the mini-split will meet most of the cooling load but the 5-ton will also cycle “on” intermittently during these peak hours, with the solar powered mini-split meeting, on average, about 85% of the peak demand.

- The third factor is how close the thermostat setpoints of the mini-split and central ducted system are to each other. Because of the way that variable capacity systems (such as the mini-split heat pumps) operate, space temperature tends to drift upward during peak hours (as can be seen in Figure 7). This is an inherent function of how variable capacity systems (including this mini-split model) modulate their output. They increase their cooling (or heating) output based on the deviation between setpoint and measured room temperature. In Economy mode, this deviation is allowed to expand slightly more than in Standard mode, in order to keep the system in lower capacity, where it operates at higher efficiency a greater proportion of the time. So, the fraction of the peak demand that is met by the solar heat pump depends in substantial part upon how close the thermostat setpoints are to each other. While a 1°F difference in setpoint might be a good selection in order to maintain continuity of space temperature as space cooling transitions from mini-split to central system, and higher mini-split operating efficiency, a 2°F difference on the other hand would allow the solar mini-split to meet all or nearly all of the peak demand on the hottest days even while operating in Economy mode.

Conclusion: While the Economy mode yields the greater yearly cooling energy savings to the customer, Standard mode yields the greatest peak demand savings to the electric utility. If the central ducted system setpoint were to be set a couple degrees higher than that of the solar heat pump, then the solar mini-split could be operated in Economy mode while still meeting 100% of the peak hour electrical demand.

5.1 Peak Demand Savings as a Function of Temperature Setpoints of the Mini-split and Central Systems

The home cooling load reaches its maximum during the hottest hours of the day. As cooling load increases throughout the day, the mini-split allows space temperature to drift upward because increasing delta-T ($T_{\text{room}} - T_{\text{stat}}$) is what pushes the mini-split to increase its capacity. The amount of space temperature increase is typically on the order of 1 to 2°F, depending upon the range of cooling load and outdoor temperature swings. Figure 17 has the same room temperature data from Figure 7 but with the mini-split thermostat setpoint shown as a blue line and the central heat pump setpoint shown as a green line. As the building cooling load increases, the upward drift in space temperature produced by the mini-split allows the central ducted system to cycle on. As the central system cycles on and caps or actually pushes indoor temperature down, it will tend to limit the mini-split’s compressor capacity. In this manner, the central system displaces some of the electrical energy savings which could have been produced by the mini-split. In what might be considered the most common configuration of the mini-split and the central system, the mini-split thermostat might use a 0.5 to 1.0°F lower setpoint. In this arrangement, the mini-split will run continuously, but not at full capacity, because the central system will intermittently cycle on as room temperature is allowed (by the mini-split) to drift upward.

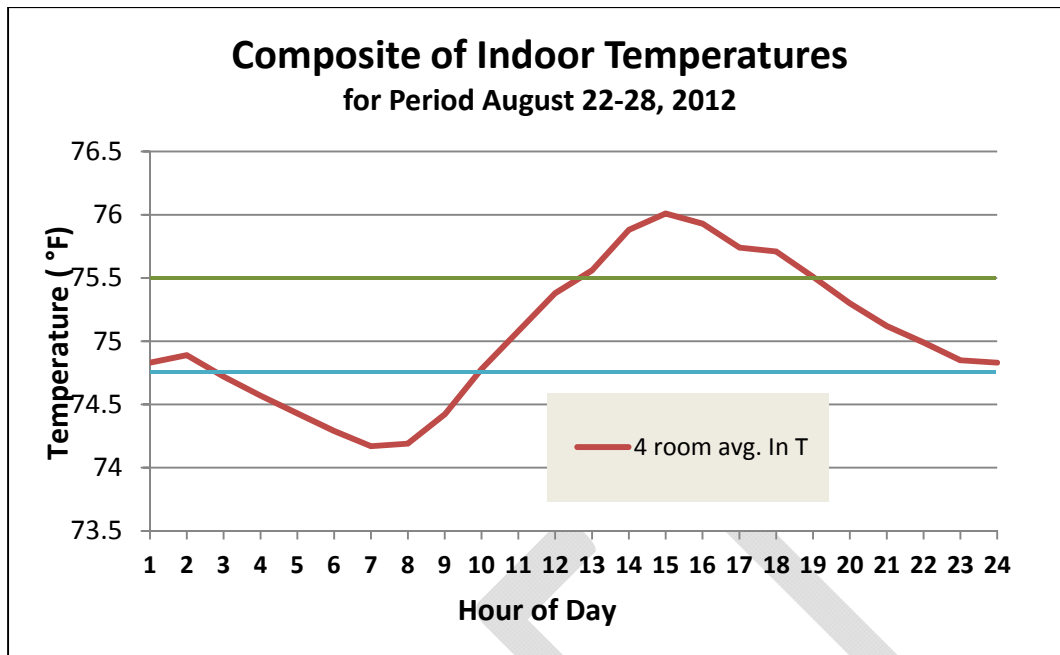


Figure 17. The red line is a measured 24-hour space temperature profile in the Building Science Lab for a 7-day period with only the mini-split conditioning the space, with space temperature setpoints used by the mini-split (blue line) and central system (orange line) illustrated.

Selecting close setpoints causes the mini-split to operate at a lower capacity factor, which in turn allows it to operate at higher efficiency. Selecting Economy mode results in additional operational efficiency. However, both of these factors -- close setpoints and use of Economy mode -- result in the mini-split being considerably less effective at displacing peak demand.

In fact, during the 12 months of solar heat pump experiments, the setpoints of the mini-split heat pump and the Building Science Lab central heat pump were about 0.5°F different. Because the setpoints were so close, the central system was more likely to activate during peak load periods of the day as the mini-split allowed the space temperature to drift upward (for more details, see Section 2.4 and Figure 7), especially when economy mode was employed. Economy mode allows the room temperature to drift upward to a greater degree before the unit goes into higher cooling capacity. Conversely, Standard mode tends to make the deadband between mini-split setpoint and room temperature tighter, thus minimizing the likelihood that the central system will cycle on. If the homeowner is willing to set the central system thermostat setpoint to perhaps 1.5 to 2°F warmer than that of the mini-split, then the central system is unlikely to cycle on even when it operates in Economy mode.

In the real world, there will be tension between what would be most convenient and comfortable for the customer, namely setting the central ducted system thermostat to a level just slightly higher than that of the mini-split (thus causing the mini-split to operate in lower capacity and higher efficiency) versus a higher temperature setting which would, for the most part, prevent or resist the central system from activating. A smaller difference between setpoints will yield a more seamless transition from mini-split to central system operation and greater occupant comfort,

since indoor space temperature will remain stable. By contrast, what would be best for the electric utility would be to have the solar-powered mini-split meet the entire cooling load during the peak periods. Of course, incentives could be put in place to encourage the customer to control the mini-split so that a larger portion of the peak demand is met by the mini-split. An “on-demand” system could also operate to disable the central system (or adjust the thermostat upward) on days (and hours) of high peak demand, thus forcing the mini-split to meet the entire space cooling load.

A discussion regarding optimizing peak demand reduction is presented in Appendix B.

DRAFT

6. HEATING SEASON ENERGY SAVINGS PRODUCED BY THE SOLAR HEAT PUMP SYSTEM

Because of limited heating season data, and because the mini-split provides solar-powered space heating much more efficiently in Economy mode, only a limited amount of Standard-mode space heating was available.

6.1 Heating Energy Savings Calculation Methodology

As was done for cooling season analysis, multivariate regression analysis was performed to account for the driving forces of both solar and delta-T (outdoor minus indoor temperature). This yielded equations which predict daily heating energy delivered by the solar mini-split system as a function of daily solar radiation and average outdoor temperature. The regression results are shown in the form of an equation which allows calculation of delivered heating (DH), as follows:

$$DH = M1 \times \text{Solar at tilt} + M2 \times \text{Outdoor Temperature (F)} + C$$

where M1 = solar coefficient, M2= temperature coefficient, and C = constant

Table 8 presents the results of the multivariate analysis for 2 different experimental variations, 100% mini-split operation (part of the day powered by solar and the remainder of the day by the grid) and Baseline (both mini-split and central system operating) with 8 batteries and Economy control mode.

Table 8

Regression analysis results for heating derived from monitored data of 100% mini-split (M-S) operation and 8 battery Economy control mode. Calculated heating energy savings (last column) are based on daily average temperature of 72°F indoors and 50°F outdoors, with solar radiation of 5500 Wh/m²-day.

	# days	M1	M2	C	r ²	kBtu/d
100% M-S economy ¹	50	-0.00065	-9.1681	668.357	0.876	206.4
8 batt economy	60	0.001073	-3.70685	279.619	0.528	100.2

¹ Note: 100% M-S economy means that these 50 days of monitored data were with the mini-split (M-S) operating 100% of the time, on solar power when that is available and on the grid when the solar resource has been depleted.

For each day of the year, the amount of heating electrical energy savings (heating energy provided to the MH Lab by the solar heat pump) is determined (calculated) in a 4-step process, similar to that which was employed for space cooling.

- **STEP 1:** The maximum amount of solar-powered heating that could be delivered to the MH Lab (based on daily solar radiation) is determined by the solar radiation level for each TMY3 day in conjunction with the regression equation in Table 8.
- **STEP 2:** The heating load of the MH Lab is determined in the following manner. For each day of the TMY3 data, the daily average outdoor temperature is used to determine delta-T (T_{amb} – 72°F). Then based on the delta-T for that day and the equation in Figure 18, the total heating load for that day is then calculated.

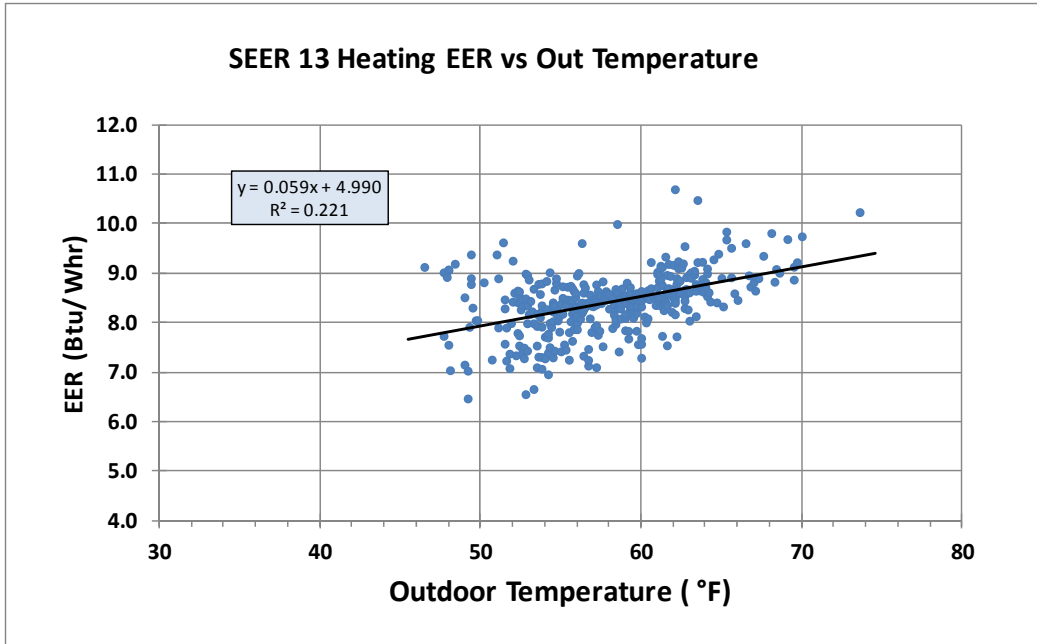


Figure 18. Daily heating load (Btu/day) versus delta-T (out – in) for the MH Lab excluding duct losses.

- STEP 3: The lesser of Step 1 or Step 2 is then the actual delivered heating.
- STEP 4: Actual heating delivered to the MH Lab by the solar powered heat pump is converted to daily heating electrical energy savings by dividing the delivered heating by the heating EER of the MH Lab central system for that day. Figure 19 provides heating EER for the MH Lab central heat pump as a function of daily average ambient temperature.

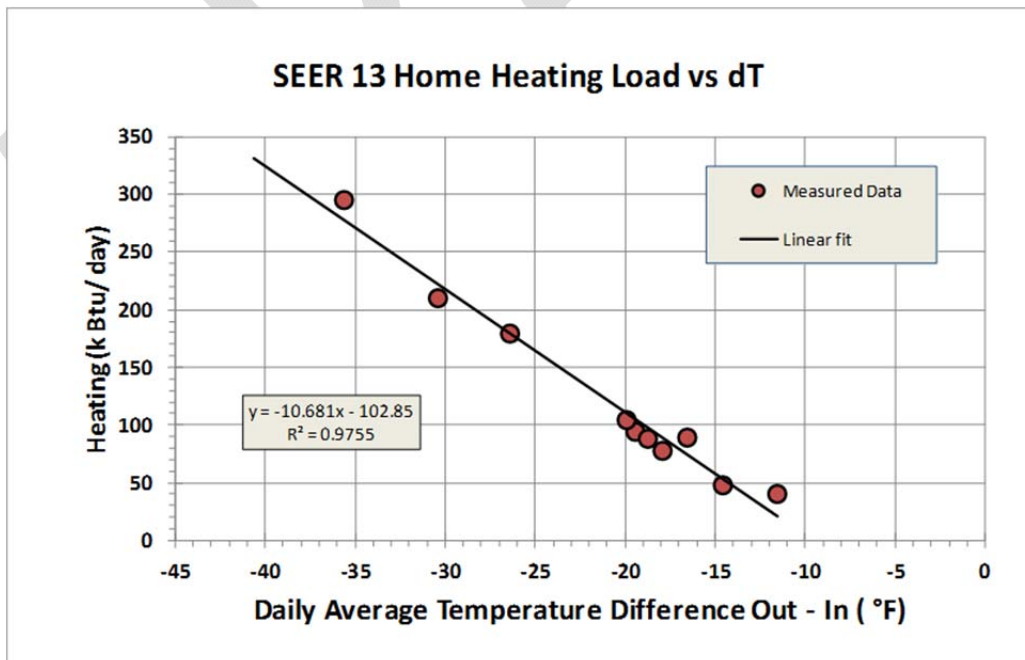


Figure 19. Measured system 15-minute heating EER for the 3-ton SEER 13 MH Lab heat pump as a function outdoor temperature.

These calculations are then performed for each day of the year for which heating is required (based on TMY3 data) for each of the four FPL service territory cities.

6.2 Seasonal Heating Energy Savings from the Solar Heat Pump

Annual heating energy consumption and heating energy savings shown in Table 9 are calculated based on TMY3 weather data for four Florida cities and the calculation methodology outlined in Section 6.1.

When the mini-split is operated with 8 batteries and Economy mode, the solar heat pump yields 213 kWh annual heating savings with 72°F setpoint. This represents heating season energy savings of 82% compared to operating only the central ducted SEER 13 heat pump. The predicted annual percentage savings are quite high for the 8 battery Economy configuration, in part due to relatively mild TMY3 winter data in the heavily weighted south Florida cities. While high percent annual heating savings are indicated, the savings are only \$21.30 per year. So while the heating savings are valuable, they only represent about 3% of total annual heating and cooling energy use to the customer. If the space temperature setpoints were increased to say 75°F, heating energy consumption and heating energy savings would be very substantially higher.

It should also be understood that occupant controlled factors could result in very different realized savings. If the Solar Heat Pump were operated in Standard mode, the mini-split heat pump would typically operate at a higher heating capacity which would result in reduced system efficiency and diminished savings.

If the mini-split were allowed to operate on the utility grid when the solar resource has been depleted, then additional savings could be achieved. Annual savings, in this case, would increase to 232 kWh/y, an 89.2% reduction compared to there being no solar heat pump system.

Table 9

Annual heating energy required by the MH Lab SEER 13 central system and annual energy savings provided by the solar heat pump system using 2 different system configurations.

	Daytona kWh	Miami kWh	West Palm Beach kWh	Ft. Myers kWh	4 city weight-avg kWh	Annual savings %
SEER 13 MHL	777	99	288	179	260	
8 Bat. Econ. savings	603	96	237	138	213	81.9%
100% MS Economy savings²	673	97	257	154	232	89.2%

² These savings are based on the assumption that the mini-split operating on the grid meets no more than 80% of the space cooling load that would otherwise be met by the SEER 13 central system.

7. HEATING SEASON PEAK DEMAND SAVINGS PRODUCED BY THE SOLAR HEAT PUMP SYSTEM

Heating peak demand has been examined for the hours of 6 AM to 8 AM on cold winter mornings during the 2012-2013 winter seasons. While the solar heat pump provided 69%-100% of peak cooling demand (depending upon whether Economy or Standard control is used and the number of batteries employed), no peak demand reduction was observed for heating, for any 6 AM to 8 AM period throughout the 12-month monitoring period. It was found that it would be very difficult for the solar heat pump to meet peak heating loads on cold winter mornings.

Why is this? First, there is no solar radiation during this peak period so all of the solar heating during this 2-hour window must be powered solely from battery storage. Second, all of the power to run the solar heat pump during the peak hours must come from the batteries. Third, the power draw of the solar heat pump is typically quite large on the coldest hours of the coldest days, so this tends to draw down the battery voltage quickly which in turn leads to a premature shut down of the inverter.

Peak demand performance is typically assessed by means of regression analysis of a sample the coldest hours of the coldest days. However, the sample size was insufficient to do that analysis for peak heating. As an alternative, a number of individual cold mornings were examined, and the resulting peak demand reduction (or lack of peak reduction) was characterized. In all cases, the solar heat pump did not operate during the critical 6 AM to 8 AM period. Plots are provided to illustrate typical peak period solar heat pump operation.

Figure 20 shows a 24-hour composite of outdoor temperature and solar heat pump operation for two very sunny but cold days. It can be seen that the solar heat pump becomes active at about noon (when battery voltages rises to a level sufficient to activate the inverter), operates throughout the afternoon and evening hours, shutting off for the night at about 11 PM (all times EDT).

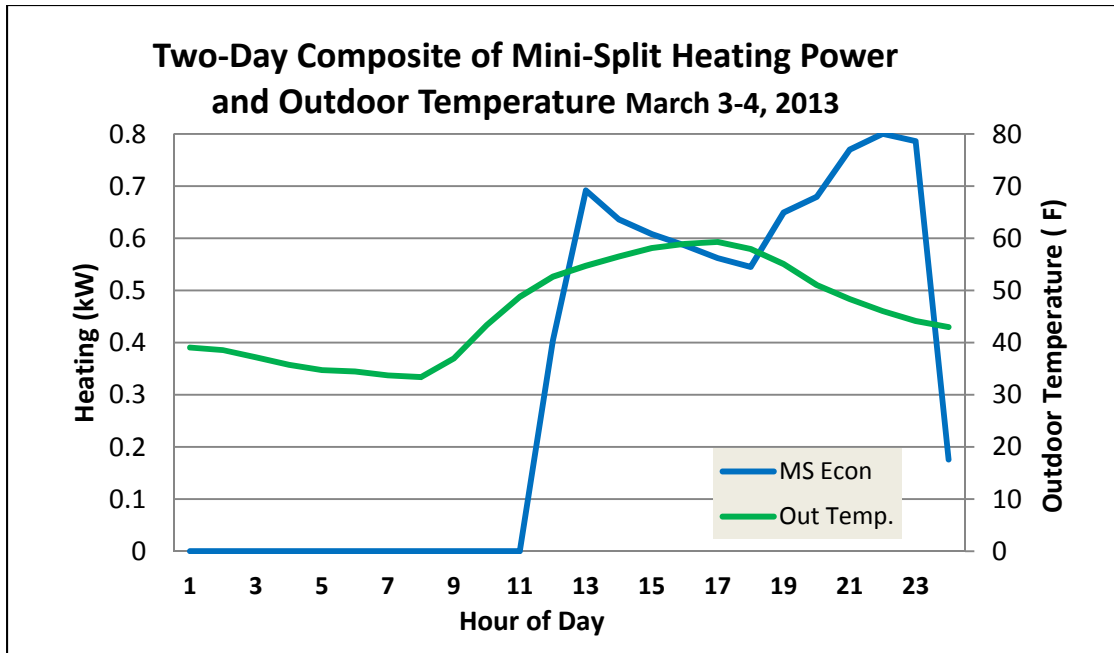


Figure 20. Twenty-four hour composite of solar heat pump operation on a cold two-day period, with average morning low of 33°F and nearly cloudless skies.

Figure 21 shows the same two-day composite period, but with more information about space heating activities. As in Figure 20, outdoor temperature and solar heat pump operation are shown. In addition, however, the mini-split power from the grid (for hours when the solar resource was no longer available) and the central heat pump power are shown. It can be noted that the central 5-ton heat pump also operated during the hours from about 1 AM to 1 PM (purple line).

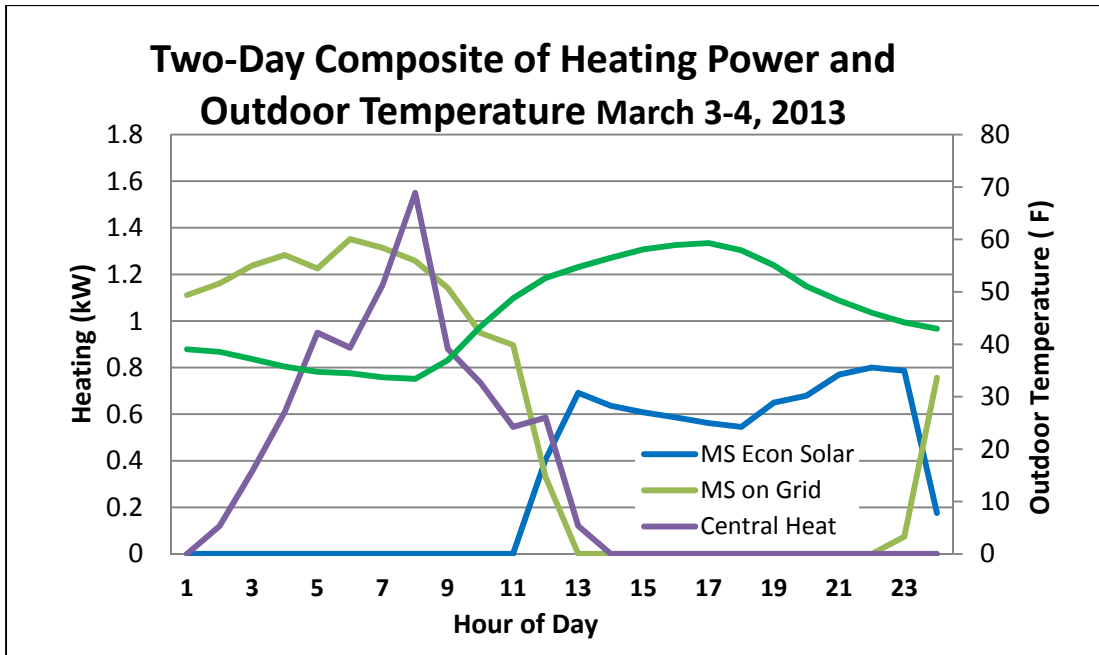


Figure 21. Twenty-four hour composite of solar heat pump operation on a cold two-day period, showing heating power for the mini-split operating on solar (blue line) and on the grid (olive green line), and heating power for the central 5-ton system (purple line).

One might guess that the central system was operating during the 1 AM to 1 PM period because the mini-split could not meet the total heating load. This might be a correct guess, but not entirely. It should be noted that thermostat of the 5-ton system was set at about 1°F lower temperature than that of the mini-split, so that it could act as back-up. As the reader will recall (see Figures 7 or 17), the mini-split (at this time operating on grid power) allows room temperature to deviate increasingly from setpoint as the need for more compressor capacity increases. As the space heating load increased, the mini-split allowed room temperature to drift lower, thus drooping into the deadband of the 5-ton system thermostat and therefore allowing the central 5-ton system to come on. The interaction between the two systems is even more complicated than this. Because the 5-ton system caps the downward space temperature droop, it prevents the mini-split from moving to higher capacity (note that the maximum power draw of the mini-split is 1800 W, per manufacturer specifications) and therefore meeting a higher proportion of the heating load.

Having said all that, it is also possible that the mini-split would not have had sufficient capacity to meet the total heating load during the cold overnight hours, even if the central system setpoint had not been so close to that of the mini-split setpoint. Since the central system uses 2.4 times as much energy per unit of heating output compared to the mini-split heat pump, the spike in central system energy consumption occurring at about 8 AM exceeds the energy consumption of the mini-split by about 20%, but its heating energy output is only about 50% of the heating output being produced by the mini-split.

If the solar heat pump system had more PV panels and a larger battery bank, sufficiently large so that it could have operated continuously through the entire peak demand period, it is likely that it

could have met 80-85% of the peak demand for the 6-8 AM period for the March 3-4, 2013 period, just based on its maximum heating capacity. However, the size and cost of that greatly oversized solar heat pump system would yield a system much less cost-effective than the as-tested system.

Figure 22 presents a composite of mini-split power and outdoor temperature for a period of milder heating weather in late March 2013. While the days March 3-4 were quite cold, with average daily temperatures of 44.3°F and 47.5°F, respectively, the period of March 27-29 had average daily temperatures of 53.7°F, 50.6°F, and 53.9°F. Again, these three days had essentially cloudless skies. Even with these milder temperature conditions and full sun, the solar mini-split only operated until about 4 AM, at which time it would shut down until about 9 AM. At this point solar radiation raised battery voltage to the level required to activate the inverter. The research team concludes, therefore, that under normal operation patterns, the solar heat pump (while operating on solar) cannot meet any of the heating 6-8 AM peak demand on peak heating days or even for moderately cold days.

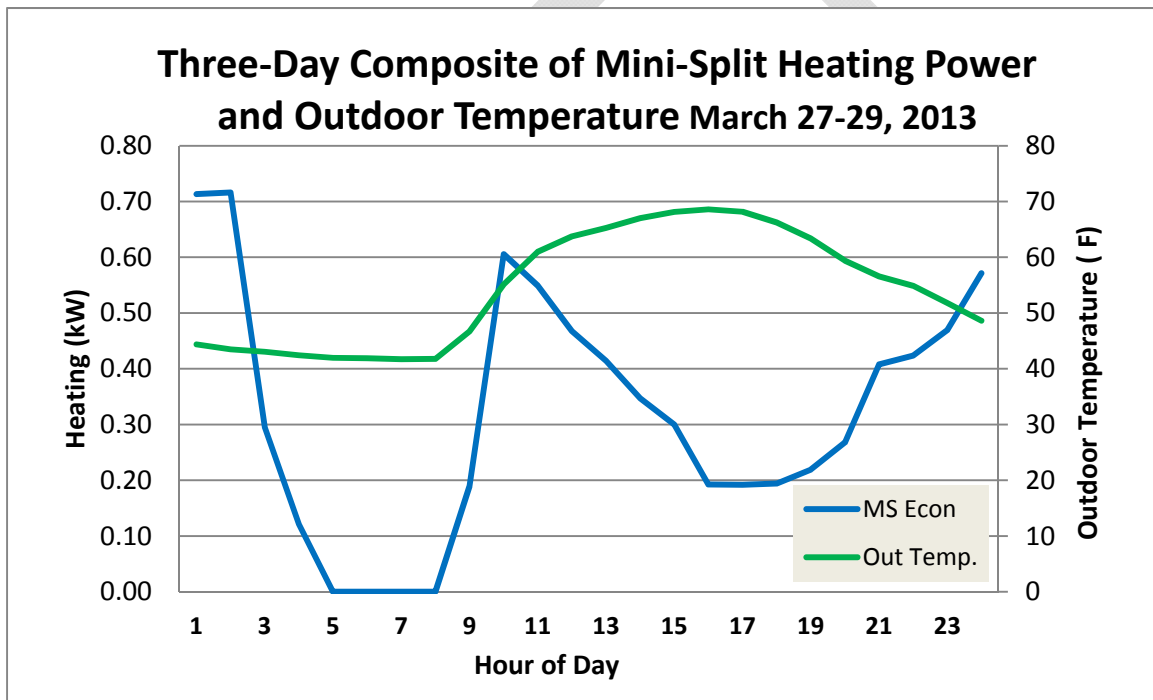


Figure 22. Composite of three moderately cold days in late March shows that there is insufficient stored battery energy to allow the solar heat pump to operate during the 6 to 8 AM peak period.

On the other hand, a management system could be implemented which would control both the solar heat pump and the central ducted system to allow solar-powered peak demand reduction. As the authors envision this control, a system such as “On Call” could (on days when a peak demand event was anticipated the following morning) be used to deactivate the solar heat pump system in the early evening perhaps around 6 PM, when the batteries would be nearly fully charged. The central ducted system would remain active and meet space heating requirements through the night. Then at 6 AM, the solar heat pump would be activated and the central system would be deactivated. With this arrangement, it is anticipated that the solar heat pump would be able to meet 2 or 3 hours of space heating peak demand.

Conclusion: Insufficient data was available to produce peak heating regression analysis. Alternatively, the research team has examined data for a number of cold winter mornings and concluded that the solar heat pump cannot meet any of the 6 - 8 AM heating peak demand. On the other hand, a large fraction of the peak demand (perhaps 85% or more) could be met by the solar heat pump if the central and mini-split heat pumps were controlled by the “On Call” system.

DRAFT

8. ECONOMIC ANALYSIS OF VARIOUS SYSTEM CONFIGURATIONS

An economic analysis has been carried out to determine the relative economic competitiveness of seven solar heat pump system configurations. It should be clarified that the energy performance results presented in Sections 4 through 7 of this report are based on 12 months of monitored data and regression analysis for the “as-tested” stand-alone solar heat pump system. In this section (Section 8), supplemental modeling of several system configurations is performed using a solar simulation tool called PV-DesignPro-S.

All of the system designs evaluated in this section had battery back-up with the exception of 1) a grid-tied solar system with a separate (not integrated) heat pump system; this was the baseline against which the other system designs were compared. Other examined designs included 2) the “as-tested” solar heat pump system, 3) the dc-powered solar heat pump system which was originally proposed but was unavailable for testing, and 4) an optimized bimodal ac-powered solar heat pump system. Three additional variations of the “as-tested” system are also evaluated in this section; 5) the “as-tested” system comparing operation with 8 batteries and 4 batteries, 6) the “as-tested” system with a lower and a higher efficiency mini-split heat pump, and 7) the “as-tested” system with expanded PV/battery capacity. All of the systems used a 1.5 ton mini-split heat pump with SEER 19.2 (SEER rating of 17 for the dc-powered mini-split), though in the case of the system 1, the mini-split operated completely independently of the solar system.

System number 1, which serves as a basis of economic comparison, is a standard grid-integrated solar system with a mini-split heat pump installed in the house but obtaining its power completely from the grid. Just to clarify, the base system consists of a standard grid-integrated PV system (PV panels, charge controller, and inverter) sending solar electricity to the house or the utility grid, with a non-integrated mini-split. The mini-split (1.5 ton, 19.2 SEER unit) heat pump is installed to serve the house but does not operate directly from the PV system. It can be considered, however, to be operating indirectly from the solar system. Because there are no batteries, this base system has no stand-alone operation nor can it serve as a back-up system in case of grid power outage.

In all cases, a substantial portion of the seasonal energy savings occurred as a result of the high efficiency of the mini-split heat pump. The ac-powered mini-split had a net efficiency that was 1.97 times that of the MH Lab central SEER 13 ducted heat pump (which has an effective SEER of 9.75 after including 25% attic duct system losses). The dc-powered mini-split’s net efficiency was 1.74 times that of the central system. The fact that in most cases all of the solar power was being delivered through the mini-split means that the mini-split can be thought of as an amplifier, in effect doubling (or nearly doubling) the delivered savings that the solar system would otherwise have provided.

There is another source of seasonal energy savings apart from solar powering of the mini-split, and that is operation of the mini-split from the grid when the solar resource has been depleted. This applies to all of the systems except the dc-powered system, which can operate only while

the sun is shining or the batteries have stored energy. While the “as-tested” solar heat pump system meets about 53% of the heating and cooling load of the house (MH Lab, in this case) from solar alone, the remaining space conditioning load can be substantially met by operation of the high efficiency mini-split operating from the utility grid. The “as-tested” solar heat pump system had a relay installed that allowed the mini-split to switch seamlessly from solar to grid when the solar resource was depleted. For this analysis, the research team assumed that 80% of the remaining heating and cooling load that had not been met by the solar heat pump would, in fact, be met by the mini-split operating off of the grid. The fact that the mini-split could provide the required space conditioning at approximately twice the efficiency of the central system, meant that the energy represented by the remaining 47% of the yearly load not met by solar would then be effectively cut in half. As a result, about 72% of the energy use that would have occurred with the central ducted system was saved by the mini-split heat pump system when operating from solar and the grid.

Economic analysis has been carried out for four solar heat pump system configurations, plus three additional variations on the “as-tested” system, to identify which systems provide the best economic performance. There are a variety of economic evaluation methods for Life Cycle Cost (LCC) analysis, each with advantages and disadvantages. This section uses payback period as the metric of economic comparison, taking into account fuel cost escalation, the time value of money, and the replacement cost for batteries every 7 years, the inverter every 10 years, and the mini-split every 15 years.

Since the objective of this economic analysis is to compare each of the systems on an even playing field rather than predicting energy outcomes for the full FPL service territory, all of the modeling is performed using the TMY3 data from Melbourne, Florida. The electricity utility rate is assumed to be \$0.10/kWh for on-peak/off-peak electricity. Following are economic assessments for seven system configurations. National Renewable Energy Laboratory’s Solar Advisor Model (SAM) software has been used to perform the economic analysis. The cash flow analysis captures installation and operating costs, taxes, incentives, and the cost of debt. SAM uses the system's hourly output for a single year generated by the performance model (and TMY data), and then calculates a series of annual cash flows for revenues from electricity sales and incentive payments, tax liabilities (accounting for any tax credits for which the project is eligible), loan principal, and interest payments. SAM reports a set of economic metrics, such as the levelized cost of energy (LCOE), which it calculates from the cash flow. Currently, residential systems cost about \$3.5/W or less. Of course, this cost will vary from contractor to contractor due to their differing degrees of buying power, overhead, installation practices, and profit margin. Each of the solar heat pump systems has 2.0 kW of PV. For this analysis, a cost of \$3.5/W was assumed for the solar portion of the grid-tied system, including the inverter and charge controller. The full cost of the solar portion of the system is \$7000. The 1.5-ton mini-split heat pump is assigned an installed cost of \$4200. The net cost of the system after a 30% Federal Tax Credit is \$7840 for systems without batteries. Analysis is also based on annual rise in retail electricity rates of 5%, a 5% inflation rate, a 5% real discount rate, and a PV panel performance degradation rate of 0.5% per year. It should be noted that the values for these assumptions, including the installed cost of PV systems, will vary by geographic region and utility.

Table 10 presents results from economic analysis results for four solar heat pump design variations. Shown are simulated seasonal electrical energy savings and payback period taking into account net system initial cost (after 30% Federal tax credit), replacement costs for batteries, inverter, and mini-split heat pump with an assumed electricity cost of \$0.10/kWh in the first year and escalating by 5% per year. Following Table 10 are descriptions and discussions in Sections 8.1-8.4 of the four solar heat pump system variations. Three additional system design variations of the “as-tested” system are presented in Sections 8.5-8.6, with economic assessments of using four batteries instead of eight batteries and the relative cost-effectiveness of installing a higher efficiency mini-split heat pump versus adding more PV/battery capacity.

Table 10. Seasonal Savings and Payback Period for Four Solar Heat Pump System Designs Taking into Account Maintenance and Component Replacement Costs over a 20-year Period

	PV produced kWh/y	PV+M-S avoided kWh/y	Mini-split on grid savings kWh/y	Seasonal savings kWh/y	Gross system cost	Net system cost ¹	Payback period years
Grid-integrated	2968	3877	1274	6151	\$11,200	\$7,840	12
“As-tested”	2734	5386	539	5925	\$15,200	\$10,640	20
DC	2441	4247	-	4247	\$12,860	\$9,002	22
Bimodal	2968	3877	1274	6151	\$13,600	\$9,520	17

¹ after 30% Federal tax credits

8.1 Analysis for a Grid-tied Photovoltaic System with Heat Pump but No Batteries

This is a traditional grid-tied PV system, consisting of PV modules, charge controller, and inverter, but which also incorporates a mini-split heat pump that operates independently of the solar system (Figure 23). The system has no batteries. Each module, when exposed to sunlight, generates dc electrical energy. An inverter converts the dc electricity to ac electricity, which can be consumed immediately by electronics in the building or exported to the grid. When the central utility’s electric grid goes down, the homeowner has no electrical service or space conditioning service, as would be the case with the systems evaluated in Sections 8.2 and 8.4, since the system has no battery back-up and the PV power must disconnect from the grid when there is a power outage.

The grid-tied PV system without battery back-up has an efficiency advantage because the batteries decrease system performance by about 6%.

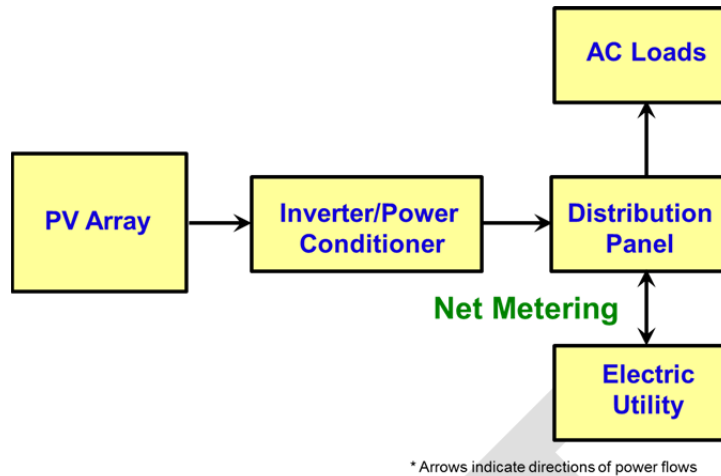


Figure 23. Utility Grid-Interactive PV System

8.1.1. System Description

For this analysis, a 2 kW grid-interactive system using the same PV modules as that of the Stand-alone System as tested this past year and a grid-tied inverter. The system cost is \$7000 for the PV system and \$4200 for the 1.5-ton mini-split, for a combined gross cost of \$11,200. Net cost is \$7840 after 30% Federal Tax credits. Life-cycle cost analysis assumes a 20-year evaluation period, modeled energy output for the system (using PV-DesignPro-S software), a 0.85 dc-to-ac derate factor (accounting for various types of losses that occur in the PV system), estimated annual PV system O&M costs of \$25, periodic replacement costs for the inverter and mini-split heat pump, and an effective SEER for the central ducted system of 9.75 (a SEER 13 system taking into account duct losses).

8.1.2. Economic performance

Figure 24 shows simulated hourly electricity from the PV system in red, electricity from the grid to the mini-split and central heat pumps in purple, electricity to house ac loads in blue, and electricity to grid in green. Peak electricity consumption and production occur during the summer months when the demand for cooling is high.

The PV system delivers a simulated 5144 kWh/y into the utility grid. In addition, the mini-split heat pump produces 306 kWh/y energy savings when the mini-split displaces heating and cooling that would otherwise occur with the central ducted system operating (more discussion on mini-split energy savings is found in Section 8.2). Together, first year net savings from this system is 5450 kWh, yielding a payback period of approximately 12 years.

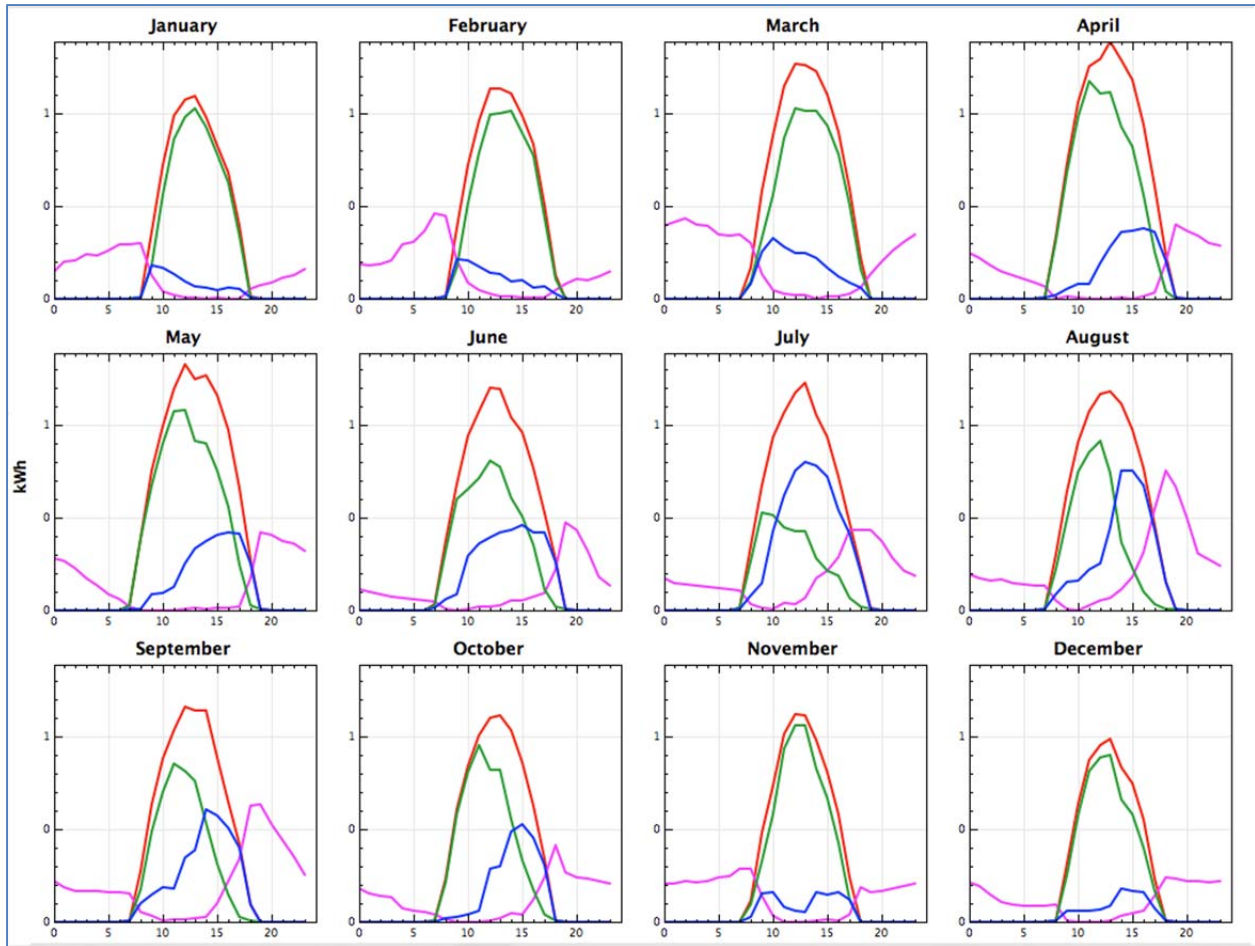


Figure 24. Grid Interactive monthly 24-hour profile PV system supply/demand energy flows.

8.1.3. Discussion

The grid tied solar system (with mini-split which operates in parallel to the solar) is found to be considerably more cost-effective than the other systems because there are no battery costs. However, this system does not provide a critical back-up service function for periods when the grid goes offline.

8.2 Analysis for the Stand-alone System as Tested This Past Year

The stand-alone solar heat pump system, as tested over the past 12 months in the Building Science Lab and described in earlier sections of this report, consists of PV modules, a charge controller, a bank of batteries, an inverter, and an ac-powered mini-split heat pump (Figure 25). The solar system provides power exclusively to the heat pump (although the inverter could be configured to provide power to other end uses within the home). Because the mini-split has a high SEER rating and has no distribution system losses, it delivers space conditioning to the building at 1.97 times the efficiency of the central ducted system.

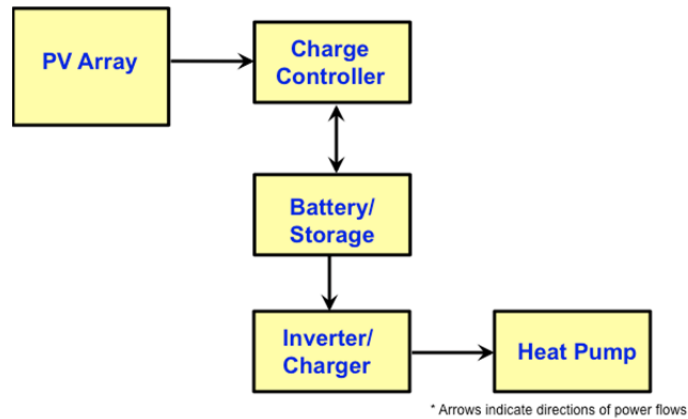


Figure 25. “As-tested” Stand-Alone Solar Heat Pump System

8.2.1. System Description

The inverter has the capability of receiving power from the grid but it cannot deliver electrical energy to the grid. The fact that the inverter can obtain power from the grid allows the mini-split to operate through all hours of the day (if so selected), thus providing significant additional energy savings compared to operating the central ducted heat pump during hours when the solar resource has been depleted.

The cost of this stand-alone solar heat pump system has been estimated to be \$15,200 based on current (September 2013) costs of system components, right-sizing the inverter (a 4 kW inverter was purchased but only 2 kW was required), and estimating contractor mark-ups, plus the \$4200 installed cost of a 1.5-ton Fujitsu 19.2 SEER mini-split heat pump. After 30% tax credits, the net system cost to the customer is estimated to be \$10,640.

8.2.2. Economic performance and discussion

The solar heat pump system saves energy in two ways. In the first place, the PV system delivers energy to the mini-split which then provides space conditioning to the residence that displaces electrical energy that would otherwise be consumed by the central ducted system (a SEER 13 heat pump with attic ducts that have delivery efficiency of 75%). These savings can be considered savings from solar energy. However, the solar generated electricity is enhanced by being delivered to the house by means of a high efficiency (SEER 19.2) mini-split (with zero cooling and heating distribution losses). Because its effective efficiency is essentially twice that of the central heat pump system, total solar savings are greatly enhance. In the second place, the mini-split heat pump can, on a regular basis, be powered by the grid after the solar resource has been depleted (based on operation of a simple relay), thus displacing additional space conditioning energy that would otherwise be consumed by the central ducted system.

On the other hand, since excess solar electricity (that which cannot be used when the space conditioning load has been satisfied) is in effect thrown away, savings are reduced.

Based on the simulation performed in PV-DesignPro-S, the PV system delivers 2734 kWh/y to the heat pump operating in Economy mode and using 8 batteries. Because the mini-split operates at 1.97 times the efficiency of the central ducted system, the combination of solar and mini-split saves 5386 kWh/y in electrical energy use that the central system would otherwise have consumed. An additional 539 kWh of annual energy savings result when the mini-split is powered by the grid during hours when the solar resource has been depleted. Combined, these result in first year energy savings of 5925 kWh. With these savings, the payback period is approximately 21 years.

8.3 Analysis for a dc-powered Solar Heat Pump System

This system is comprised of an array of PV modules, a charge controller, a bank of batteries, and a dc-powered mini-split heat pump (Figure 26). No inverter is required since the electrical load is a dc-powered heat pump.

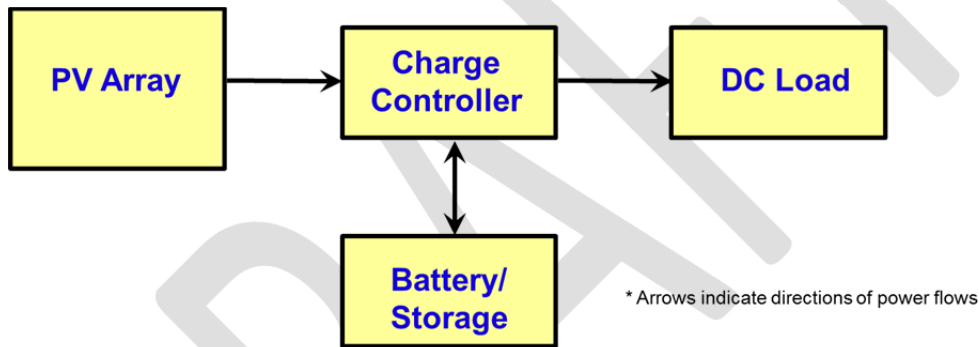


Figure 26. Solar Powered Heat Pump System

8.3.1. System Description

This dc-powered system (this is the SplitCool system which was originally proposed for this project) is similar to the preceding “as-tested” ac system (including PV modules, charge controller, and batteries). However, there are several important differences. This system would have no inverter, the mini-split heat pump would operate on dc power, there would be no critical-service ac-circuit within the house (to provide power to the homeowner during grid outages), and the mini-split could operate only when the solar resource is available (i.e., there is no way to operate the heat pump on the grid). PV-DesignPro-S software was used to simulate annual solar energy production and consumption. The full cost of the system is estimated to be \$12,860 and the net system cost is estimated to be \$9,002 (after tax credits). These first costs are lower than for the ac-powered system because no inverter is required. PV system efficiency is higher because the 10-15% inefficiency losses from the inverter are avoided. On the other hand, the SEER 19.2 ac mini-split has an approximate 13% efficiency advantage over the SEER 17 dc-powered mini-split.

8.3.2. Economic performance

Based on the simulation, the dc-powered system delivers 2441 kWh/y to the dc-heat pump (SplitCool) from the PV/battery system. Because the dc-powered mini-split has 1.74 times the efficiency of the central ducted system, this yields savings of 4247 kWh/y of avoided energy consumption of the central system. There are no additional savings from operating the mini-split using grid power, since the dc unit cannot operate on ac current. With these savings, the payback period is approximately 22 years.

8.3.3. Discussion

The payback period of the dc-powered solar heat pump is a little longer compared to the “as-tested” ac-powered solar heat pump. It could also be argued that there are additional factors that might make the ac-powered mini-split more attractive. First, ac-powered mini-splits are being widely used around the world and have a reputation for excellent reliability. It is less certain that dc-powered mini-splits are reliable. Second, when service and repair are required, it will be more difficult to get service and parts for the dc system. Third, the ac-powered system offers more versatility, by potentially providing critical service to a variety of ac end uses such as communication, lighting, and refrigeration during periods of grid power disruption. Fourth, the dc-powered system can only supply power to dc appliances, so excess solar power (not consumed by the heat pump) will go to waste, whereas excess power in the ac-powered system could be delivered to other ac appliances.

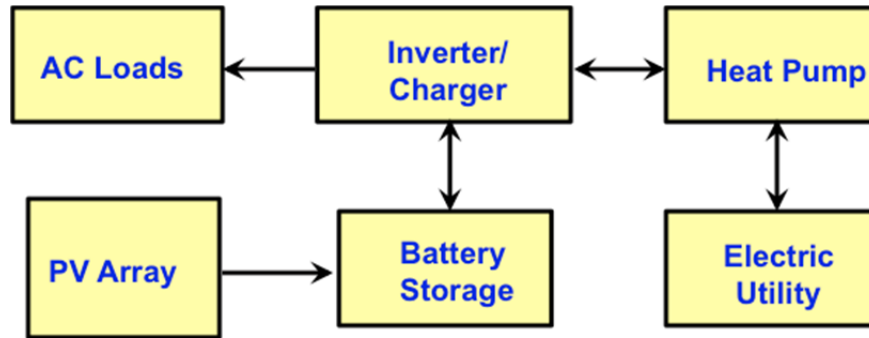
8.4 Analysis for an Optimized Solar Heat Pump System with Bimodal Inverter

An optimized bimodal, grid-interactive solar heat pump system with battery backup is proposed as a significant improvement compared to the “as-tested” system that can help with reliability of the battery bank. This system consists of an array of PV modules, charge controller, bank of four batteries, bimodal inverter, and 1.5-ton SEER 19.2 ac-powered mini-split heat pump (Figure 27). The system can operate as a grid-interactive system and as an Uninterrupted Power Supply. The inverter would have two-way energy flow capability (intermittently purchasing electrical energy from the grid and selling electrical energy to the grid). Because of battery storage and the dc-to-ac inverter, a critical-service ac-circuit could also be provided to the house to meet ancillary service to communication, lighting, refrigeration, and other uses during grid power interruption. When solar is unavailable, power from the grid would maintain the standby load circuits through the batteries/inverter.

It should be noted that a four-battery storage system was selected for this system to optimize cost-effectiveness. An eight-battery system could also be examined, but it would have the disadvantage of costing about \$1500 more at first cost and at each of the 7-year battery replacement cycles. On the other hand, a bank of eight batteries would allow the system to provide improved power back-up to the home during periods when the grid goes down. For the homeowner, then, the choice is whether to pay more to have greater back-up when the grid goes down or whether to have a more cost-effective system that provides reduced back-up capability during power outages. Since the larger battery bank also helps the utility with

meeting peak demand, incentives from the utility could be provided to the customer to incentivize purchase of the larger battery storage.

In normal operation, the inverter would use utility power, as needed, to charge the battery bank to maintain a minimum SOC. When utility grid goes down, the batteries can serve as a power source for the ac critical loads. When the batteries are fully charged, excess power generated by the PV array can be exported to the grid.



* Arrows indicate directions of power flows

Figure 27. Bimodal PV System

8.4.1. System Description:

The proposed optimized solar-powered heat pump system would have essentially the same components as the “as-tested” stand-alone system except that the battery bank would use four batteries instead of eight and the inverter would have bimodal capability. To improve battery life, the utility grid is designed to charge the batteries when SOC falls to 80% and discontinue charging at 85% SOC. Electrical energy would flow rather freely back and forth between the solar/battery system and the grid. In this design, power would be provided to the mini-split and also to a separate 120V critical loads circuit from the inverter/batteries. This would serve the function of providing an uninterruptable power supply to critical end uses on a relatively continuous basis. Additionally, battery/inverter power would also be available to this circuit during grid power outages, for shorter periods (for minutes to hours) and for more extended periods (multiple days resulting from storm or other causes). While the SOC range would be limited to 5 percentage points during normal operation, during grid outages, the SOC range could be increased by a factor of about 10 to allow expanded storage and delivery of available solar electricity.

8.4.2 Economic performance

The system cost is estimated to be \$13,600 (\$1600 less than the “as-tested” system because it uses 4 fewer batteries) including the \$4200 mini-split heat pump. After 30% federal tax credits, the net system cost is projected to be \$9520.

The bimodal system generates 2968 kWh/y in PV electricity. Of this 2968 kWh/y, 1968 kWh/y of solar power goes to the heat pump operating in Economy mode, which then generates 3877 kWh/y in avoided energy consumption by the central ducted heat pump system. Another 1000 kWh/y is projected to be consumed by other household ac end uses or be sold to the utility. Additionally, an additional 1274 kWh/y of avoided space conditioning energy consumption occurs when the mini-split operates on the grid. With these savings, the payback period is approximately 17 years.

8.4.3 Discussion

Compared to the “as-tested” stand-alone system, this optimized system is about 10% less expensive and yields about 4% greater energy savings. Additionally, this bimodal system will be much more reliable because of greatly enhanced battery life. While the batteries in the “as-tested” system failed after about 12 months of service, it is anticipated that the batteries in this proposed bimodal system should have a life-expectancy of seven years.

Since batteries are expensive and represent a weak link in the “stand-alone” system and dc-powered system concepts, it is anticipated that the small range of SOC cycling will greatly extend the life of the batteries. This would, in some ways, be comparable to the success of some brands of hybrid auto electrical storage system, which have had very low rates of battery failure over a 10-year operation period, achieved in large part by having a very narrow range of SOC operation. Using this configuration, the inverter would be available to serve both the mini-split and other critical loads. The only time that the critical loads circuit would be unavailable would be if the grid has been down for an extended period and the solar resource is insufficient to maintain the battery bank charge. When the utility grid goes down for longer periods (days), the battery SOC operation can be expanded to allow greater operational performance from the system. With the battery SOC widened for only a few days per year, the life of the batteries would still be greatly extended while the robust back-up function is preserved for periods of grid outage.

8.5 A Cooling Season Optimized System (4 batteries versus 8 batteries)

Economic performance has also been examined for a smaller battery bank (4 batteries versus 8 batteries) for the “as-tested” system. As was discussed in Section 2.3.2, the amount of battery storage required for good system performance varies substantially between the cooling season and the heating season. In our monitoring results, the 4-battery system performed reasonably well during cooling weather. However, the 4-battery system performed very poorly during heating weather. Even the 8-battery system performed only marginally during the heating season, especially at peak hours. Since the FPL service territory is heavily weighted toward cooling (with cooling degree days on the order of 5 to 10 times that of heating degree days across most of the service territory), it might make sense to optimize the system for the cooling season.

When modeling (based on regression analysis of monitored data) is done with 8 batteries and 4 batteries, the predicted annual savings for the “as tested” stand-alone system is found to be 2683 kWh/y and 2101 kWh/y, respectively, with Standard control. When operated in Economy mode, the 8-battery and 4-battery options yielded 3322 kWh/y and 2516 kWh/y savings, respectively. Since the extra four batteries represent about \$1600 of extra cost to the customer, and the savings from having 4 additional batteries is only \$58 per year (assume \$0.10/kWh) for Standard control and \$81 per year for Economy control, it appears that sizing the system for cooling optimization (4 batteries) is the more cost-effective approach.

On the other hand, having 8 batteries yields a more favorable outcome for peak demand and is likely to make the system more functional to the customer as a back-up system during grid outages.

8.6 Evaluation of Two Additional System Design Alternatives

The economic benefits of two options 1) installing a higher efficiency mini-split and 2) installing greater PV and battery capacity are examined.

- 1 Purchasing a higher efficiency mini-split.* Analysis has been done to identify the incremental cost of higher efficiency mini-split heat pumps. The cost of purchasing mini-split equipment only (installation additional) is shown in Figure 28 for $\frac{3}{4}$ -ton, 1-ton, 1.5-ton, and 2-ton systems. It can be seen that while there is no strong correlation between SEER and cost, there is a general upward price increase trend with increase in SEER rating. For this cost analysis, we have chosen to focus on 1-ton systems, because there is a fairly good sample size and the data trend is reasonably well behaved. For this size of system, there is an increase in cost of about \$600 (from about \$1200 to about \$1800) as SEER goes from 16 to 25. The 1-ton systems, therefore, show equipment an efficiency cost increment of approximately \$67 per SEER rating point. Extrapolating the price increment to 1.5-ton units, this would be \$100 per SEER point.

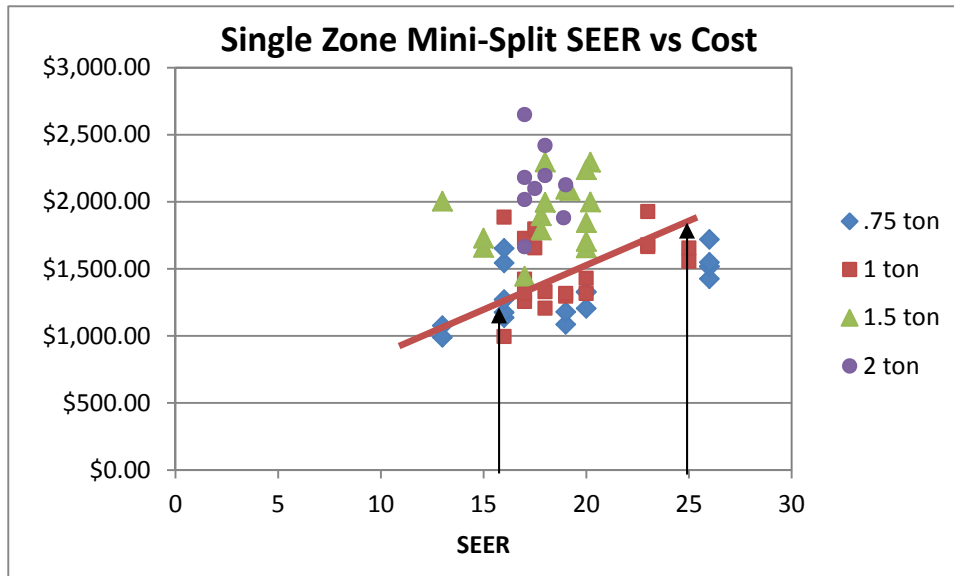


Figure 28. Equipment cost versus SEER rating for four sizes of mini-split heat pumps based on an on-line survey, including a best-fit line for the 1-ton units. (Source: survey performed by Carlos Colon in 2011.)

To examine the cooling energy savings related to mini-split SEER rating, we will begin at the low end of the efficiency spectrum, with a SEER 16 rating. We will also assume that the solar heat pump system has been configured so that the mini-split can be operated from the grid as well as from solar. Simulations found that the SEER 19.2 mini-split saves 4442 kWh/y in cooling energy savings when operated from both solar and the grid (Table 6). These savings are derived under the assumption that this mini-split delivers all of the solar-source cooling, that it operates off of the grid to meet 80% of the remaining yearly cooling that would otherwise be met by the MH Lab SEER 13 central ducted system, and that the SEER 13 central system operates at an effective SEER of 9.75 because of duct losses.

- Given that the 19.2 SEER mini-split saves 4442 kWh/y, we calculate that the annual cooling savings would be 3842 kWh if using a SEER 16 mini-split.
- Given that the 19.2 SEER mini-split saves 4442 kWh/y, we calculate that the annual cooling savings would be 5242 kWh if using a SEER 25 mini-split.
- Yearly cooling savings from going from SEER 16 to SEER 25 is then 1400 kWh.
- If we assume that heating energy savings are equal to 15% of the cooling savings (this is based on HDD being about 15% of CDD in the FPL service territory), then yearly heating savings from going from SEER 16 to SEER 25 is then 210 kWh.

Annual cooling and heating electricity savings to the customer from installing a SEER 25 heat pump versus a SEER 16 unit would be 1610 kWh/y (\$161/year). Given that the installed cost of the SEER 25 system is estimated to be \$900 more than that of the SEER 16 system, the payback period for purchasing a higher efficiency mini-split is less than 8 years.

- 2 *Adding greater PV/battery capacity.* For this analysis, 500 W of additional PV capacity with proportional additional battery capacity is added to the “as-tested” system. Incremental net

cost will be \$963 (\$700 for the 500 W of PV and \$675 for the battery each with 30% tax credit). Energy savings produced by the incremental PV/battery system is found to be 474 kWh/y (\$47/y). Therefore, the incremental cost of \$963 for the added PV and battery capacity yields a payback of about 20 years. Because the payback period for purchasing a high efficiency mini-split is less than 8 years, it is clear that purchasing increased mini-split efficiency is a much better investment.

DRAFT

9. Summary and Conclusions

Lab research was conducted to evaluate annual and peak energy savings from operation of a solar powered mini-split heat pump system in a home also served by a central ducted heat pump system. The mini-split can also operate on grid power when the solar resource has been depleted. Energy and peak demand savings are based on TMY3 simulation and weighted for four cities (Daytona Beach, West Palm Beach, Miami and Ft. Myers). The five configurations evaluated over a 12-month period were:

- PV power, 8 battery back-up, mini-split with Economy control
- PV power, 8 battery back-up, mini-split with Standard control
- PV power, 4 battery back-up, mini-split with Economy control
- PV power, 4 battery back-up, mini-split with Standard control
- PV power, 8 battery back-up, with mini-split also operated on the grid (100% MS) when the daily solar resource had been depleted.

Regression analysis and simplified simulation using TMY3 data provided savings results for these five configurations.

A more complex hourly model was used to simulate several variations on the as-tested system and a base-line system (grid-integrated solar system with no batteries).

FPL also requested answers to the following:

- Which system type (PV-grid integrated solar system with no batteries and separate mini-split heat pump versus the as-tested solar heat pump system with batteries) is more cost-effective and what level of peak demand reduction is achievable by each?
- Which upgrade is more cost-effective; 1) money to upgrade heat pump efficiency or 2) money to expand the PV/battery system?

The results of this analysis are presented in Section 8 and briefly summarized in the following list.

1. The “as-tested” solar heat pump system (with battery back-up) meets up to 72% of annual space conditioning energy consumption, but the economic returns are not attractive with payback on the order of 20 years. Furthermore, there are significant maintenance requirements and on-going costs associated with the batteries that further cut into possible savings. On the other hand,
 - a. The solar heat pump system produces substantial cooling peak demand reduction (2.20 kW) which can be attractive to the utility. It was, on the other hand, ineffective in meeting heating peak demand.
 - b. As configured and operated in the MH Lab, the mini-split can meet up to 54% of the annual space conditioning requirement from solar alone. Another 18 percentage points of space conditioning savings can be achieved by operating the high efficiency mini-split from utility grid power thus displacing energy that would otherwise be consumed by the lower efficiency central ducted heat pump system, bringing savings to 72% (4442 kWh/y).

- c. The system can also potentially provide 120V ac service for other appliances during periods when the grid goes down.
2. Batteries are the weak link in the stand-alone solar heat pump system. When subjected to nearly daily cycling from 45% to 90% state-of-charge (SOC), the batteries experienced dramatically diminished storage capacity by the end of 12 months.
3. The inverter proved to be more inefficient (84% monitored efficiency) than originally anticipated compared to expected 90-95% efficiency. It will be important, for future stand-alone applications, to find a higher efficiency inverter.
4. A bimodal inverter (able to both receive from and deliver to the central grid) is needed in order to use excess solar energy that is available on sunny days with limited space conditioning loads.
5. An optimized bimodal stand-alone system design is proposed in this report that will make the system more cost-effective by delivering all of the available solar energy either to the mini-split, the house, or to the utility grid, and by greatly extending the life of the batteries.
6. A grid-tied PV system, with a mini-split heat pump operating independently of the PV but without batteries, was modeled and found to have a payback period of about 12 years. It cannot, however, provide back-up for when the grid goes down. It meets 100% of the cooling peak demand of the HVAC system when operated in tandem with the high efficiency SEER 19.2 mini-split heat pump but 0% of the heating peak demand.
7. The solar heat pump system with battery back-up provides considerably more yearly cooling and heating electricity savings while operating in Economy mode.
 - a. Indoor RH control was very good for both control modes typically 39% for Standard mode and 46% for Economy mode.
8. The “as-tested” solar heat pump system (using Standard control) achieved 100% peak demand savings on the hottest hours of the hottest days – on the order of 2.2 kW reduction. By contrast, Economy mode produces peak savings of about 85% during those same hours. If the “as-tested” system is operated with only 4 batteries, 85% of the peak cooling demand is met in Standard mode and 69% is met in Economy mode.
9. A direct current-powered solar heat pump system would be slightly less cost-effective compared to the “as-tested” system. It would deliver lower energy savings but is expected to have a lower first cost. On the other hand, the dc mini-split would be unable to provide high-efficiency space conditioning using power from the grid during periods when the solar resource has been depleted and would not be able to provide space conditioning or 120V ac back-up service when the grid goes down.
10. An optimized bimodal stand-alone solar heat pump system is proposed in this report as a means to yield longer battery life and lowered battery maintenance/replacement costs while also reducing or even eliminating the solar power that must be discarded by the “as-tested” system during periods of low space conditioning loads.

11. A 4-battery (instead of 8-battery) version of the “as-tested” system might be slightly more cost-effective to the homeowner but less effective in summer peak demand reduction and at providing critical service during grid outages.
12. Installing a higher efficiency mini-split system is cost-effective, with a payback of less than 8 years for the added cost for higher efficiency.
13. Installing more PV/battery capacity is less cost-effective, with a payback on the order of 20 years.

DRAFT

APPENDIX A

Performance Analysis of Components of the Stand Alone System

When this research project began, the dc-powered SplitCool heat pump was not available from the manufacturer. FSEC then offered to monitor the energy delivery efficiency of the inverter (which would not have been required for the dc heat pump) in order to account for this inefficiency when simulating the dc-heat pump system performance. Power meters were installed at various junctions of the solar heat pump system, thus providing data that can be used to determine the efficiency of each component of the system. Figure A-1 illustrates system components and energy flow patterns.

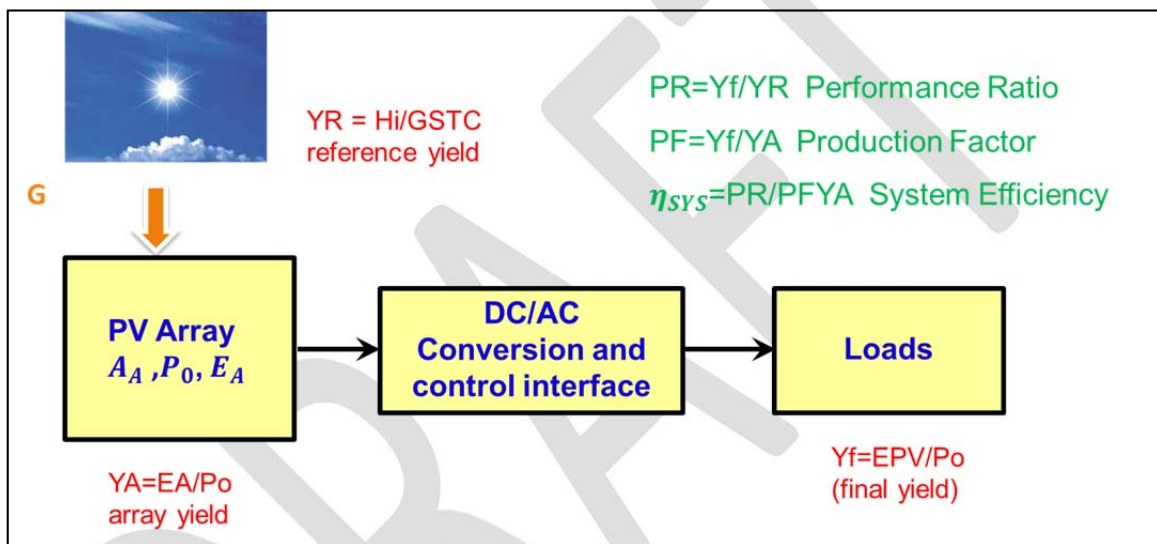


Figure A-1. System Operation Energy Flow Patterns and Definitions.

The method of analysis presented here provides a means of evaluating the performance of the monitored solar heat pump system and each component separately. An understanding of some PV terminology is helpful in understanding this analysis. PV system power rating refers to the nameplate dc power rating of the PV array provided by the module manufacturer. This is the sum of the ratings for all of the PV modules connected, and refers to their electrical power output under Standard Test Conditions (STC). STC for a PV array are an irradiance of 1000 W/m^2 incident on the modules, spectral distribution of 1.5 atmospheres, and cell temperature of 25°C (77°F). PV system yield, Y_A , is defined as the array dc energy output divided by the PV system power rating. Moreover, final PV system yield, Y_f , is defined as the net ac output energy divided by the dc nameplate power of the array under STC. The higher this number, the more energy the array has generated relative to its potential. Reference yield, Y_R , is defined by the total plane-of-array (POA) solar irradiation incident on the array, H_{POA} , divided by the reference irradiance at STC, which is 1000 W/m^2 . The performance ratio (PR) is simply the final PV system yield divided by the reference yield (Y_R). This parameter allows for a more appropriate comparison of one PV system to another by normalizing the difference in irradiance incident on

the individual arrays. The higher PR is, the better the system is using its potential. A low PR value means production losses due to technical or design problems are high. The production factor (PF) is defined as final PV system yield divided by reference yield (YR) (Figure A-2). Finally, system efficiency is simply the performance ratio (PR) divided by the production factor (PF). The empirical relationship between PF and PR is shown in Figure A-3.

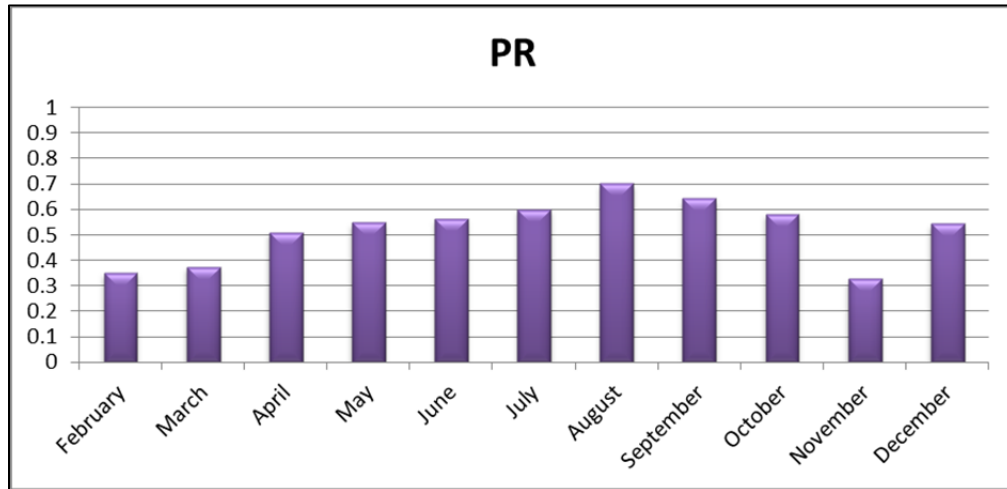


Figure A-2. Calculated Performance Ratio (PR) values are determined based on monitored data from the “as-tested” solar heat pump system for each month of the year.

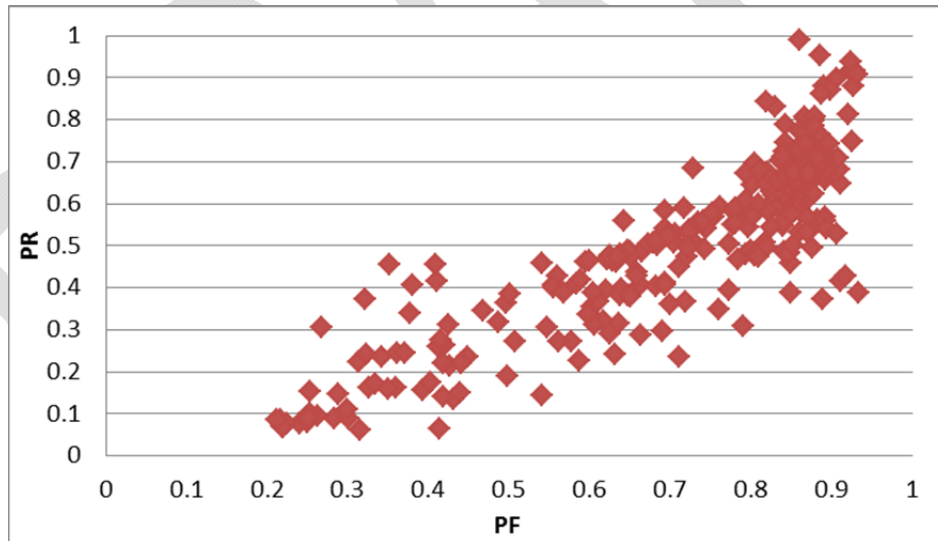


Figure A-3. Performance Ratio plotted versus Production Factor based on monitored data.

Lower monthly PF values indicate that system production is limited by low consumption (low space conditioning loads) during that month.

Between the sun and the electrical end use, various inefficiencies emerge. PV system losses (or PV system derate factor) is determined for the system through each system component. It is the product of all of the system efficiencies and miscellaneous sub-factors including: module

mismatch and nameplate tolerance, inverter, wiring losses, charge controller, and battery bank charging and discharging.

The first is panel mismatch. To determine the module mismatch and nameplate tolerance, the four PV module strings' operating voltages and currents were measured using an IV curve tracer (PV600). Measurements were taken at the combiner box for the array. Plane-of-array irradiance values and modules temperatures were measured using a reference PV cell and thermocouple. Due to the dynamic nature of PV module performance and constantly changing operating conditions, the performance specifications of a module or array have meaning only when the rating conditions are given. Measured operation data were translated to the Standard Test Condition (STC) using translation formulas for temperature and irradiance, the two principal factors affecting PV performance. String measurements were taken. The instantaneous efficiency for each array was developed. As can be seen, the four PV panel strings have an average derate factor of 6.5% (Table A-1). The efficiency loss of the PV strings is caused by differences in maximum power point voltage. The panel with the lowest voltage pulls voltage down for the other panel in the string.

Table A-1

Analysis of the solar heat pump system PV strings (1 modules per string) over the period July 15, 2012 – July 15, 2013 finds that PV module mismatch produces losses of 6 to 7% for each of the four strings of panels.

	Vmp Volts	Imp Amps	Pmax Watts	Voc Volts	Isc Amps	FF	PF %	Irradiance (W/m ²)	Temp. deg C	Vmp(trans) Volts	Imp(trans) Amps	Pmax(trans) Watts	Voc(trans) Volts	Isc(trans) Amps	ΔP Watts
String #1	55.3	4.94	273	69.0	5.28	0.750	95.4	634	42.8	60.16	7.78	468.28	72.87	8.32	-6%
String #2	54.9	4.98	273	68.9	5.39	0.736	94.9	638	42.8	59.63	7.81	465.64	72.81	8.44	-7%
String #3	55.1	5.05	278	69.0	5.44	0.741	95.7	640	41.7	59.58	7.89	470.01	72.62	8.50	-6%
String #4	55.6	5.03	280	69.0	5.45	0.744	95.3	647	41.1	59.98	7.78	466.41	72.49	8.42	-7%

The average module mismatch and nameplate tolerance value is 0.94, which means that the strings are only delivering 94% of the potential energy that could be produced under ideal mismatch and nameplate tolerance circumstances. This is a typical value for an average efficiency crystalline module. Based on a comprehensive data analysis, the average efficiency for all the other components has been calculated as follows:

Inverter = 0.84
 Charge Controller = 0.96
 Battery Bank = 0.94
 Wiring = 0.98

When all of these losses are considered together, the resulting system derating factor is 0.70. This is calculated as the product of all system derating sub-factors (0.94 x 0.84 x 0.96 x 0.94 x 0.98 = 0.70).

The largest surprise from this analysis was the low efficiency of the inverter. The research team had been expecting overall dc to ac conversion efficiency through the inverter to be closer to 90-95%.

APPENDIX B

Improving Solar Heat Pump System Control to Achieve Maximum Peak Demand Savings

For the cooling season, peak demand savings are likely to be achieved on all peak days, especially when the mini-split is operated in Standard mode, which tends to produce maximum cooling output. The reason for this is that the hottest hours generally have substantial solar radiation, and if not, the battery is nearly always near full charge at this peak time. Furthermore, the solar heat pump is always producing cooling during the hours of 4 PM to 6 PM on these hotter than average days, either by solar directly from the PV or from stored energy in the batteries.

For the heating season, peak demand savings can in most cases be achieved during the utility's peak demand period but only by careful scheduling of heat pump operation using a timer. Another way to express this is that the homeowner would need to be significantly motivated to get the solar powered heating to occur during the winter peak period. The project research team implemented several timer schedules with the objective of having the mini-split operate fully during the 6-8 AM peak demand period. We were generally not successful, because the batteries can carry forward only a limited amount of energy.

There is tension between several operational factors. On one hand, we want to allow the system to operate for as many hours as possible on solar power, so that little or no collected solar power is thrown away. However, since we would also like to shift the heat pump operation to the coldest hours of the cold winter morning, this means shutting down the solar powered space heating fairly early in the evening on a cold winter night. On our first try, we scheduled the heat pump to operate on solar till 12:30 AM (EDT) and then turn back on at 5:30 AM (EDT). This worked well on moderately cold nights with low temperature of 45°F to 50°F. For colder nights, too much of the stored battery power was expended by 11:30 PM, so that the battery SOC was too low at 6 AM.

March 3, 2013 was the coldest day of the 2012-2013 heating season, with a low of 34°F and a high of 55°F. Space heating was needed for every hour of the day in part because of the relatively high space heating setpoint of 76°F (this elevated temperature was chosen in order to increase the potential for the heating system to operate on a maximum number of days; for our modeling we use 72°F as the house heating setpoint). Solar powered heating occurred from about 11:55 (EDT) till 2250 (EDT), but then remained off till 1130 (EDT) the next day when the batteries reached their cut-in battery voltage (27.0V for a five minute period; this is user selectable).

If the batteries are “resting” (no power being drawn out of the battery and none being pushed into the battery), then battery voltage is a good indicator of SOC. Figure B-1 shows the relationship between battery voltage (BV) and state of charge (SOC) based on manufacturer data for a resting battery. Battery voltage is not, however, a good indicator of battery SOC under most operational circumstances, because power flows into and out of the batteries.

- If power is being delivered into the batteries from the PV panels, then BV is pushed upward by the force of the current being pushed into the batteries.

- If power is being drawn from the batteries from the mini-split heat pump, then BV is drawn downward by the force of the current being drawn from the batteries.
- If the PV panels are delivering power to the batteries and the heat pump is drawing power from the batteries, the net effect will be higher or lower BV (compared to resting BV) based on whether the PV power delivery is greater than the heat pump power draw. Under bright sun, the PV system was typically delivering power that was on the order of twice that of the power draw of the heat pump.

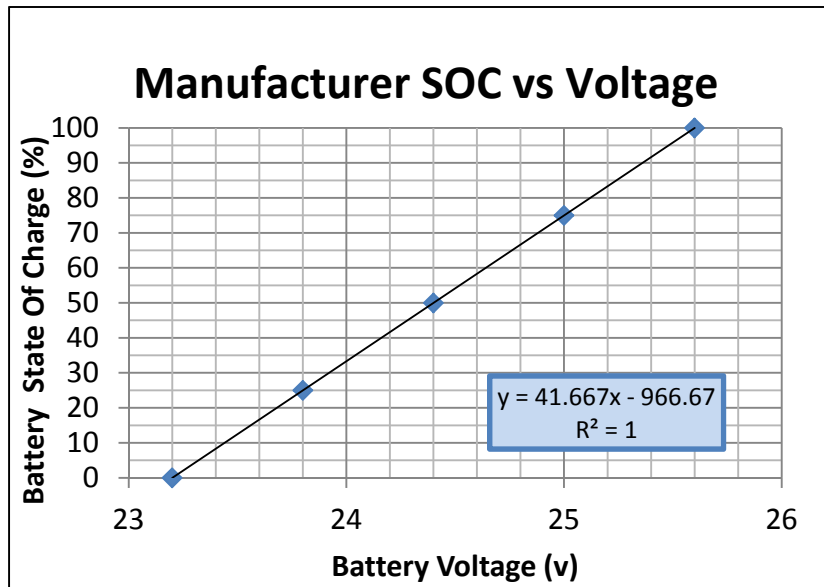


Figure B-1. Battery SOC versus Battery Resting Voltage (data from battery manufacturer).

The greater the (net) draw of power, the greater will be the downdraft on BV compared to its resting voltage. Also, the greater the (net) input of power to the batteries, the greater will be the updraft of BV compared to its resting voltage. These power fluxes create system control problems because the BV cutout (shut off) will be prematurely reached if the mini-split is drawing at a maximum rate (such as on a cold winter morning). The manufacturer of the inverter/charge controller equipment has assured us that better controllers are now being introduced which can provide accurate SOC measurement. Once this SOC control option is readily available, customers will be more able to manage the scheduling of the heat pump system. If a utility cost structure or other incentive was available to the customer to provide incentive to operate the mini-split heat pump from solar, battery power, or both during peak periods, then the customer could schedule solar-powered heating operation (delivered by means of battery storage) for the winter morning peak demand period with greater effectiveness (compared to our none-too-successful attempts to schedule operation based on BV).

A couple of other options might also be available to help meet winter peak demand (recall that the solar heat pump meets 100% or near 100% of cooling peak in nearly all circumstance) by means of utility intervention (such as “on call” control). One possibility, for a cold winter night, is that the utility could use their remote activation technology to deactivate the heat pump during the preceding evening and overnight and then activate the heat pump on solar power (through the

batteries) for the period starting at 6 AM. Another complementary option could include automatically charging the bank of batteries using power from the electric grid on cold nights, during a nighttime period such as 10 PM till 1 AM, thus ensuring that the bank of batteries would have sufficient power to operate the mini-split heat pump through the entire peak demand period.

DRAFT